TMMOB İnşaat Mühendisleri Odası

Teknik Dergi

Technical Journal

Volume 30 Issue 2 March 2019

TEKNİK DERGİ PUBLICATION PRINCIPLES

Teknik Dergi is a scientific and technical journal indexed by the Science Citation Index Expanded. Annually six issues are published, three in Turkish in the months of January, May and September, three in English in March, July and November. Its main principles of publication are summarized below:

1. Articles reporting original scientific research and those reflecting interesting engineering applications are accepted for publication. To be classified as original, the work should either produce new scientific knowledge or add a genuinely new dimension to the existing knowledge or develop a totally new method or substantially improve an existing method.
2. Articles reporting preliminary results of scientific studies and those which do not qualify as full articles but provide useful information for the reader can be considered for publication as technical notes.
3. Discussions received from the readers of the published articles within three months from publication are reviewed by the Editorial Board and then published together with the closing remarks of the author.
4. Manuscripts submitted for publication are evaluated by two or three reviewers unknown to the authors. In the light of their reports, final decision to accept or decline is taken by the Editorial Board. General policy of the Board is to get the insufficient manuscripts improved in line with the reviewers' proposals. Articles that fail to reach the desired level are declined. Reasons behind decisions are not declared.
5. A signed statement is taken from the authors, declaring that the article has not been published as a "journal article or book chapter". In case the Editorial Board is in the opinion that the article has already been published elsewhere with minor changes or suspects plagiarism or a similar violation of ethics, then not only that article, but none of the articles of the same authors are published.
6. Papers reporting works presented as conference papers and developed further may be considered for publication. The conference it was presented to is given as a footnote in the first page.
7. Additionally, a document signed by all authors, transferring the copyright to UCTEA Chamber of Civil Engineers is submitted together with the manuscript.

UCTEA Turkish Chamber of Civil Engineers

Teknik Dergi

Technical Journal

Volume 30 Issue 2 March 2019

UCTEA
Turkish Chamber of Civil Engineers
Necatibey St. No: 57, Kızılay 06440 Ankara, Turkey
Tel: +90.312.294 30 00 - Faks: +90.312.294 30 88
E-mail: imo@imo.org.tr - www.imo.org.tr

Publisher:
Cemal GÖKÇE
On behalf of UCTEA Turkish Chamber of Civil Engineers

Administrative Officer:
Bahaettin SARI

Volume 30 - Issue 2 - March 2019

Published bi-monthly. Local periodical.

Date of Print: 01 March 2019 / Number of copies: 1.000

ISSN: 1300-3453

Printed by:
Lotus Life Ajans Rek.Tan.Bas.Yay.Org.Amb.İth.İhr.San.ve Tic.Ltd.Şti.
Sokullu Cad. Perçem Sok. No: 9/A Çankaya / Ankara - Tel: 0.312.433 23 10

UCTEA Turkish Chamber of Civil Engineers

Teknik Dergi

Teknik Dergi is indexed by

- Science Citation Index Expanded
- Scopus
- Journal Citation Reports / Science Edition
- Engineering Index
- Concrete Abstracts (American Concrete Institute)
- National Technical Information Service (US NTIS)
- CITIS
- Ulrich's International Periodical's Directory
- TÜBİTAK / ULAKBİM

Teknik Dergi is a peer reviewed open access periodical publishing papers of original research and interesting practice cases. It addresses both the research community and the practicing engineers.

Reviewers:

This list is renewed each year and includes reviewers who served in the last two years of publication.

Ayda Şafak AĞAR ÖZBEK
Ragıp AKBAŞ
Sami Oğuzhan AKBAŞ
Rıfat AKBIYIKLI
Özge AKBOĞA KALE
Burcu AKÇAY ALDANMAZ
Cihan Taylan AKDAĞ
Cem AKGÜNER
M. Vefa AKPINAR
Atakan AKSOY
Zuhal AKYÜREK
Fatih ALEMDAR
Pelin ALPKÖKİN
Sinan ALTIN
Hilmi Doğan ALTINBİLEK
Adlen ALTUNBAŞ
Fuat ARAS
Davit ARDITI
Deniz ARTAN İLTER
Hakan Nuri ATAHAN
Shady ATTIA
Mustafa Tamer AYVAZ
Lale BALAS
Selim BARADAN
Bekir Oğuz BARTIN
Bilge BAŞ
Zeynep BAŞARAN BUNDUR
Cüneyt BAYKAL
Zerrin BAYRAKDAR
İdris BEDİRHANOĞLU
Serkan BEKİROĞLU
Mehmet BERİLGEN
Saadet Arzu BERİLGEN
Niyazi Özgür BEZGİN
Selçuk BİLDİK
Senem BİLİR MAHÇİÇEK
Barış BİNİCİ
İlknur BOZBEY
Zafer BOZKUŞ
Burcu BURAK BAKIR
Erdem CANBAY
Zekai CELEP
Cihan CENGİZ
Halim CEYLAN
Ömer CİVALEK
Mustafa CÖMERT
Ali Fırat ÇABALAR
Barlas Özden ÇAĞLAYAN
Özgür ÇAKIR
Gülben ÇALIŞ
Necati ÇATBAŞ
Erkan ÇELEBİ
Kutay ÇELEBİOĞLU
Ahmet Ozan ÇELİK
Oğuz Cem ÇELİK
Osman Nuri ÇELİK
Hilmi Berk ÇELİKOĞLU
Kemal Önder ÇETİN
Mecit ÇETİN
Reha ÇETİNKAYA
Safiye Feyza ÇİNİCİOĞLU
Erdal ÇOKÇA
Kutlu DARILMAZ
Cem DEMİR
Ender DEMİREL
Mehmet Cüneyd DEMİREL
Fatih DİKBAŞ
Seyyit Ümit DİKMEN
İrem DİKMEN TOKER
Ahmet Anıl DİNDAR
Emrah DOĞAN
Nurhan ECEMİŞ ZEREN
Özgür EKİNCİOĞLU
Alper ELÇİ
Şebnem ELÇİ
Nilay ELGİNÖZ KANAT
Murat Altuğ ERBERİK
E. Mete ERDEMGİL
Saffet ERDOĞAN
Esin ERGEN PEHLEVAN
Ayşen ERGİN
Gökmen ERGÜN
Esra Ece ESELLER BAYAT
Tuğba ESKİŞAR TEFÇİ
Güngör EVREN
Antonio FORMISANO
Nuray GEDİK
Ergun GEDİZLİOĞLU
Haluk GERÇEK
Ilgın GÖKAŞAR
Çağlar GÖKSU
Burcu GÜLDÜR ERKAL
Fazlı Erol GÜLER
Zeynep GÜLERCE
Taylan GÜNAY
Necmettin GÜNDÜZ
Abdurrahman GÜNER
Ülker GÜNER BACANLI
Aslı Pelin GÜRGÜN
İpek GÜRSEL DİNO
Gürşans GÜVEN IŞIN
Soner HALDENBİLEN
Murat HAMDERİ
Zeki HASGÜR
Abdul HAYIR
Nejan HUVAJ SARIHAN
Zeynep IŞIK
Sabriye Banu İKİZLER
Eren İNCİ
Pınar İNCİ
Erdal İRTEM
Recep İYİSAN
Nihat KABAY
M. Rifat KAHYAOĞLU
Volkan KALPAKÇI
Erhan KARAESMEN
Halil KARAHAN
Himmet KARAMAN
Mustafa KARAŞAHİN
İlker KAZAZ
Cevza Melek KAZEZYILMAZ ALHAN
Mustafa Kubilay KELEŞOĞLU
Elçin KENTEL
Havvanur KILIÇ
Ufuk KIRBAŞ
Veysel Şadan Özgür KIRCA
Gökhan KİRKİL
Niyazi Uğur KOÇKAL
Önder KOÇYİĞİT
Mete KÖKEN
Ali Ümran KÖMÜŞÇÜ
Özgür KURÇ
Akif KUTLU
Semih KÜÇÜKARSLAN
Hilmi LUŞ
Kasım MERMERTAŞ
Mehmet Murat MONKUL
Yetiş Şazi MURAT
Elif OĞUZ
Mehmet Hakkı OMURTAG
Sema ONURLU
Engin ORAKDÖĞEN
Şeref ORUÇ
Okan ÖNAL
Akın ÖNALP
Aybike ÖNGEL
Bihrat ÖNÖZ
Ali Hakan ÖREN
Murat ÖZEN
Pelin ÖZENER
Abdullah Tolga ÖZER
Eren Arman ÖZGÜVEN
Hakkı Oral ÖZHAN
Zeynep Huri ÖZKUL BİRGÖREN
Beliz ÖZORHON ORAKÇAL
Sadık ÖZTOPRAK
Turan ÖZTURAN
Baki ÖZTÜRK
Mustafa ÖZUYSAL
Tolga Yılmaz ÖZÜDOĞRU
Nilüfer ÖZYURT ZİHNİOĞLU
Bekir Yılmaz PEKMEZCİ
Şamil Şeref POLAT
Gül POLAT TATAR
Selim PUL
Selman SAĞLAM
Mehmet SALTAN
Altuğ SAYGILI
Hasan SAYGIN
Neslihan SEÇKİN
Serdar SELAMET
Serdar SOYÖZ
Ayşe Filiz SUNAR
Erol ŞADOĞLU
Burak ŞENGÖZ
Aykut ŞENOL
Ali Ünal ŞORMAN
Özcan TAN
Ali Hamza TANRIKULU
Serhan TANYEL
Ergin TARI
Taha TAŞKIRAN
Gökmen TAYFUR
Berrak TEYMUR
H. Onur TEZCAN
Mesut TIĞDEMİR
Şahnaz TİĞREK
Vedat TOĞAN
Onur Behzat TOKDEMİR
Nabi Kartal TOKER
Mustafa TOKYAY
Ali TOPAL
Cem TOPKAYA
Ahmet TORTUM
Gökçe TÖNÜK
Nursu TUNALIOĞLU
Eda TURAN
Ahmet TÜRER
Kaan TÜRKER
Handan TÜRKOĞLU
Cüneyt TÜZÜN
Eren UÇKAN
Berna UNUTMAZ
Mehmet UTKU
Volkan Emre UZ
Deniz ÜLGEN
Aslı ÜLKE KESKİN
Alper ÜNLÜ
Ahmet YAKUT
İsmail Özgür YAMAN
A. Melih YANMAZ
Mert Yücel YARDIMCI
Ufuk YAZGAN
Anıl YAZICI
Emine Beyhan YEĞEN
İrem Zeynep YILDIRIM
Koray Kamil YILMAZ
M. Tuğrul YILMAZ
Mehmet YILMAZ
İsmail YÜCEL
Yeliz YÜKSELEN AKSOY
Nabi YÜZER
Ahmet Şahin ZAİMOĞLU

UCTEA Turkish Chamber of Civil Engineers

Teknik Dergi

Volume: 30 Issue: 2 March 2019

CONTENTS

Foreword

THE FIRST YEAR OF BILINGUAL TEKNİK DERGİ

In line with a decision taken in 2017 to convert Teknik Dergi into a bilingual periodical, bilingual publication has started with the January 2018 issue, following a period of preparatory arrangements. Initially, the Board had been concerned about the possible complications caused by this conversion. Fortunately, no complications have taken place and the first year of bilingual publication could be completed smoothly and successfully.

One major concern was a sustainable inflow of English manuscripts. First year observations indicated no need for concern. Two thirds of the manuscripts received that year were in English. In other words, the number of English manuscripts doubled the Turkish ones. However, it is not granted that this tendency will continue. The Board has the impression that the potential authors were initially enthusiastic to submit English manuscripts without paying the due attention to the quality of contents and the drafting rules. Consequently, the decline rate was higher for the English manuscripts compared to that for the Turkish ones. These fluctuations are expected to settle gradually and the authors to observe the Teknik Dergi principles and paper drafting rules more carefully. Consequently, the number of submitted manuscripts will possibly decrease a little and the manuscript quality will probably improve.

Most of the manuscripts submitted by foreign authors had to be declined probably because of their authors underestimating Teknik Dergi publication policies and standards. Originality is another concern for the scientifically high quality manuscripts submitted by foreigners. The Board may sometimes be in doubt if the paper might have been published elsewhere. However, the “Statement of Originality” signed by the author(s) is expected to warn the authors about the ethical requirements of Teknik Dergi.

An important objective of the bilingual publication policy is to enlarge Teknik Dergi audience by reaching the international civil engineering community and thus to increase citation and the impact factor. Although a short term observation is not a reliable indication, the Board tends to interpret the minor improvement recently observed optimistically.

Besides its printed copy distribution, Teknik Dergi has also been published electronically for a considerable while. Realising the popularity and effectiveness of electronic publishing, the Board has recently decided to limit the printed copy distribution to a list of selected bodies including university libraries and civil engineering chairs in Turkey. All members of the Turkish Chamber of Civil Engineers will be notified about the publication of each issue and a link will be given, since Teknik Dergi is a free access publication.

With our best wishes…

Tuğrul Tankut
On behalf of the Editorial Board

Teknik Dergi, 2019 8913-8935, Paper 528

Residual Displacement Demand Evaluation from Spectral Displacement

Müberra ESER AYDEMİR[1]
Cem AYDEMİR[2]

ABSTRACT

In this study, residual displacement demands are investigated for SDOF systems with a period range of 0.1-3.0 s for near-field and far-field ground motions. The effects of stiffness degradation and post yield stiffness ratio in residual displacements are investigated. The modified-Clough model is used to represent structures that exhibit significant stiffness degradation when subjected to reverse cyclic loading. The elastoplastic model is used to represent non-degrading structures. For inelastic time history analyses, Newmark's step by step time integration method was adapted in an in-house computer program. Based on time history analyses, a new simple equation is proposed for residual displacement demand of a system as a function of structural period (T), ductility (μ), strain hardening ratio (α) and spectral displacement (S_d).

Keywords: Residual displacement, stiffness degradation, ductility demand, spectral displacement.

1. INTRODUCTION

Although it is preferable to design a structure that behaves elastically in the event of severe earthquake motions, current earthquake – resistant design provisions allow the nonlinear response of structures because of economic factors. Seismic design procedures aim at controlling earthquake damage to structural elements and many types of nonstructural elements by limiting lateral deformations on structures. Structural performance is usually estimated using peak deformation demands. However, the past earthquakes have shown that the excessive permanent lateral deformations at the end of the earthquake motion (i.e. residual displacement) of a system -in addition to peak demands- is one of the major parameters to determine whether the structural system can continue its function or the system should be strengthened/repaired or the system should be rebuilt. Besides, the necessity to

Note:
- This paper has been received on October 16, 2017 and accepted for publication by the Editorial Board on October 09, 2018.
- Discussions on this paper will be accepted by May 31, 2019.

• https://dx.doi.org/10.18400/tekderg.344597

1 İstanbul Aydın University, Dep. Of Civil Engineering, İstanbul, Turkey - muberraaydemir@aydin.edu.tr https://orcid.org/0000-0002-4609-4845

2 İstanbul Aydın University, Dep. Of Civil Engineering, İstanbul, Turkey - cemaydemir@aydin.edu.tr https://orcid.org/0000-0003-4531-5084

consider the residual displacements and residual drifts in seismic performance assessment is addressed in Vision 2000 (1995) and FEMA356 (2000) guidelines. Therefore, it is important to estimate residual structural displacement demands for the evaluation and rehabilitation of structures.

Residual displacement ratios have been the topic of several investigations so far. The first well-known studies on residual displacement were conducted by Riddell and Newmark (1979a, b) pointing out that the magnitude of residual displacements is strongly affected by the unloading– reloading rules of the hysteresis model. Mahin and Bertero investigated the dispersion of the residual displacements of SDOF systems assuming a peak-ductility for each SDOF system (1981). MacRae and Kawashima (1997) worked on SDOF systems with ductility demands of 2, 4 and 6 for 11 ground motions. They concluded that post-yield stiffness has an important effect on the residual displacement levels. Similarly, to these previous studies, Pampanin et. al. (2002) worked on residual displacement ratios for equivalent SDOF systems for 20 earthquake motions and three different hysteretic models. They have concluded that without considering residual deformations, the performance of systems cannot be compared to other systems that sustain residual deformations. Ruiz Garcia and Miranda conducted the most extensive researches on residual displacement ratios for both SDOF and multistory structures (2005; 2006a, b; 2008). They proposed simplified expressions to estimate mean residual displacement ratios of existing structures and also, they reported that the amplitude and heightwise distribution of residual drift demands depend on the frame mechanism, structural overstrength and hysteretic behavior. Hatzigeorgiou et.al. (2011) and Christidis et.al. (2013) conducted parametric studies on SDOF systems to derive empirical equations for maximum displacement from residual displacements. More recently, Liossatou and Fardis (2014) investigated the effects of hysteresis rules representing the cyclic degradation of stiffness and strength and the energy dissipation of typical RC structures on residual displacement ratios whereas D'Ambrisi and Mezzi (2015) proposed a method to evaluate the residuals of the response parameters of a reinforced concrete plane frame. In a very recent study conducted by Ruiz Garcia and Guerrero (2017), a new functional form to estimate mean residual displacement ratios for soft soil sites is presented.

As all of these previous studies mainly focus on the normalized residual displacement ratios, the main difference lies in the definition of these ratios. For the case of residual displacements, several normalization alternatives have been proposed by various researchers. Mahin and Bertero (1981) and Farrow and Kurama (2003) used yield displacement to normalize residual displacement and they called this ratio as the residual displacement ductility. MacRae and Kawashima (1997) used maximum possible residual displacement demand for normalization. Pampanin et.al. (2002), Ruiz Garcia (2004), Ruiz Garcia & Miranda (2005) and Borzi et.al. (2011) used the ratio of residual displacement to maximum inelastic displacement as the key parameter. Similarly, the ratio of residual displacement to elastic spectral displacement is used by Ruiz Garcia and Miranda (2005; 2006a, b; 2008); this ratio is called residual displacement ratio.

The objective of this study is to present the results of an investigation conducted to provide more information on the residual displacement for degrading and non-degrading structures when subjected to near-field and far-field earthquake ground motions. In particular, this study tried to: (1) investigate SDOF systems with a period range of 0.1-3.0 s and five levels of ductility (μ = 2, 3, 4, 5, 6); (2) focus on elastoplastic and stiffness degrading structures with

strain hardening ratios of α = -10%, -5%, -2%, 0, 2%, 5% and 10%; (3) use a set of near-field and far-field ground motions and (4) propose a new equation for residual displacement demands of SDOF systems as a function of spectral displacement (Sd), structural period (T), ductility ratio (μ) and post yield stiffness ratio (α).

2. ANALYSIS PROCEDURE

2.1. Hysteretic Behavior

Numerous hysteretic models have been proposed to represent the cyclic behavior of reinforced concrete structures. One of the most common hysteretic models used for reinforced concrete structures is Modified-Clough model which is the improved form of the original model proposed by Clough and Johnston that includes the effect of stiffness degradation. This model is based on the Clough model, and several studies have concluded that the Modified-Clough model is more accurate and capable of reproducing the behavior of properly designed reinforced concrete structures (Miranda and Ruiz Garcia, 2002). The influence of stiffness degradation on the seismic demands of structures has been the topic of several studies (Clough and Johnston, 1966; Rahnama and Krawinkler, 1993; Gupta and Krawinkler, 1998; Gupta and Kunnath, 1998; Borzi et.al.,2011). In 2009, to enhance the understanding of degradation and dynamic instability by developing practical suggestions, where possible, to account for nonlinear degrading response in the context of current seismic analysis procedure FEMA P440A guideline was prepared (FEMA, 2009). Another research conducted by Ayoub and Chenouda (2009) has focused on the development of response spectra plots for inelastic degrading structural systems subjected to seismic excitations and conclusions regarding the behavior and collapse potential of different structural systems are drawn. Figure 1 shows the Elastoplastic (EP) and Modified-Clough (MC) hysteretic models.

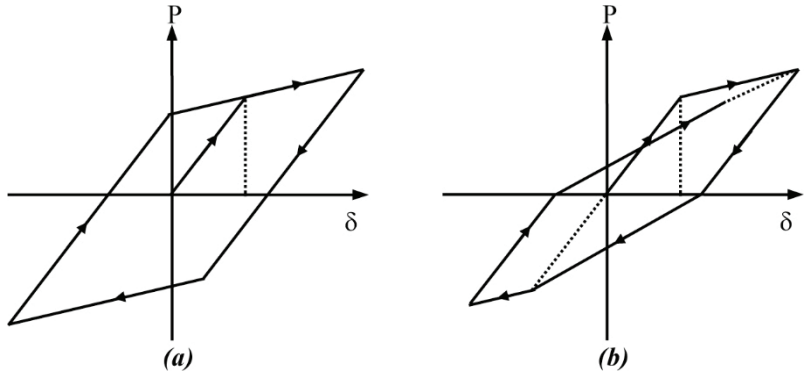

Fig. 1 - Load-deformation hysteretic models used in this study:
***(a)** Elastoplastic (EP); **(b)** Modified-Clough (MC)*

The post yield stiffness ratio, α is the ratio of the post-yield stiffness of a SDOF system to its elastic stiffness. An (α) value larger than zero implies hardening behavior and smaller than zero implies softening behavior. P-δ effect caused by gravity loads acting on the deformed configuration of the structure will always lead to a decrease in stiffness and effective strength

and an increase in lateral displacements. If the P-delta effect causes a negative post-yield stiffness in any story, it may affect significantly the interstory drift and may lead to incremental collapse if the structure has not sufficient strength. Therefore, if certain target ductility is required, more strength must be provided for the structural system. In the present study, post yield stiffness ratios of α = -10%, -5%, -2%, 0, 2%, 5% and 10% are considered, respectively, to study the strain hardening / softening effect on residual displacements.

2.2. Method of Analysis and Seismic Input

The present study focuses on residual displacement demands of SDOF systems with Elastoplastic (non-degrading) (EP) and Modified-Clough (degrading) (MC) hysteretic behavior with linear hardening or softening. The dynamic equation of motion of an SDOF system is given by Eq. (1)

$$m\ddot{u} + c\dot{u} + f_s(u) = -m\ddot{u}_g \tag{1}$$

where m is the mass, u is the relative displacement, c is the viscous damping coefficient, $\int_s(u)$ is the resisting force and $\ddot{u}_g$ is the acceleration of ground motion. Newmark's step by step time integration method is adapted in an in-house computer program for inelastic time history analyses. Time history analyses were carried out with the time step selected as the minimum of followings; original earthquake ground motion time step, 1/25 of structural period and 0.01 s.

Seismic excitation consists of real near-field and far-field earthquakes. A set of 70 near-field and 70 far-field acceleration time-histories are used in this study. The selection of near field and far field ground motions are based on the earthquakes given in ATC40 (1996) and ATC 63 (2007) documents. Details of selected ground motions are listed in Tables 1 and 2. Also, Figure 2 shows the magnitude- source distance- PGA relation for the far field and near field ground motions, respectively.

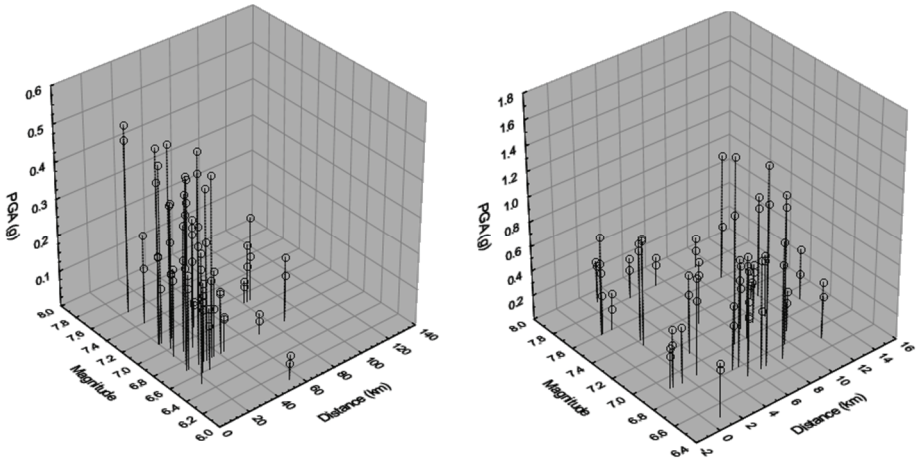

Fig. 2 - Magnitude- source distance- PGA relation for the used ground motions

These accelerograms are downloaded from the strong motion database of the Pacific Earthquake Engineering Research (PEER) Center (Last access 2017). Near-field seismic ground motions are usually characterized by intense velocity and displacement pulses; besides, forward directivity and permanent translation are generally the two main causes for the velocity pulses observed in near-field regions. Thus, the near-fault ground motion data set is evaluated in detail to distinguish records that contain pulse-like signal effects. The near-field ground motion set used for the presented study consists of 30 records with pulse signal and 40 records without pulse signal. The residual displacement demands are described separately for near-fault records that either do or do not contain pulse signals.

A total of 294000 analyses have been conducted for SDOF structures with period range of 0.1-3.0 s, five levels of ductility (μ = 2, 3, 4, 5, 6), 140 ground motions, seven strain hardening ratios (α = -10%, -5%, -2%, 0, 2%, 5%, 10%) and two types of hysteretic behavior (EP and MC).

3. RESULTS AND DISCUSSION

As mentioned before, for residual displacement demands, several normalization alternatives have been proposed by various researchers. For simplicity, it is generally appropriate to normalize the residual displacements (D_{res}) with respect to elastic spectral displacement (S_d) of a SDOF system subjected to same acceleration time history which is called residual displacement ratio and is expressed as follows:

$$D_s = \frac{D_{res}}{S_d} \tag{2}$$

Thus, the results of conducted statistical study have been presented in the terms of residual displacement demands (D_{res}) and residual displacement ratios (D_s), respectively. The effects of analysis variables on these parameters are given below.

3.1. Effect of Hysteretic Behavior

3.1.1. Effect of stiffness degradation

In Figure 3, variations of mean residual displacement demands (D_{res}) against ductility are shown for elastoplastic and Modified Clough hysteretic models with strain hardening ratio of 0%. The results are presented for far field ground motions set. It can be seen from the figure that; residual displacement demands of elastoplastic systems are almost always larger than degrading systems for all strain hardening ratios.

The variations of mean residual displacement ratios (D_s) for Elastoplastic and Modified Clough hysteretic models for far field ground motion sets shown in Figure 4. It can be seen from the figures that mean residual displacement ratios are greater for elastoplastic systems than degrading systems for all strain hardening ratios. For all cases, it is observed that residual displacement ratios remain nearly constant for T > 0.5 s. For T<0.5 s, there is tendency for residual displacement ratio to increase with the ductility demand.

Table 1 - Far field ground motions used in analyses

Earthquake	Station/No	M	Dist. (km)	Comp. 1	PGA (g)	PGV (cm/s)	Comp. 2	PGA (g)	PGV (cm/s)	Site class
Loma Prieta 18/10/89	Coyote Lake Dam/57217	7.1	21.8	CYC195	0.151	16.2	CYC285	0.484	39.7	C
Loma Prieta 18/10/89	Monterey City Hall/47377	7.1	44.8	MCH000	0.073	3.5	MCH090	0.063	5.8	C
Loma Prieta 18/10/89	SC Pacific Heights/58131	7.1	80.5	PHT270	0.061	12.8	PHT360	0.047	9.2	B
Northridge 17/01/94	Lake Hughes 9/127	6.7	28.9	L09000	0.165	8.4	L09090	0.217	10.1	C
Northridge 17/01/94	Wrightwood - Jackson Flat/23590	6.7	68.4	WWJ090	0.056	10	WWJ180	0.037	7	C
Northridge 17/01/94	Sandberg Bald Mtn/24644	6.7	43.4	SAN090	0.091	12.2	SAN180	0.098	8.9	C
Northridge 17/01/94	MT Wilson-Cit Sta./24399	6.7	36.1	MTW000	0.234	7.4	MTW090	0.134	5.8	C
Loma Prieta 18/10/89	Anderson Dam Downstream/1652	7.1	20	AND250	0.244	20.3	AND340	0.24	18.4	C
Northridge 17/01/94	Castaic Old Ridge/24278	6.7	25.4	ORR090	0.568	52.1	ORR360	0.514	52.2	C
Northridge 17/01/94	LA Century City North/24389	6.7	18.3	CCN090	0.256	21.1	CCN360	0.222	25.2	D
Cape Mendocino 1992	Rio Dell Overpass/89324	7	22.7	RIO270	0.39	43.9	RIO360	0.55	42.4	D
Loma Prieta 18/10/89	Golden Gate Bridge/1678	7.1	85.1	GGB270	0.233	38.1	GGB360	0.123	17.8	C
Northridge 17/01/94	Ucla Grounds/24688	6.7	16.8	UCL090	0.278	22	UCL360	0.474	22.2	C
Northridge 17/01/94	LA Univ. Hospital/24605	6.7	34.6	UNI005	0.493	31.1	UNI095	0.214	10.8	D
Landers 28/06/92	Yermo Fire Station/22074	7.4	26.3	YER270	0.245	51.5	YER360	0.152	29.7	D
Friuli, Italy-01, 1976	Tolmezzo/8012	6.5	16	TMZ000	0.35	22	TMZ270	0.31	30.8	C
Loma Prieta 18/10/89	Foster City - APEEL 1/58375	7.1	43.9	A01000	0.26	31.9	A01090	0.28	46.3	E
Loma Prieta 18/10/89	Hollister - South & Pine/47524	7.1	28.8	HSP000	0.371	62.4	HSP090	0.177	29.1	D
Northridge 17/01/94	Downey-Birchdale/90079	6.7	40.7	BIR090	0.165	12.1	BIR180	0.171	8.1	D
Northridge 17/01/94	LA-Centinela/90054	6.7	30.9	CEN155	0.465	19.3	CEN245	0.322	22.9	D
Imperial Valley 15/10/79	Delta/6605	6.9	32.7	DLT262	0.238	26	DLT352	0.351	33	D
Loma Prieta 18/10/89	APEEL 2- Redwood City/1002	7.1	47.9	A02043	0.274	53.6	A02133	0.22	34.3	E
Northridge 17/01/94	Montebello/90011	6.7	86.8	BLF206	0.179	9.4	BLF296	0.128	5.9	D
Superstition Hills 24/11/87	Salton Sea Wildlife Refuge/5062	6.6	27.1	WLF225	0.119	7.9	WLF315	0.167	18.3	D
Loma Prieta 18/10/89	Treasure Island/58117	7.1	82.9	TRI000	0.1	15.6	TRI090	0.159	32.8	E

Table 1 - Far field ground motions used in analyses (continue)

Earthquake	Station/No	M	Dist. (km)	Comp. 1	PGA (g)	PGV (cm/s)	Comp. 2	PGA (g)	PGV (cm/s)	Site class
Kocaeli 17/08/99	Ambarli/-	7.8	78.9	ATS000	0.249	40	ATS090	0.184	33.2	E
Morgan Hill 24/04/84	Appel 1 Redwood City/58375	6.1	54.1	A01040	0.046	3.4	A01310	0.068	3.9	E
Düzce 12/11/99	Ambarlı/-	7.3	193.3	ATS030	0.038	7.4	ATS300	0.025	7.1	E
Kobe 16/01/95	Kakogawa/0	6.9	26.4	KAK000	0.251	18.7	KAK090	0.345	27.6	D
Northridge 17/01/94	Beverly Hills – Mulhol/522	6.7	17.2	MUL009	0.42	58.9	MUL279	0.52	62.7	D
Kobe 16/01/95	Shin-Osaha/932	6.9	19.2	SHI000	0.24	37.8	SHI090	0.21	27.9	D
Loma Prieta 18/10/89	Capitola/47125	7.1	20.1	CAP000	0.53	35	CAP090	0.44	29.2	D
San Fernando 1971	LA - Hollywood Stor FF/326	6.6	22.8	PEL090	0.211	18.9	PEL180	0.171	14.9	D
Chi – Chi Taiwan 1999	HWA003/-	7.6	56.1	HWA003-N	0.14	19.1	HWA003-W	0.05	10.4	A
Chi – Chi Taiwan 1999	TCU045/1018	7.6	26	TCU045-E	0.47	50.05	TCU045-N	0.51	46.4	C

Table 2 - Near field ground motions used in analyses

Earthquake	Station/No	M	Dist. (km)	Comp. 1	PGA (g)	PGV (cm/s)	Comp. 2	PGA (g)	PGV (cm/s)	Site class	Pulse Type*
Imperial Valley 15/10/79	El Centro Array #6/230	6.9	1.35	E06140	0.45	67	E06230	0.45	113.5	D	P
Imperial Valley 15/10/79	El Centro Array #7/200	6.9	0.56	E07140	0.34	51.7	E07230	0.47	113.1	D	P
Irpinia, Italy 1980	Sturno/935	6.9	10.8	STU000	0.23	36.9	STU270	0.32	71.9	C	P
Superstition Hills-02 1987	Parachute Test Site/5051	6.5	0.95	PTS225	0.43	134.3	PTS315	0.38	53.1	D	P
Loma Prieta 18/10/89	Saratoga Aloha/58065	7.1	8.5	STG000	0.51	41.6	STG090	0.33	45.9	C	P
Imperial Valley 15/10/79	Chihuahua/6621	6.9	7.3	CHI012	0.27	24.9	CHI282	0.254	30.1	D	NP
Cape Mendocino 1992	Petrolia/89156	7	8.1	PET000	0.59	49.6	PET090	0.66	88.6	C	P
Landers 28/06/92	Lucerne/260	7.4	2.2	LCN260	0.73	133.5	LCN345	0.79	28.2	B	P
Loma Prieta 18/10/89	Gilroy Array #4/57382	7.1	14	G04000	0.417	38.8	G04090	0.212	37.9	D	NP

*P: Pulse, NP: No Pulse

Table 2 - Near field ground motions used in analyses (continue)

Earthquake	Station/No	M	Dist. (km)	Comp. 1	PGA (g)	PGV (cm/s)	Comp. 2	PGA (g)	PGV (cm/s)	Site class	Pulse Type*
Düzce 12/11/99	Bolu/Bolu	7.3	12	BOL000	0.728	56.4	BOL090	0.822	62.1	D	NP
Kocaeli 17/08/99	Gebze/-	7.8	10.9	GBZ000	0.244	50.3	GBZ270	0.137	29.7	B	NP
Düzce 12/11/99	Lamont 1061/1061	7.3	11.4	1061-E	0.107	11.5	1061-N	0.134	13.7	C	NP
Northridge 17/01/94	Rinaldi Receiving Station/77	6.7	6.5	RRS228	0.87	148.1	RRS318	0.47	74.8	D	P
Northridge 17/01/94	Sylmar Olive View/24514	6.7	5.3	SYL090	0.6	77.6	SYL360	0.84	129.6	C	P
Kocaeli 17/08/99	İzmit/-	7.8	7.2	IZT090	0.23	38.28	IZT180	0.17	22.33	B	P
Chi – Chi Taiwan 1999	TCU065/-	7.6	0.57	TCU065-E	0.79	125.3	TCU065-N	0.58	92.1	D	P
Loma Prieta 18/10/89	Gilroy Array #1/47379	7.1	9.64	G01000	0.41	31.6	G01090	0.47	33.9	B	NP
Chi – Chi Taiwan 1999	TCU102/-	7.6	1.49	TCU102-E	0.3	91.67	TCU102-N	0.17	66.4	C	P
Düzce 12/11/99	Düzce/-	7.3	6.58	DZC180	0.4	71.12	DZC270	0.51	84.2	D	P
Gazli, USSR, 1976	Karakyr/9201	6.8	5.46	GAZ000	0.7	66.2	GAZ090	0.86	67.7	D	NP
Imperial Valley 15/10/79	Bonds Corner/5054	6.9	2.66	BCR140	0.6	46.7	BCR230	0.78	44.9	D	NP
Nahanni, Canada, 1985	Site 1/6097	6.8	9.6	S1010	1.11	43.9	S1280	1.2	40.6	C	NP
Nahanni, Canada, 1985	Site 2/6098	6.8	4.93	S2240	0.52	29.6	S2330	0.36	31.9	C	NP
Loma Prieta 18/10/89	Bran/13	7.1	10.72	BRN000	0.46	51.4	BRN090	0.5	44.5	C	NP
Loma Prieta 18/10/89	Corralitos/57007	7.1	3.85	CLS000	0.64	56	CLS090	0.48	47.5	C	NP
Cape Mendocino 1992	Cape Mendocino/89005	7	6.96	CPM000	1.49	124.6	CPM090	1.04	42.5	C	NP
Northridge 17/01/94	Sepulveda VA/637	6.7	8.44	SPV270	0.75	77.6	SPV360	0.93	76.3	C	NP
Northridge 17/01/94	Saticoy/90003	6.7	12.09	STC090	0.34	31.47	STC180	0.46	60.1	D	NP
Kocaeli 17/08/99	Yarımca/-	7.8	4.83	YPT060	0.23	69.7	YPT150	0.32	71.9	D	NP
Chi – Chi Taiwan 1999	TCU067/-	7.6	0.62	TCU067-E	0.5	92.02	TCU067-N	0.32	51.3	C	NP
Chi – Chi Taiwan 1999	TCU084/-	7.6	11.48	TCU084-E	1.01	128.8	TCU084-N	0.43	48.1	C	NP
Denali, Alaska, 2002	TAPS Pump Sta. #10/Ps10	7.9	2.74	PS10-047	0.33	115.7	PS10-317	0.3	65.9	D	NP
Northridge 17/01/94	Pacoima Dam (upper left)/24207	6.7	7.01	PUL104	1.58	55.7	PUL194	1.29	104	A	P
Tabas, Iran, 1978	Tabas/9101	7.35	2.05	TAB-T1	0.86	123.5	TAB-L1	0.85	99.1	B	NP
Imperial Valley 15/10/79	Aeropuerto Mexicali/6616	6.9	0.34	AEP045	0.33	42.8	AEP315	0.26	24.8	D	P

*P: Pulse, NP: No Pulse

3.1.2. Effect of post yield stiffness ratio

In Figure 5, variations of mean residual displacement demands (D_{res}) against strain hardening ratio are shown for elastoplastic (left) and Modified Clough (right) hysteretic models. The results are presented for a system with ductility demand of 4.

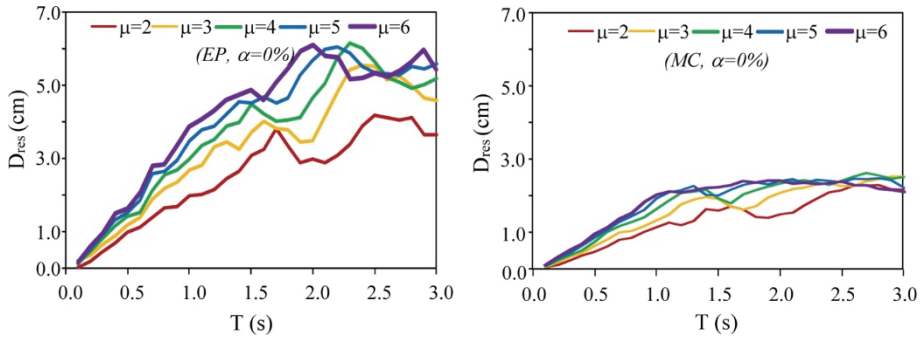

Fig. 3 - Variations of mean residual displacements against ductility for EP (left) and MC (right) behavior using far field ground motions for 0% hardening ratio

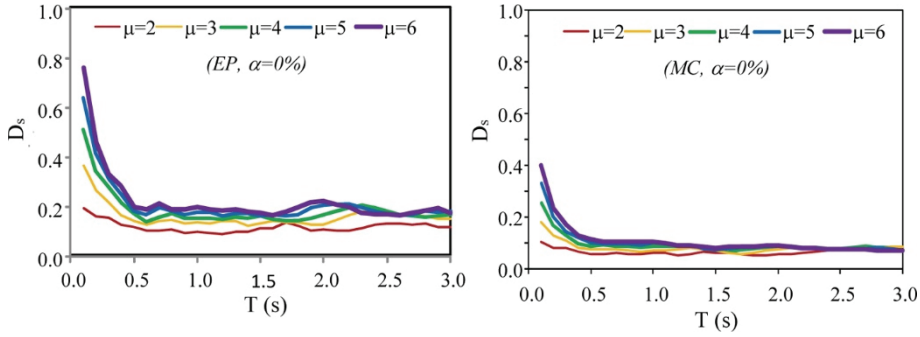

Fig. 4 - Variations of mean residual displacement ratio against ductility for EP (left) and MC (right) behavior using far field ground motions for 0% hardening ratio

The top and bottom graphs in Figure 5 represent the results for far field ground motions and near field ground motions, respectively. It can be seen from the figure that, strain hardening / softening has a significant effect on seismic response and residual displacement demands. As the post yield stiffness ratio varies from positive to negative, residual displacement demands increase severely. The increase rate of residual displacement demand is 7-10 times for elastoplastic systems whereas the corresponding value is 3-4 times for degrading systems.

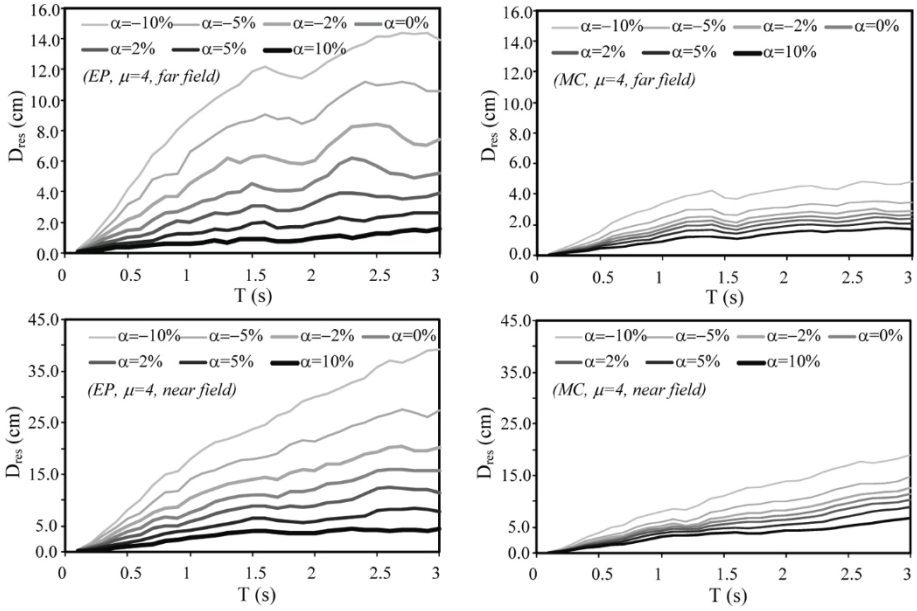

Fig. 5 - Variations of mean residual displacements against strain hardening ratio for EP (left) and MC (right) behavior using far field (upper) and near field ground motions (lower).

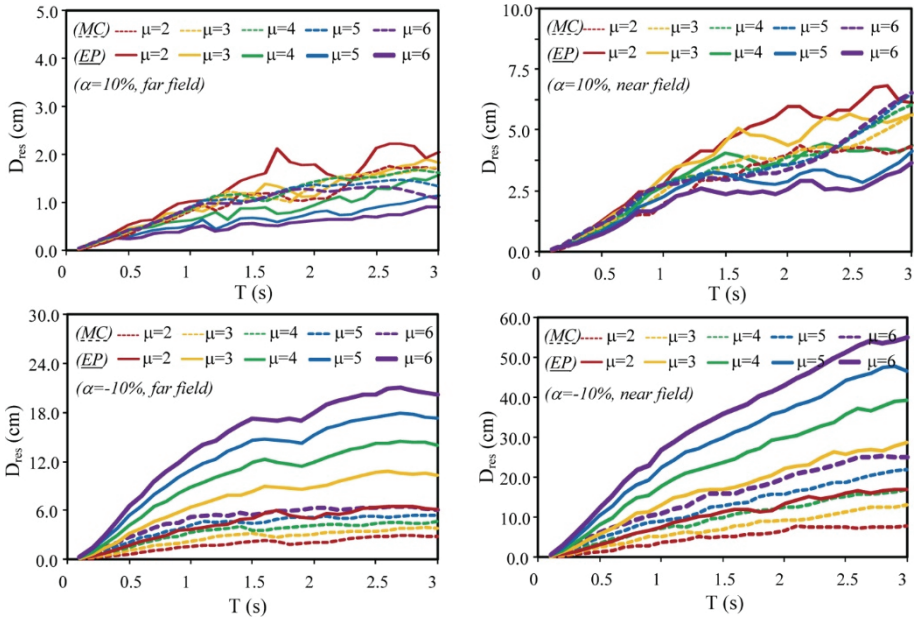

Fig. 6 - Variations of mean residual displacements for EP (solid line) and MC (dashed line) behavior using far field (left) and near field ground motions (right).

In Figure 6, variations of mean residual displacement demands (D_{res}) with hysteretic model are shown together. The results are presented for two different strain hardening ratios. For negative post yield stiffness ratio, in other words strain softening case, residual displacement demands increase as the ductility demands increase. Besides, elastoplastic residual displacement demands are always greater than the corresponding ones of degrading model. But, as the post yield stiffness ratio is positive –strain hardening case– the relation between the residual displacement demand and ductility changes significantly. The minimum residual displacement demands occur when the ductility demand is the maximum for the positive post yield stiffness ratio as can be seen in top graphs in Figure 6.

In Figure 7, variations of mean residual displacement ratios (D_s) against strain hardening ratio is shown for elastoplastic and degrading hysteretic models. The results are presented for a system with ductility demand of 4. The top graphs represent the results of far field ground motion set whereas the bottom graphs correspond to the results of near field ground motion set. It can be seen from the figure that, as the post yield stiffness ratio varies from positive to negative, mean residual displacement ratios increase severely. Although the residual displacement ratio variation is very close to each other for stiffness degrading systems, there is an evident difference between the residual displacement ratios of elastoplastic systems.

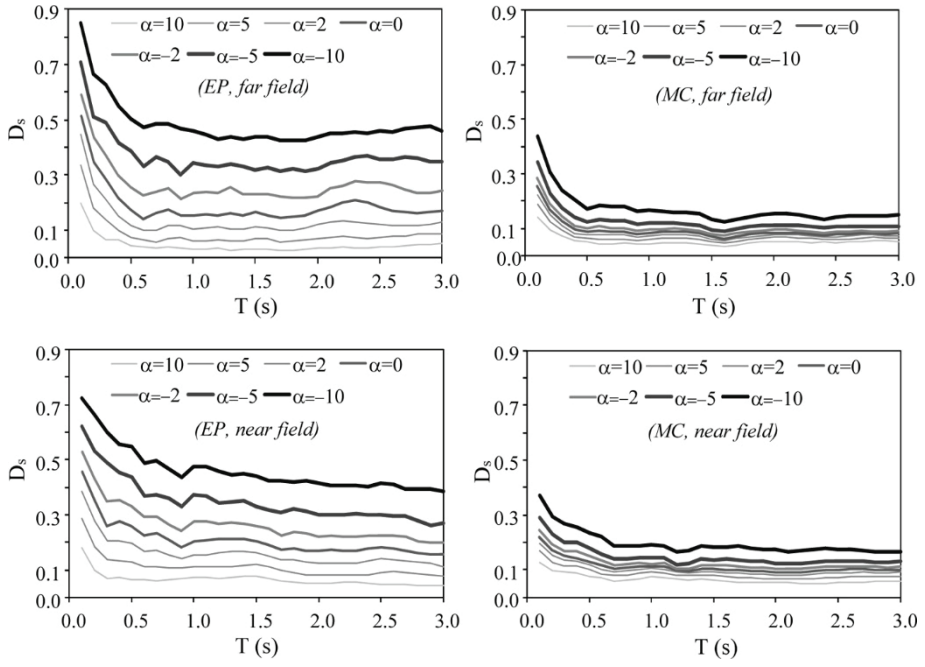

Fig. 7 - Variations of mean residual displacement ratio against strain hardening ratio for EP (left) and MC (right) behavior using far field (upper) and near field ground motions (lower).

3.2. Effect of Ground Motions

3.2.1. Effect of fault distance

The effects of near and far field data on residual displacement demands (D_{res}) are shown in Figure 8 for elastoplastic and Modified Clough hysteretic models for different values of post yield stiffness ratio. The solid lines represent the results for far field ground motions whereas the dashed lines show the results for near field ground motions. It can be seen from the figures that; residual displacement demands for near field ground motions are greater than the ones for far field ground motions. This condition is almost always valid for both hysteretic models and all post yield stiffness ratios.

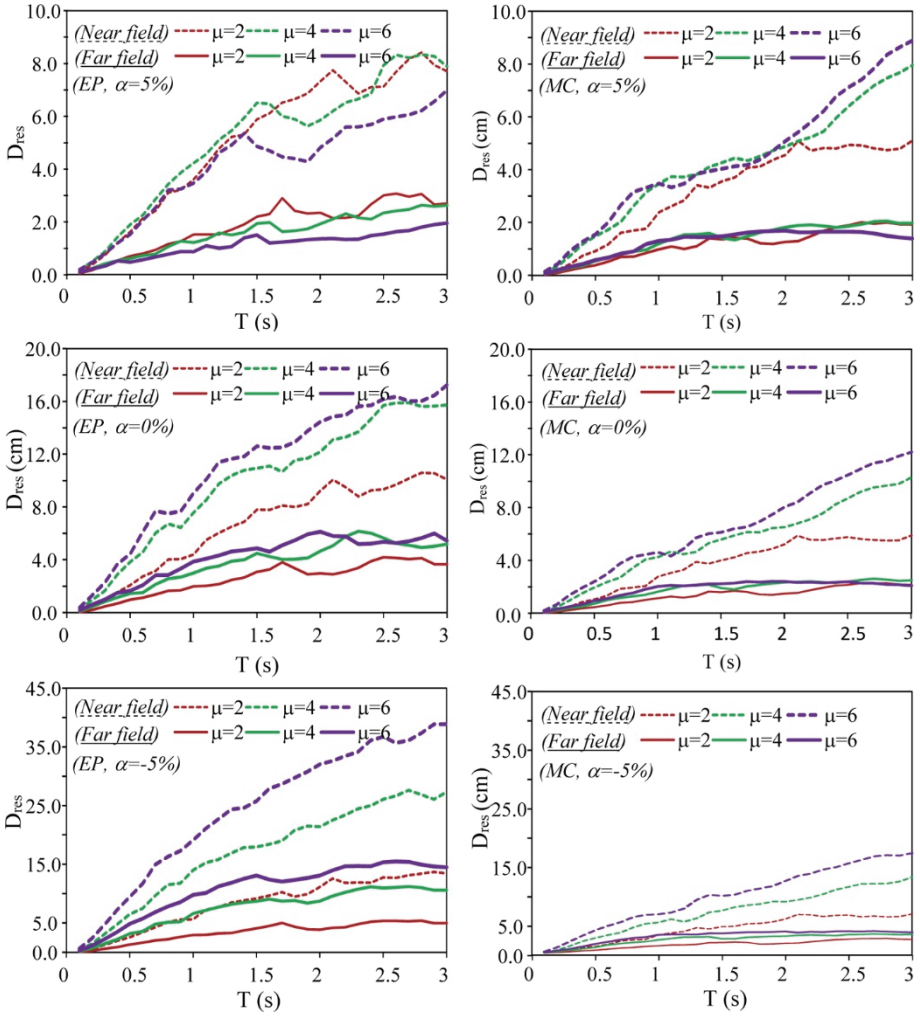

Fig. 8 - Variations of mean residual displacements for EP (left) and MC (right) behavior using far field (solid) and near field ground motions (dashed)

Figure 9 shows the effects of near and far field data on residual displacement ratios (D_s). Results are presented for elastoplastic and Modified Clough hysteretic models and different values of post yield stiffness ratio. The solid lines represent the results for far field ground motions whereas the dashed lines show the results for near field ground motions. It is seen from the figures that mean residual displacement ratios of near and far field ground motions are quite similar to each other within the period range covered and remain nearly constant especially for T> 0.5 s. This condition is almost always valid for both hysteretic models and all post yield stiffness ratios.

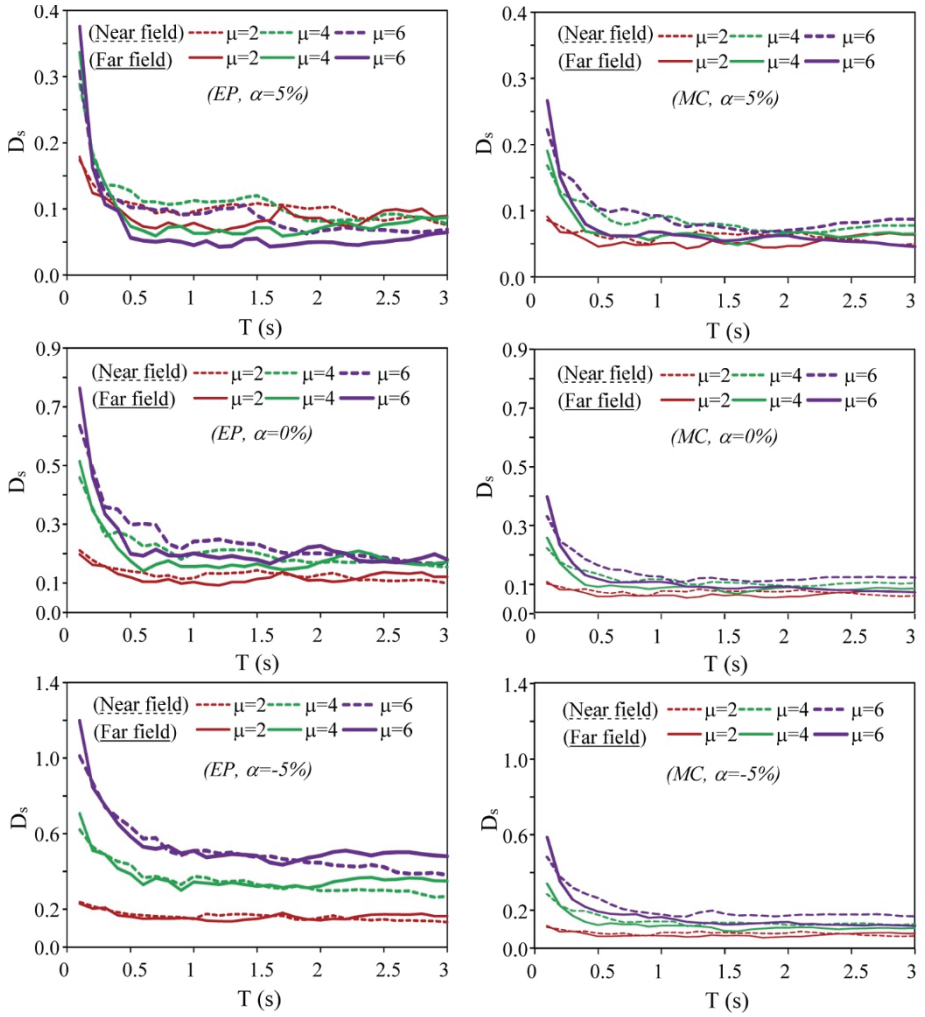

Fig. 9 - Variations of residual displacement ratios for EP (left) and MC (right) behavior using far field (solid) and near field ground motions (dashed)

3.2.2. Effect of pulse like features

The effect of pulse like features for near field earthquakes on residual displacement demands is also investigated. In Figures 10 and 11, variations of mean residual displacement demands (D_{res}) for pulse and no pulse type records are presented individually considering two hysteretic models and strain hardening ratios of 5% and 0%. As it is seen from the figures, pulse like features have an obvious effect on residual displacement demands for both hysteretic models and strain hardening ratios. Although the same behavior is valid for other strain hardening ratios, they are not included in the figures for the sake of clarity.

The effect of pulse like features for near field earthquakes on mean residual displacement ratio is also investigated. In Figures 12 and 13, variations of mean residual displacement ratios (D_s) for pulse and no pulse type records are presented.

It can be concluded from the figures that, the effects of pulse like features on mean residual displacement ratios are not as obvious as on residual displacement demands. This behavior is valid for other strain hardening ratios but they are not included in the figures for the sake of clarity.

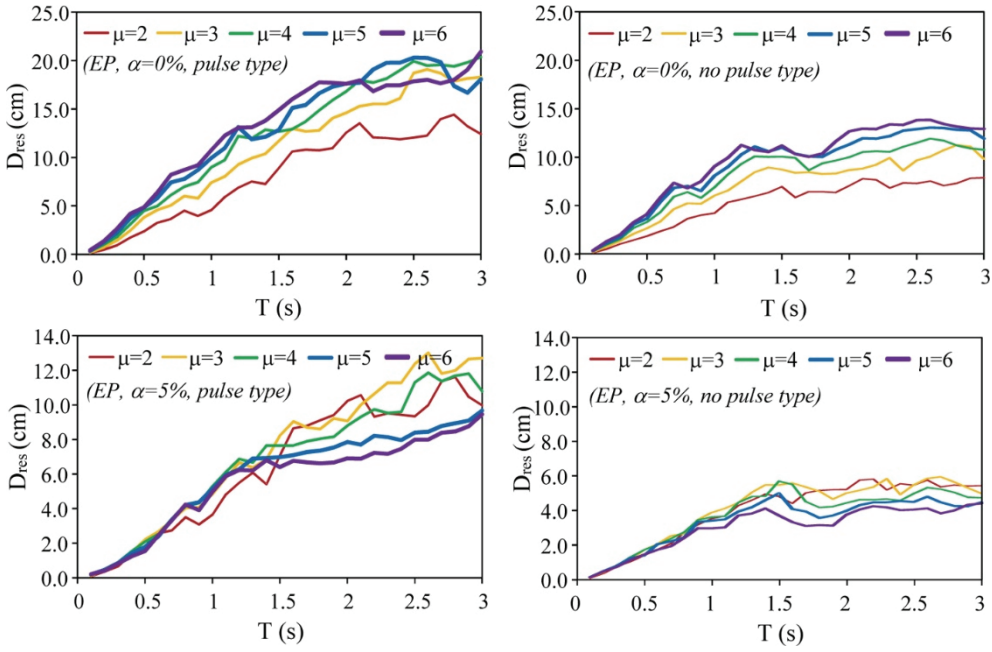

Fig. 10 - Variations of mean residual displacements for EP behavior using pulse type (left) and no pulse type ground motions (right). (α = 0% (upper), α = 5% (lower))

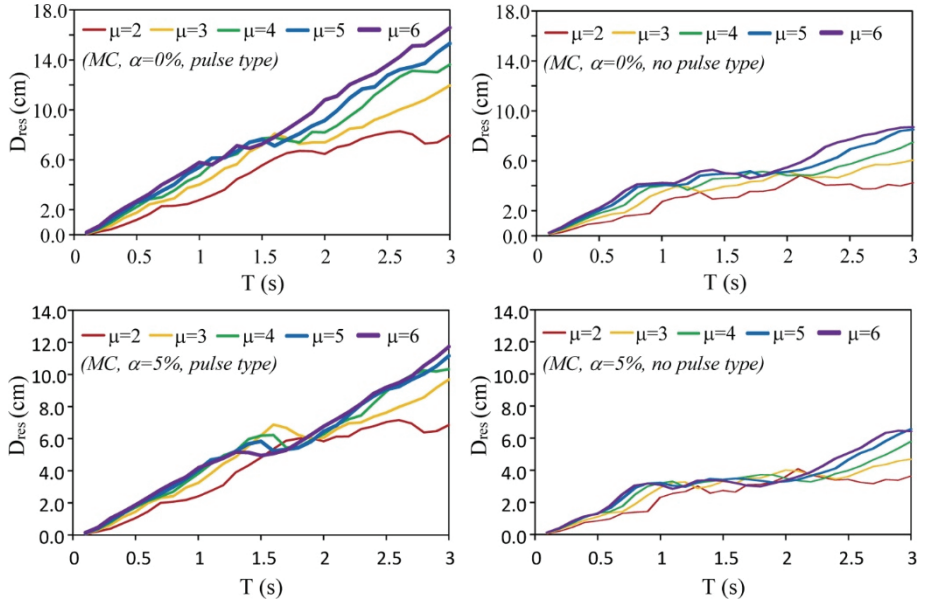

Fig. 11 - Variations of mean residual displacements for MC behavior using pulse type (left) and no pulse type ground motions (right). (α = 0% (upper), α = 5% (lower))

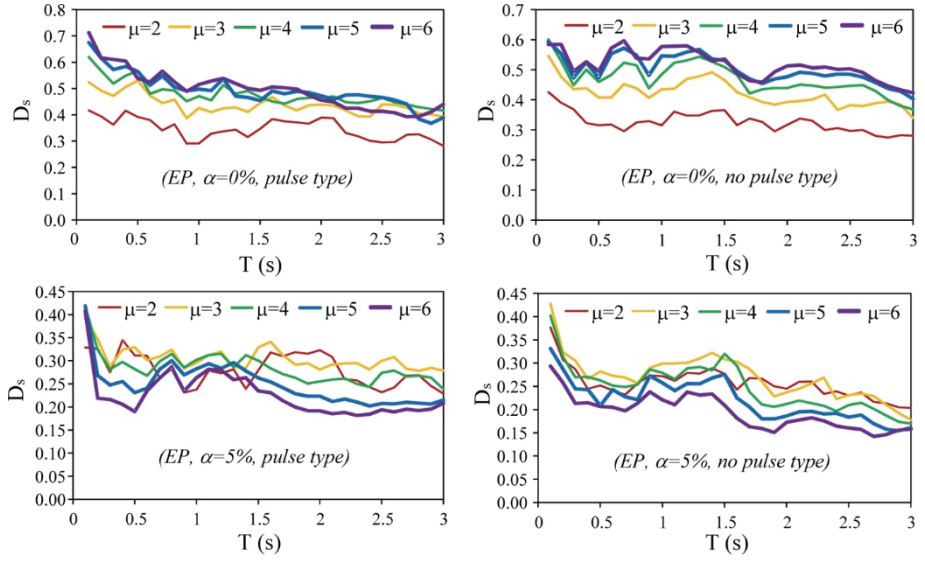

Fig. 12 - Variations of mean residual displacement ratios for EP behavior using pulse type (left) and no pulse type ground motions (right). (α = 0% (upper), α = 5% (lower))

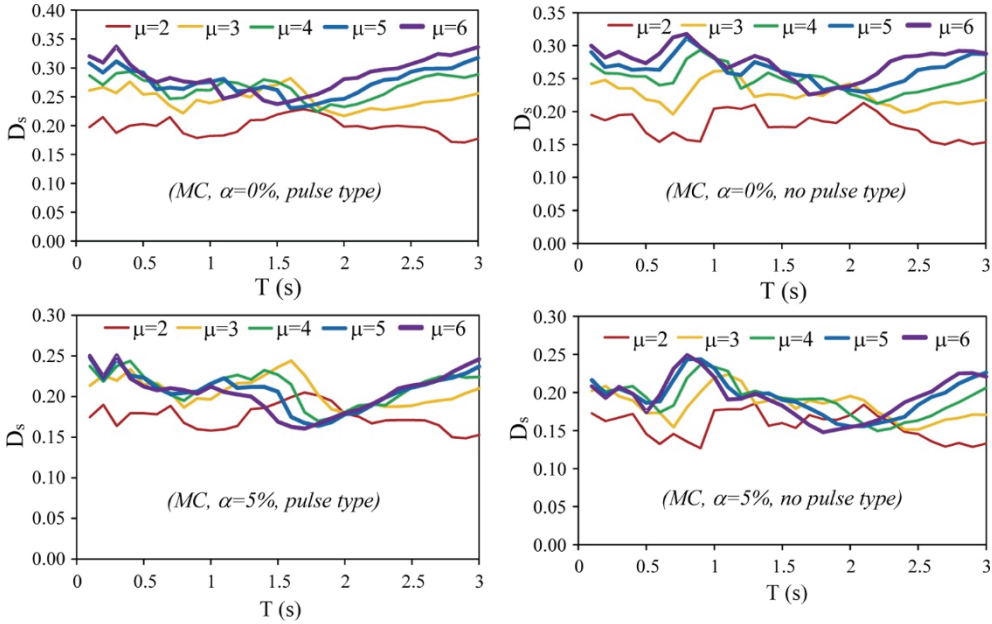

Fig. 13 - Variations of mean residual displacement ratios for MC behavior using pulse type (left) and no pulse type ground motions (right). (α = 0% (upper), α = 5% (lower))

4. SIMPLIFIED EQUATION TO ESTIMATE RESIDUAL DISPLACEMENTS

A complete nonlinear regression analysis is carried out on the basis of the data obtained by the procedure described above. Correlations of structural variables on residual displacements are presented in Table 3. As it is seen from the matrix, the most effective parameters on residual displacement are spectral displacement and post yield stiffness ratio. Moreover, the correlation between spectral displacement and structural period is 0.7, a relatively high value as expected. Thus, a simplified equation to predict residual displacement would include these parameters as variables.

Table 3 - Correlation matrix of structural variables on mean residual displacement values

	Ductility ratio (μ)	Period (T)	Post yield stiffness ratio (α)	Spectral displacement (S_d)	Residual displacement (D_{res})
μ	1.00				
T	0.00	1.00			
α	0.00	0.00	1.00		
S_d	0.00	*0.70*	0.00	1.00	
D_{res}	*0.22*	*0.42*	*-0.55*	*0.61*	1.00

Using the Levenberg-Marquardt method (More, 1977) in the regression module of STATISTICA (1995), nonlinear regression analyses were conducted to derive simplified expressions for estimating mean residual displacements for elastoplastic and stiffness degrading models, respectively. The resulting regression formula is appropriately simplified and expressed as;

$$D_{res} = \beta \cdot S_d \tag{4}$$

where β (=D_s) is given by

$$\beta = (a + b\mu + c\alpha + d\mu T + e\mu\alpha + f\mu\alpha^2) \tag{5}$$

and μ is ductility, T is period and α is post yield stiffness ratio. Although the expression of β coefficient is proposed to be a quadratic surface equation, as given in Equation 5, some terms which are considered to be insignificant are dropped. It is also worth noting that, since the effects of pulse like features on mean residual displacement ratios (D_s) are not appreciable, the coefficient of the proposed equation for near field case is obtained for all near field record data. The coefficients "a – f" are summarized in Table 4 for considered hysteretic models.

Table 4 - Parameter Summary for Eq. (4)

Model/ Record Set	Coefficients of quadratic surface						Correlation Coefficient, R
	a	b	c	d	e	f	
EP / Far field	0.158	0.062	0.0161	0.0036	-0.0177	0.00048	0.99
MC / Far field	0.123	0.022	0.0044	-0.0024	-0.0043	0.00015	0.98
EP / Near field	0.169	0.104	0.016	-0.0173	-0.0156	0.00040	0.99
MC / Near field	0.092	0.0417	0.0068	-0.0021	-0.0055	0.00015	0.99
EP / Far+Near field	0.167	0.0978	0.016	-0.0144	-0.0159	0.00041	0.99
MC / Far+Near field	0.096	0.0374	0.0065	-0.0013	-0.0054	0.00015	0.99
EP + MC/ Far field	0.140	0.0422	0.0102	0.00056	-0.0110	0.00032	0.80
EP + MC/ Near field	0.130	0.07297	0.0114	-0.0097	-0.0106	0.00028	0.87
All data	0.132	0.0676	0.0112	-0.0078	-0.0106	0.00028	0.88

It should be remembered that the proposed equation is valid for inelastic structures (i.e. $\mu \geq 2$) since there is no residual displacement for elastic structures.

Figure 14 shows the fitness of the regressed function of the mean residual displacements for elastoplastic and stiffness degrading models for both near field and far field records, all ductility values and strain hardening ratios. In Figure 14, Elastoplastic and Modified Clough hysteretic models are presented on the left and right, respectively. The vertical axis shows the calculated D_{res} values whereas the horizontal axis shows the corresponding values obtained with proposed equation Eq. (4).

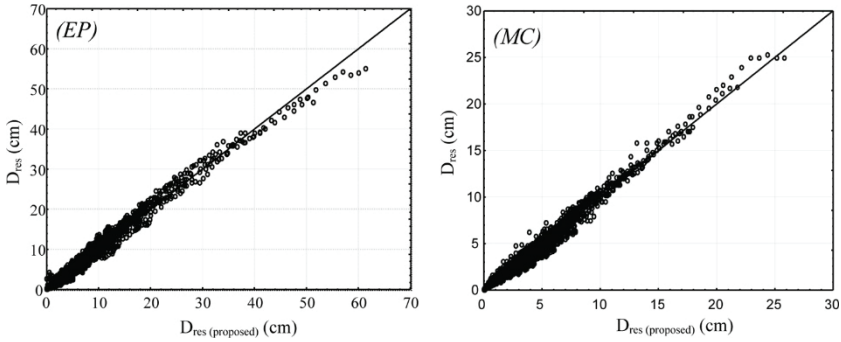

Fig. 14 - Comparison of calculated residual displacements with corresponding values obtained with proposed equation (Eq.4)

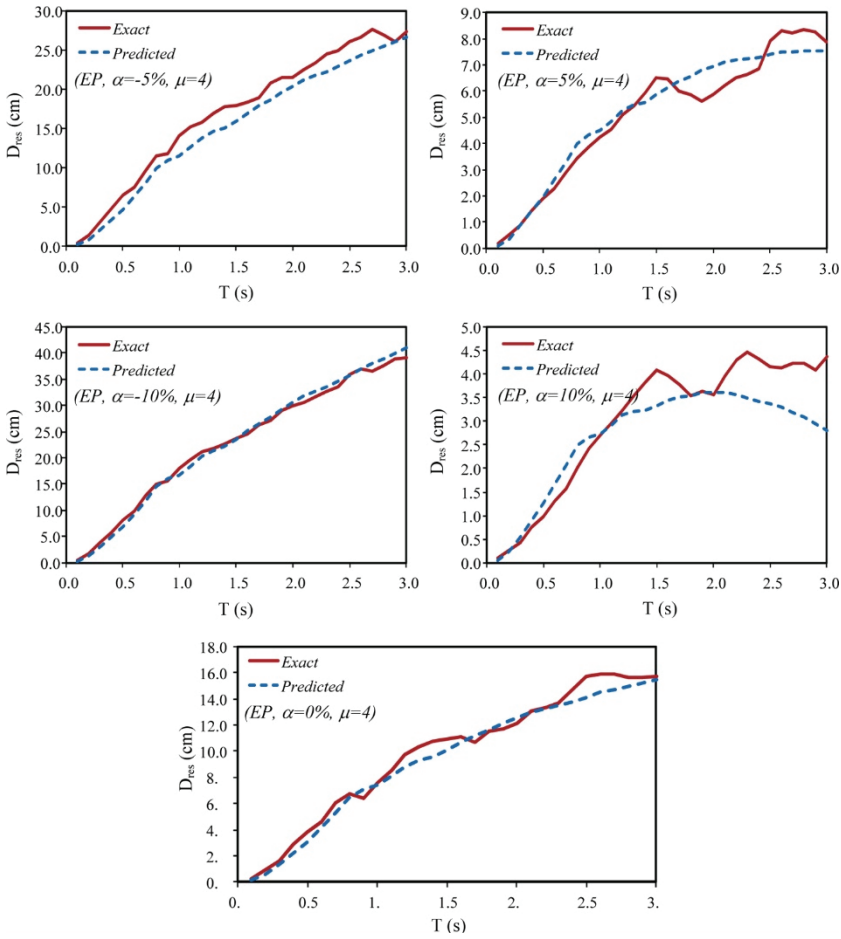

Fig. 15 - Comparison of exact (non-linear dynamic analysis) residual displacements (solid line) to those computed with Eq. (4) (dashed line).

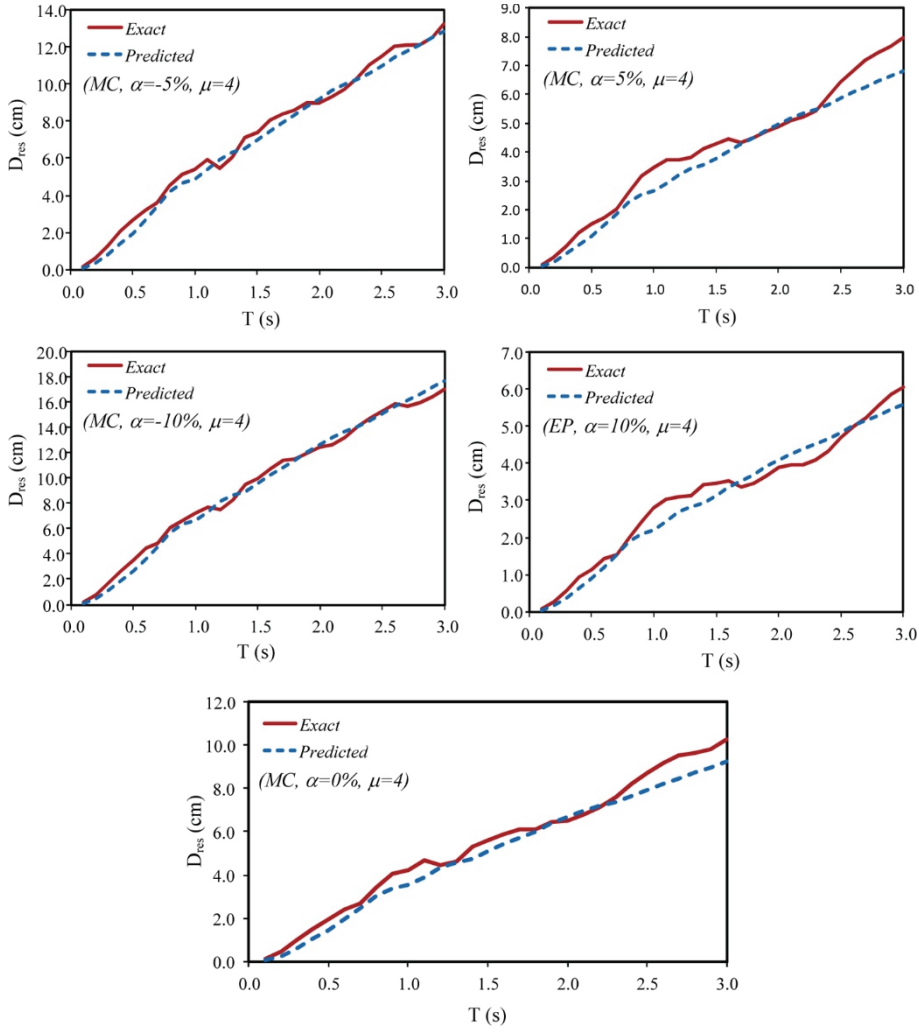

Fig. 16 - Comparison of exact (non-linear dynamic analysis) residual displacements (solid line) to those computed with Eq. (4) (dashed line).

Figures 15 and 16 demonstrate the fitness of the proposed function for the mean residual displacements for elastoplastic (EP) and Modified-Clough (MC) models, respectively. In these figures, the dashed line represents the values obtained from the proposed function (Eq.4) and the solid line represents the actual mean values of residual displacements obtained from non-linear dynamic analyses.

The comparison of proposed equation with existing residual displacement estimation equations is also completed. A very common measure of "goodness of fit" given by Eq. (6) is used for the comparison of proposed equation and the equation proposed by Ruiz Garcia

and Miranda (2006c). The standard error values calculated for the cases considered are reported in Table 5. From these measures, it can be concluded that the proposed equation to estimate residual displacements provide good results.

$$SE_{of\ prediction} = \sqrt{\left\{ \frac{\sum (x_{exact} - x_{predicted})^2}{n} \right\}} \tag{6}$$

Table 2 - Computed Measures of "goodness of fit" for Eq. (4)

Equation	Standard Error, SE
Proposed eq.	1.15
Ruiz Garcia and Miranda (2006c)	6.22

5. CONCLUSIONS

In this study, residual displacement demands are investigated for SDOF systems with degrading and non-degrading behavior for a period range of 0.1-3.0 s considering far-field and near-field effects. For this purpose, the modified-Clough model is used to represent structures that exhibit significant stiffness degradation and the elastoplastic model is used to represent non-degrading structures. The effects of negative strain hardening on the displacement demand of structures are also investigated. A new equation is proposed for mean residual displacement demand of SDOF systems as a function of structural period (T), ductility ratio (μ), strain hardening ratio (α) and spectral displacement (S_d). The following conclusions can be drawn from the results of this study.

- Residual displacement demands are larger for elastoplastic systems than degrading systems for all post yield stiffness ratios, under both far-field and near-field ground motion records. Besides, as the post yield stiffness ratio varies from positive to negative, the residual displacement variation presents a reverse behavior according to varying ductility demands. This is partially in agreement with earlier findings by other researchers such as Riddell and Newmark (1979a) and MacRae and Kawashima (1997).
- Residual displacement demands are found to be much greater for near field ground motion set rather than far field ground motions set. This statement is also in consistent with the results of study conducted by Farrow and Kurama (2003).
- Residual displacement ratios of near and far field ground motions are quite similar to each other for whole period range and remain nearly constant especially from the period point of 0.5 s.
- Pulse like features of near field earthquakes have an obvious effect on residual displacement demands for both hysteretic models and strain hardening ratios. However, the effects of pulse like features on mean residual displacement ratios are not as obvious

as on residual displacement demands because of the normalization using spectral displacement.

- As the post yield stiffness ratio varies from positive to negative, residual displacement demands increase drastically. The reason lies in the fact that, for systems with negative post-elastic stifnesses that the deformation is predominantly in one direction whereas for systems with positive post-elastic stifnesses the deformation is about the zero displacement position. The rate of increase is greater for elastoplastic systems than degrading systems.
- Similarly, to residual displacements, mean residual displacement ratios (D_s) are greater for elastoplastic case rather than Modified Clough model for all strain hardening ratios and both ground motion sets. As the post yield stiffness ratio decreases, mean residual displacement ratios increase explicitly.
- A new equation (Eq. (4)) is proposed to represent the mean residual displacement demands for considered records, ductility values, strain hardening ratios and structural periods as a function of structural period (T), ductility ratio (μ), strain hardening ratio (α) and spectral displacement (S_d). The proposed simplified expression provide a good approximation of mean residual displacement ratios of SDOF systems having non-degrading or degrading behavior; with this simple equation, it is possible to obtain probable residual displacement demand of a system due to structural period, ductility and spectral displacement for any earthquake.

References

[1] Applied Technology Council (1996). ATC 40: The Seismic Evaluation and Retrofit of Concrete Buildings. 2 volumes. Redwood City, California.

[2] Applied Technology Council (2007). ATC 63: Recommended Methodology for Quantification of Building System Performance and Response Parameters - 75% Interim Draft Report, Redwood City, California.

[3] Ayoub A, Chenouda M (2009). Response spectra of degrading structural systems. Engineering Structures, 31, 1393-1402.

[4] Borzi B, Calvi GM, Elnashai AS, Faccioli E, Bommer JJ (2011). Inelastic spectra for displacement-based seismic design. Soil Dynamics and Earthquake Engineering, 21(1), 47–61.

[5] Christidis AA, Dimitroudi EG, Hatzigeorgiou GD, Beskos DE (2013). Maximum seismic displacements evaluation of steel frames from their post-earthquake residual deformation. Bulletin of Earthquake Engineering, 11(6) : 2233–2248.

[6] Clough RW, Johnston SB (1966). Effect of stiffness degradation on earthquake ductility requirements. In: Proc of the Japan Earthquake Engineering Symposium, Tokyo, Japan, 227–232.

[7] D'Ambrisi A, Mezzi M (2015). Design value estimate of the residuals of the seismic response parameters of RC frames. Bulletin of Earthquake Engineering, 13(5), 1491-1511.

[8] Farrow KT, Kurama YT (2003). SDOF demand index relationships for performance-based design. Earthquake Spectra, 19(4):799–838.

[9] Federal Emergency Management Agency (2000). NEHRP guidelines for the seismic rehabilitation of buildings. ReportFEMA356:, Washington, DC.

[10] Federal Emergency Management Agency (2009), Effects of Strength and Stiffness Degradation on Seismic Response FEMA P440A, Washington, DC.

[11] Gupta A, Krawinkler H (1998). Effect of stiffness degradation on deformation demands for SDOF and MDOF structures. Proc., 6th Natl. Conf. on Earthquake Engineering, Earthquake Engineering Research Institute, Oakland, California.

[12] Gupta B, Kunnath SK (1998). Effect of hysteretic model parameters on inelastic seismic demands. Proc., 6th Natl. Conf. on Earthquake Engineering, Earthquake Engineering Research Institute, Oakland, California.

[13] Hatzigeorgiou GD, Papagiannopoulos GA, Beskos DE (2011). Evaluation of maximum seismic displacements of SDOF systems from their residual deformation. Engineering Structures, 33 : 3422–3431.

[14] Liossatou E, Fardis MN (2014). Residual displacements of RC structures as SDOF systems. Earthquake Engineering & Structural Dynamics, doi: 10.1002/eqe.2483.

[15] MacRae GA, Kawashima K (1997). Post-earthquake residual displacements of bilinear oscillators. Earthquake Engineering & Structural Dynamics, 26(7):701–716.

[16] Mahin SA, Bertero VV (1981). An evaluation of inelastic seismic design spectra. Journal of The Structural Division, ASCE, 107(9):1777–1795.

[17] Miranda E, Ruiz-Garcia J (2002). Influence of stiffness degradation on strength demands of structures built on soft soil sites, Engineering Structures, 24:(10), 1271-1281.

[18] More JJ (1977). Levenberg – Marquardt algorithm: implementation and theory. Conference on numerical analysis, Dundee, UK.

[19] Pacific Earthquake Engineering Research Center. PEER Strong motion database. http://peer.berkeley.edu/smcat. Last access: 2017

[20] Pampanin S, Christopoulos C, Priestley MJN (2002). Residual deformations in the performance-based seismic assessment of frame structures, No. ROSE-2002/02. Technical report, European School for Advanced Studies in Reduction of Seismic Risk, University of Pavia, Italy.

[21] Rahnama M, Krawinkler H (1993). Effects of soft soil and hysteresis model on seismic demands. Rep. No. 108, John A. Blume Earthquake Engineering Center, Stanford Univ., Stanford, California.

[22] Riddell R, Newmark NM (1979a). Statistical analysis of the response of nonlinear systems subjected to earthquakes. Research Report 468. Un. of Illinois at Urbana-Champaign, Urbana, ILL, 291pp.

[23] Riddell R, Newmark NM (1979b). Force-deformation models for nonlinear analysis. Journal of Structural Division, ASCE, 105(12):2773–2778.

[24] Ruiz-Garcia J (2004). Performance-based assessment of existing structures accounting for residual displacements. Dissertation, Stanford University, California.

[25] Ruiz-Garcia J, Miranda E (2005). Performance-based assessment of existing structures accounting for residual displacements, No. 153. Technical report, The John A. Blume Earthquake Engineering Center, Stanford University, California.

[26] Ruiz-Garcia J, Miranda E (2006a). Evaluation of residual drift demands in regular multistorey frames for performance-based seismic assessment. Earthquake Engineering & Structural Dynamics, 35(13):679–694.

[27] Ruiz-Garcia J, Miranda E (2006b). Residual displacement ratios of SDOF systems subjected to near-fault ground motions. Proceedings of the 8th. US National Conference on Earthquake Engineering, EERI, Paper No. 380, San Francisco, California.

[28] Ruiz-Garcia J, Miranda E (2006c). Residual displacement ratios for assessment of existing structures. Earthquake Engineering & Structural Dynamics, 35:315–336.

[29] Ruiz-Garcia J, Miranda E (2008). Probabilistic seismic assessment of residual drift demands in existing buildings. In The 14th World Conference on Earthquake Engineering, Beijing, China.

[30] Ruiz-Garcia J, Guerrero H (2017). Estimation of residual displacement ratios for simple structures built on soft soil sites. Soil Dynamics & Earthquake Engineering, 100: 555-558.

[31] SEAOC (1995). Vision 2000: Performance based seismic engineering of buildings, Volume I. Technical report, Structural Engineers Association of California, Sacramento, California.

[32] StatSoft Inc (1995). STATISTICA V.12.0 for Windows. Tulsa, OK, USA.

Teknik Dergi, 2019 8937-8959, Paper 529

Cost and Time Management Efficiency Assessment for Large Road Projects Using Data Envelopment Analysis

Changiz AHBAB[1]
Sahand DANESHVAR[2]
Tahir ÇELIK[3]

ABSTRACT

Upon the completion of national road projects, their cost and time deviations are often reported. These deviations from the projected values are a result of complications in the time and cost management of such projects. Controlling the cost and time overrun of projects is important for successful implementation and efficient project management. However, few studies have attempted to measure the project cost and time management efficiency in civil engineering. Thus, this issue requires further investigation. In this study, large road projects that had poor cost and time management were selected. The chosen projects were configured as Decision Making Units (DMUs) in a Data Envelopment Analysis (DEA). It is a non-parametric modern mathematical tool for measuring relative managerial performance and determining efficient DMUs. The cost and time management efficiency of the projects was calculated using this tool, and the resulting values were ordered according to importance. The identified results demonstrate that additional works, inaccurate initial project scope, increase or change in the scope of the project, and design changes are four common critical causes that strongly impact both time and cost management efficiency.

Keywords: Data envelopment analysis, management performance evaluation, project management efficiency, project management, cost and time overrun.

1. INTRODUCTION

Cost and time overruns are common phenomena in large civil engineering projects. These variables are defined as discrepancies between predicted cost and duration with actual total cost, and time taken at project completion. Exceeding the budget and running over the

Note:
- This paper has been received on January 08, 2018 and accepted for publication by the Editorial Board on November 12, 2018.
- Discussions on this paper will be accepted by May 31, 2019.
- https://dx.doi.org/10.18400/tekderg.375664

1 Eastern Mediterranean University, Department of Civil Engineering, Famagusta, Northern Cyprus - changiz.ahbab@emu.edu.tr - https://orcid.org/0000-0002-0780-1375

2 Eastern Mediterranean University, Department of Industrial Engineering, Famagusta, Northern Cyprus - sahand.daneshvar@emu.edu.tr - https://orcid.org/0000-0002-8597-3463

3 Cyprus International University, Department of Civil Engineering, Nicosia, Northern Cyprus - tcelik@ciu.edu.tr - https://orcid.org/0000-0002-2943-0640

schedule for the implementation of projects is a significant problem. This has encouraged researchers to conduct detailed studies on the causes that impact the contracted cost and schedule.

Arditi et al. [1] investigated the sources of cost overrun in public projects. In the first statistical treatment of the problem, Flyvbjerg et al. [2] studied the frequency and magnitude of cost overrun in transport infrastructure projects. They concluded that transport infrastructure projects generally exceed their time and/or cost, and also identified the cost as a highly uncertain criteria. They also found that 90% of transportation infrastructure projects experience cost escalation, indicating that cost overrun is a pervasive phenomenon. Assaf and Al-Hejji [3] studied the sources of extensions in the duration of large construction projects and identified the causes leading to delay. It was found that approximately 2/3 of large projects experience different degree of time overruns. In other studies, the cost overrun causes impacting projects were identified and categorized [4]. Ahsan and Gunawan [5] inspected and analysed the cost and time variation of 100 international development projects. They identified the major causes of time extension and cost overrun. Ahbab and Celik [6] proved the existence of time and cost overrun by obtaining the critical causes affecting time and cost criteria in large road projects. Cheng [7] studied the important causes impacting on the cost of a project, and developed new methods to control and avoid cost overrun. The aim of these investigations is to assist project managers by highlighting critical causes and directing their efforts to complete the project successfully [8, 9, 10, 11].

There are different criteria for benchmarking a completed project as successful. The parties involved in a project (Investor, client, contractor, consultant, and end-consumer) may assess the outcome differently. For instance, the success of a project was traditionally compared to the output and interrelation of time, cost, and quality through the Barnes' Iron Triangle [12].

Empirical and academic research has revealed that project managers play a vital role in delivering projects within the specified timeframe, and budget of the contract. This starring role in large projects is of high importance. Olsen [13] defined successful project management as the delivery of a project within the time, cost, and quality constraints. Munns and Bjeirmi [14] noted the importance of good project management leading to a higher possibility of project success. It is obvious that the extent to which the project manager controls the budget and schedule will affect the probability of success. The importance of applying project management, and project management methods has been widely researched by Besner and Hobbs [15], Chou and Yang [16], de Carvalho et al. [17], and Joslin and Muller [18]. Based on these studies, it can be concluded that the role of efficient project management is particularly important.

Efficiency can be defined as the extent of the deviation between actual performance and anticipated performance, and should be compared with an objective function [19]. Investing in building organizational project management expertise will lead to greater efficiencies in projects [20].

Serrador and Turner [21] have demonstrated that project efficiency and project success correlates moderately strongly with the overall project success. Project management efficiency can be characterized as utilization of effective project administration techniques to accomplish the clearly defined project scope and goals with minimum possible deviation.

Iyer and Banerjee [22] measured and ranked managerial efficiency in terms of the schedule during project execution.

Investors and project owners are attentive to ensuring a successful project through efficient project management, mostly in terms of time and budget variables. Project Management Efficiency can be affected by different causes, leading to cost deviations and delays in the project.

It is believed that there is a vital need for greater focus on extracting the causes that critically reduce the efficiency of project managers. To achieve this goal and obtain reliable results, mathematical methods can be applied to compute management efficiency or make a comparison between project management efficiencies.

The comparison of projects in terms of management efficiency can be undertaken by different parametric and nonparametric methods. Nonparametric methods do not consider the studied data as following a certain distribution, and place no (or very restricted) assumptions on the data. Nonparametric methods are mostly used for nominal or ordinal datasets, whereas parametric methods are applied to data sets with interval or ratio scales [23].

Common nonparametric techniques are Data Envelopment Analysis and Free Disposable Hull analysis. The Distribution-Free Approach, Stochastic Frontier Approach, and Thick Frontier Approach are parametric methods for efficiency measurement [24].

Data Envelopment Analysis is a powerful tool and is extensively used because of its advantages in determining efficiency, such as the ability to handle multiple inputs and outputs in a model, no assumptions about the input weights, and the ability to relate the resources expended on a certain activity to the level of success for that particular action [25] and [26].

Thus, due to advantages of this tool as an effective mathematical model for determining project efficiencies, authors consider it feasible and reasonable to apply this technique. Another incentive for using this tool is the ability to compare project management efficiencies based on the multiple defects influencing the time and cost criteria. To the best knowledge of the authors, this is the first time that Data Envelopment Analysis has been applied to large transportation projects to assist decision makers in efficient project management.

In this study, 63 large transportation projects with cost and time deviations were selected from the projects sponsored and financed by the Asian Development Bank. The selected projects are large in terms of cost criteria, with estimated total cost in between 12 and 1566 million dollar. Through project completion reports, Bank evaluates and rates the success of its projects according to relevance, effectiveness, efficiency, and sustainability [27]. On average, each report is about 60 pages and contains the project description, evaluation of the bank in design and execution of the project, performance, and overall assessment and recommendations at the end. Detailed Information about outputs of the project including scope and objectives, authorized and actual costs detected responsible causes for overruns, disbursements, schedule and extension causes, and implementation arrangements are also provided.

The identified causes of time and cost overruns were extracted from project completion reports and sorted in terms of the number of replications. Then, using Data Envelopment Analysis as a robust tool, the relative efficiency scores of project management for the selected

projects were computed and sorted accordingly. Using this methodology, the causes that negatively impacted the efficiency of project management and led to unsuccessful project status were recognized and extracted. These causes should be considered and addressed by policy and decision makers as critical negative efficiency causes. Additionally, more attention to these causes will help to improve the project management efficiency, and increase the likelihood of project success.

The first objective of this paper is to compute and compare the time and cost management efficiency of projects (Decision making units) regarding their contributing causes using Data Envelopment Analysis. Then, the importance of causes that adversely affect the management efficiency in terms of time and cost is quantified by applying sensitivity analysis. In this way, policy and decision makers in Asian Development Bank, government transportation departments, contract affairs units, project managers, and contractor companies will be able to improve their management efficiency. It is believed that the developed analytical tool can be used to benchmark the managerial efficiency through mitigation of the seriously continuing problems of time delays and cost overruns and objectively recognize management efficiency gaps. The rest of article is organized as follows. First, Data Envelopment Analysis methodology is illustrated. Second, Data aggregation, selection and preparation is described. Then, achieved results are discussed. As a final point, conclusions are provided.

2. DATA ENVELOPMENT ANALYSIS

Data Envelopment Analysis (DEA) is a powerful service management and benchmarking technique developed by Charnes, Cooper, and Rhodes (CCR) in 1978 to evaluate non-profit, and public-sector organizations [28]. Since its inception, this method has been used to identify ways of improving services that are not visible using other techniques. It is an evaluation tool for a set of entities called decision making units (DMUs) with multiple inputs and multiple outputs. It is also a decision-making tool that measures the relative efficiency of comparable units. The CCR model is the first and most fundamental DEA model to evaluate the relative efficiency of DMUs.

Consider a set of homogenous DMUs as DMU_j *(j=1,…, n)*. Each DMU consumes *m* inputs to produce *r* outputs. Suppose that $X_j = (x_{1j},...,x_{mj})$ and $Y_j = (y_{1j},...,y_{rj})$ are vectors of input and output values for DMU_j, respectively, and let $X_j \geq 0$ and $Y_j \geq 0, Y_j \neq 0$. The Production Possibility Set (PPS) T_C can be constructed by considering the following postulates.

The observed activities $(X_j, Y_j) \quad j = 1,2,\ldots n$ belong to T_C;

If an activity *(X, Y)* belongs to T_C, then activity *(tX, tY)* belongs to T_C for any positive scalar *t*. This property is called the constant returns-to-scale assumption;

For any activity *(X, Y)* in T_C, any semi-positive activity $(\overline{X}, \overline{Y})$ with $\overline{X} \geq X$ and $\overline{Y} \leq Y$ is included in T_C;

Any convex combination of activities in T_C belongs to T_C;

T_C is the smallest set that satisfies the above four properties.

With respect to the above assumptions, T_C can be defined as follows:

$$T_C = \{(X,Y) \mid X \geq \sum_{j=1}^{n} \lambda_j X_j,\ Y \leq \sum_{j=1}^{n} \lambda_j Y_j, \lambda_j \geq 0, \forall j\} \tag{1}$$

Now, for the evaluation of DMUs, DMU_o with (X_0, Y_0) as the input–output vector is written from an input orientation with some free value θ such that $(\theta X_0, Y_0)$ belongs to PPS. Thus,

$$\begin{array}{ll} Min & \theta \\ S.t & (\theta X_0, Y_0) \in T_C \end{array} \tag{2}$$

Based on the definition of T_C, the following linear programming problem is obtained:

$$\begin{array}{ll} Min & \theta \\ S.t & -\sum_{j=1}^{n} \lambda_j X_j + \theta X_0 \geq 0 \\ & \sum_{j=1}^{n} \lambda_j Y_j \geq Y_0 \\ & \lambda_j \geq 0,\ j = 1,\ldots,n. \\ & \theta\ free \end{array} \tag{3}$$

The dual of the above linear programming problem is used to obtain values for the input weights v_i and the output weights u_r:

$$\begin{array}{ll} Max & \theta = \sum_{r=1}^{s} u_r y_{ro} \\ s.t & \sum_{i=1}^{m} v_i x_{io} = 1 \\ & \sum_{r=1}^{s} u_r y_{rj} - \sum_{i=1}^{m} v_i x_{ij} \leq 0 \quad j = 1,2,\ldots,n \\ & v_i \geq 0 \quad i = 1,2,\ldots,m \\ & u_r \geq 0 \quad i = 1,2,\ldots,s \end{array} \tag{4}$$

In vector format, this can be written as follows:

$$\begin{array}{ll} Max & \theta = UY_o \\ s.t & VX_o = 1 \\ & UY_j - VX_j \leq 0 \quad j = 1,2,\ldots,n \\ & U \geq 0 \\ & V \geq 0 \end{array} \tag{5}$$

DMU_o is said to be CCR-efficient if $\theta^* = 1$ and there exists at least one optimal (V^*, U^*) with $V^* > 0$ and $U^* > 0$. DMU_o is said to be CCR-weak efficient if $\theta^* = 1$ and there exists $V^* \geq 0$ and $U^* \geq 0$ where at least one of V^* or U^* is equal to zero. Otherwise, DMU_o is CCR-inefficient, that is, $\theta^* \neq 1$.

Clearly, the optimal solution for both (3) and (4) is the same, which shows the efficiency value of the evaluation of DMU_o (X_0, Y_0). The optimal solutions of these models give us other useful information about DMU_o.

Assume that DMU_o (X_0, Y_0) is evaluated by model (3) and $\lambda^* = (\lambda_i^*, \dots, \lambda_j^*, \dots \lambda_n^*)$ with an objective function value of θ^* as its optimal solution. In vector λ^*, $\lambda_j^* > 0$ shows the effect of DMU_j in θ^* toward the efficiency value of DMU_o. Then, DMU_j can be considered as a benchmark in the efficiency improvement process of DMU_o. Alternatively, if it is assumed that (U^*, V^*) with an objective function of θ^* is the optimal solution of model (4) for DMU_o (X_0, Y_0), u_r^* $(r = 1, \dots, s)$ and v_i^* $(i = 1, \dots, m)$ can be considered as the weight or degree of importance of the r^{th} output and i^{th} input, respectively, in the efficiency value. Similarly, models based on variable returns-to-scale [29] may be used for this purpose.

Obviously, if u_r^* or v_i^* are equal to zero, the associated output or input has no effect on the efficiency of DMU_o [30].

One of the proposed methods for understanding the importance of inputs and outputs in the DMU efficiency values is to compute the average of the optimal weight values for u_r^* and v_i^* and compare these average values. Another significant method for the sensitivity analysis is to eliminate the inputs and outputs one by one, and compute the efficiency of the DMUs with the remaining inputs and outputs. Any decrement in the average efficiency value of a DMU shows the degree of importance of the eliminated input or output [31].

Furthermore, the sensitivity analysis for individual efficient DMUs may be employed to retain their efficiency against small changes in input or output values [32].

In this study, constant returns-to-scale are assumed for the evaluation of the observed DMUs. This is because the inherent nature of the construction industry means that increasing the number of contributing causes will increase the potential cost and time overrun.

3. DATA AGGREGATION, SELECTION, AND PREPARATION

International organizations and government departments routinely collect records and provide reports about national and international projects. The World Bank, Asian Development Bank, and the US Department of Transportation are among several organizations that frequently publish project data. Sometimes, researchers use the published data as secondary data. The advantages over primary data include the reduced time and expense of obtaining the data, the higher quality of the data, and the enhanced objectivity, accuracy, validity, and reliability of the data [33].

In this research, the Project Completion Reports published by Asian Development Bank were used as secondary data. Afterward 63 projects that suffered time and/or cost overruns were

selected (See Appendix2). Quantity of time and cost deviations in percentage from authorized duration and budget reported in each document were carefully computed and obtained. In the next step of this research, the documents were carefully scanned to find the causes that had adverse effects on time and cost criteria in the projects. As a result, 66 causes were identified as having an adverse influence leading to either time or cost overrun. To identify the most significant causes for each criterion, the number of repetitions of each cause was counted and sorted. Tables 1 and 2 list the affecting causes that were repeated 10 times or more within the projects. (See Appendix 1 for full list of adverse time and cost causes and their number of replications.)

Table 1 - Ranking of the first twenty critical causes influencing the time of the project

Code	Causes of Delay	No. Repetition	Rank
19	Long period between time of bidding and contract award	16	1
33	Delay in mobilization by contractor	13	2
43	Severe weather problems (heat, cold, snow, rain, cyclone)	12	3
58	Poor procurement procedure	11	4
21	Design changes	10	5
31	Poor performance of contractor	10	5
14	Slowness of the owner's decision-making process	10	5
20	Increase in quantity of work (Additional works)	9	6
7	Poor project management, construction management and supervision	8	7
52	Increase or change in scope of the Project	8	7
63	Delay in Land Acquisition	8	7
35	Slow or Delayed material or equipment delivery to project site	7	8
2	Inaccurate initial project scope and cost estimate	7	8
64	Delay in appointment of consultant	7	8
17	Delay in Approval of feasibility study, drawings and material	6	9
50	Complicated administrative and governmental procedures (institutional problems)	6	9
18	Financial difficulties of owner/Client	5	10
44	Political issues-Changes	5	10
42	Poor and unforeseen site conditions (Location, ground, geological, events, security, ETC)	5	10
36	Unavailability or shortage of required materials in the local market on time	5	10

In the next step, the data were prepared and modelled using the Performance Improvement Management software [34]. A total of 51 projects were input related to the 20 most frequent causes of time overruns and 38 projects with the 10 most frequent causes of cost overruns were also modelled. This combinations of selection was considered because the number of selected projects has to be higher than the maximum between (m × s) and [3 × (m+ s)], being m and s the number of input and output criteria [35]. The output from each model was the inverse time and cost overrun percentage.

Table 2 - Ranking of the first ten critical causes influencing the cost of the project

Code	Causes of Cost Overrun	No. Repetition	Rank
37	Fluctuation and escalation in prices	21	1
47	Change in exchange rate	13	2
53	Underestimated and inaccurate appraisal	12	3
52	Increase or change in scope of the project	11	4
62	Increase in the amount of land acquisition, price, and Compensation	11	4
21	Design changes	10	5
2	Inaccurate initial project scope and cost estimate	7	6
20	Increase in quantity of work (Additional works)	7	6
42	Poor and unforeseen site conditions (Location, ground, geological, events, security)	7	6
61	Additional project management, consultancy and administration costs	6	7

4. RESULTS AND DISCUSSIONS

The main purpose of this paper is to draw attention to the performance and managerial efficiency of large road projects in terms of time and cost criteria. Therefore, in this step, the project management efficiency of the projects was measured using the Performance Improvement Management software [34]. This was done by applying the CCR model considering the causes affecting each of the time and cost criteria. The relative managerial efficiency measurement is provided as an efficiency score by the software. The results are summarized in Tables 3 and 5 for time and cost, respectively.

Time and cost management efficiency can be defined as a set of management techniques which minimizes the overall effect of adverse causes leading to time and cost overrun. In other word, managing tasks by reducing the effect of adverse causes and reach to the best output, which is the completion of the project in specified time and budget. Managerial efficiency can be expressed as a relative measure. Different project management teams have different efficiency in taking decisions and controlling cost and time criteria in presence of

affecting causes. Their ability in prioritizing the tasks, taking actions against causes and minimizing defects of causes will show the extent of their success in efficient time and cost management.

Table 3 - Managerial relative efficiency score for time criteria of 51 projects

Project	Efficiency Score	Project	Efficiency Score	Project	Efficiency Score	Project	Efficiency Score
01	39.40	16	17.13	32	100	48	12.93
02	100	18	16.13	33	100	49	98.39
03	15.45	19	67.12	34	23.04	50	100
04	100	20	16.90	35	100	51	100
06	100	21	100	36	100	52	6.54
07	100	22	100	37	100	53	30.93
08	100	23	100	39	100	55	100
09	6.83	24	60.37	41	14.55	56	100
10	100	25	100	42	90.97	59	12.06
12	60.65	26	15.81	43	100	61	14.70
13	36.30	29	100	44	100	62	100
14	100	30	4.15	46	6.09	63	36.17
15	100	31	50.60	47	100		

As can be seen in Table 3, the relative managerial efficiency in terms of time for 27 out of 51 projects is 100%. This can be interpreted as follows:

1) Despite presenting various difficulties and delays, the different parties involved in the management of these projects succeeded in accomplishing the project efficiently. For instance, project 29 partially and efficiently overcame seven causes that affected the project time. Those causes were the long-time gap between project preparation and real start date of construction, the lack of knowledge in regional owners and local contractors with the circumstances of the Fédération International des Ingénieurs-Conseils (FIDIC), delays in the approval of some changes by the owner, the unavailability or shortage of required materials in the local market, equipment and manpower shortages, unforeseen events, and a tsunami. Those unexpected issues resulted in a time overrun of only 15% (See Appendix 2).

2) In project 49, the relative efficiency score in time management is 98.39%. Project managers faced with only two causes in this project including unforeseen events and the unavailability or shortage of required materials in the local market which are in common with project 29. This project was accomplished with 33% of time overrun (See Appendix 2).

This evidence shows that the project managers of this project could not able to efficiently overcome the common causes in compare with other project which overcome more causes with less time overrun.

In the second step, the focus was on the causes that critically influenced and impacted the managerial efficiency. Therefore, projects with less than 100% efficiency were investigated. A table was prepared based on the number of repetitions of causes in the selected inefficient projects. The causes were then sorted and those having the most critical effect on time criteria, leading to inefficient project management, are presented in Table 4.

Table 4. Number of repetitions of causes influencing time management efficiency in the inefficient projects

Code* / Project	33	21	7	43	31	19	14	58	2	52	17	35	18	20	23	63
01							x	x								
03		x			x				x				x			
09		x				x		x		x	x					x
12						x		x								
13		x	x		x											x
16						x		x	x	x				x		x
18	x			x					x	x		x				
19																
20			x	x	x								x			
24									x	x			x	x		
26	x	x		x									x	x		x
30	x	x	x		x											
31	x				x	x	x				x				x	
34			x	x	x		x				x					
41	x		x				x	x							x	
42							x					x				
46		x	x									x				
48	x	x				x		x			x				x	
49																
52	x	x	x	x		x						x		x	x	
53	x															
59	x	x		x						x						
61				x			x									
63	x								x							
Repetition	10	9	7	7	6	6	6	6	5	5	4	4	4	4	4	4
*	Refer to Appendix 1															

Based on Table 4, it can be concluded that delays in mobilization by the contractor, project design changes, and poor project management and supervision are the three main causes that severely affect the time management of projects.

Simultaneously, the efficiency of cost management was also studied, and Table 5 summarizes the managerial cost efficiency score for the investigated projects. This table clearly implies that 11 of the 38 projects are efficient in terms of cost management criteria. It clarifies that project managers could able to accomplish those 11 projects with efficient cost management despite presence of adverse causes that impacts the authorized cost. The other 27 project managers could not fully succeed in managing the cost against causes efficiently in comparing with successful project managers. For example, the US$ 465 million project represented by project 36 is an efficient project. The different parties responsible for the management of this project dealt with inaccurate cost estimates in appraisal, changes in the scope of the project, changes in land acquisition prices, and design changes to complete the project with a cost overrun of just 2.2%. Meanwhile project 37 was affected by three causes which are common with project 36. Effect of causes and inefficient cost management led this project to 75% of cost overrun from $762 million to $1,333 million. In this point, in line with the reasons in time management efficiency part, the importance of efficient cost management is concluded. However, 27 out of the 38 projects investigated are inefficient projects.

Table 5 - Managerial relative efficiency score for cost criteria of 38 projects

Project	Efficiency Score	Project	Efficiency Score	Project	Efficiency Score	Project	Efficiency Score
01	96.95	24	7.94	36	100	51	21.17
02	35.54	25	51.69	37	5.14	52	100
04	100	27	100	38	15.26	54	48.70
06	100	28	95.03	39	7.40	55	3.42
10	100	29	100	40	4.49	57	100
14	6.27	30	47.61	41	4.74	58	13.96
15	100	32	22.95	44	54.98	59	100
16	1.87	33	19.90	45	23.22	63	14.56
20	11.85	34	38.82	46	4.02		
21	13.02	35	100	47	21.79		

Parallel to time management efficiency calculation, Table 6 lists the main causes observed in projects with cost management efficiency scores of less than 100%. This table indicates that fluctuations and escalations in the prices of material, equipment, and labour have the most impact on the cost managerial efficiency score. As the projects being studied are international road projects, changes in the US dollar exchange rate also impacted the efficiency. Underestimated and inaccurate appraisals and increases in the land acquisition price and compensation were other influential causes.

Another point that needs more attention is that there are four common critical causes in Tables 4 and 6. These are the increased quantity of work by additional works (20), inaccurate initial project scope (2), increases or changes in the scope of the project (52) and design changes (21). These causes strongly impact the management efficiency of both time and cost criteria.

Table 6 - Number of repetitions of causes influencing cost management efficiency in inefficient projects

Code* / Project	37	47	53	62	52	20	21	42	2	10	61
01	x										
02	x						x	x		x	
14		x			x				x		
16	x		x		x	x					
20	x									x	
21	x	x				x				x	
24			x	x	x	x	x	x			
25		x							x		
28					x		x	x			
30	x										
32	x										
33		x			x	x		x			
34	x					x		x	x		
37			x	x			x				
38	x	x									x
39	x	x	x	x							
40	x		x	x	x	x	x				x
41	x								x		
44		x									
45	x	x		x							
46	x		x							x	
47	x				x						x
51	x			x							
54	x			x							
55	x	x	x	x				x	x		
58	x	x	x				x				
63		x	x								
Repetition	19	11	9	8	7	6	6	6	5	4	3
*	Refer to Appendix 1										

In order to investigate the significance of the aforementioned 10 cost causes on the cost management performance, and effect of previously defined 20 time causes on time management performance, sensitivity analysis tool was adopted. With the help of sensitivity analysis, authors verified the influence of every single cause on the overall efficiency of the management team assigned for projects. This specific analysis enabled the identification of the degree of deviation in other words, the magnitude of impact of each cause in terms of effect on the efficiency of project management of construction projects. The sequential steps followed in this study for identifying the magnitude of impact of each cause on management efficiency are; (1) Elimination of each cause as input from the critical causes list one by one, (2) Computation of the efficiency value of project managers subsequent to execution of step (1), (3) calculation of the rate of declines in value from previous efficiency average in order to determine the level of significance for each cause.

For each project, decrease in management efficiency score compared to original one reflects the importance of eliminated cause in that project management performance. As performed by Montoneri et al [31], amount of deviation in the new efficiency average of all projects from the original efficiency average indicates the level of significance for the eliminated cause.

Tables 7 and 8 present the results of sensitivity analysis and the change in the new efficiency average compared with the original efficiency score average for the time and cost criteria.

According to the results summarized in Table 7, the deviations given by omitting design changes (cause 21), delay in mobilization by contractor (cause 33), and poor project management (cause 7) from the original average value are greater than for the other inputs. Thus, it can be concluded that these causes have a greater impact on the efficiency of the time management of projects. (See Appendix 1)

Table 7 - Results of sensitivity analysis and deviations in time criteria

Cause Code	New Efficiency Average	Cause Code	New Efficiency Average	Cause Code	New Efficiency Average	Cause Code	New Efficiency Average
2	67.71	19	67.71	35	67.71	50	66.74
7	52.04	20	65.75	36	67.71	52	67.71
14	57.34	21	24.27	42	58.74	58	63.02
17	67.54	31	67.49	43	61.35	63	63.78
18	67.71	33	42.09	44	62.56	64	66.66
Average of efficiency scores in Table 3: **67.71**							

As can be seen from Table 8, the studied projects are most sensitive to underestimated and inaccurate appraisals (cause 53), changes in the exchange rate (cause 47), and an increase in the quantity of work (cause 20). Based on the results, these causes have a greater impact on the cost management efficiency than other causes.

Table 8 - Results of sensitivity analysis and deviations in cost criteria

Cause Code	New Efficiency Average	Cause Code	New Efficiency Average
2	37.96	47	37.07
20	37.35	52	44.77
21	47.64	53	29.66
37	41.63	61	42.56
42	46.42	62	47.17
Average of efficiency scores in Table 5: **47.17**			

The results obtained by the sensitivity analysis using the Performance Improvement Management software are in line with the results in Tables 3 and 5. In the same way, these results confirm that the causes investigated here not only impact on the final cost and time of projects, but also influence the efficiency of time and cost management.

4.1. Importance of time and cost management efficiency

An awareness of the extent of the interaction between time and cost management efficiency is an important point. This may help decision makers and project managers to undertake countermeasures to reduce the probability of time and cost overruns. Consequently, in the last part of the current study, projects that suffered both time and cost overruns were selected.

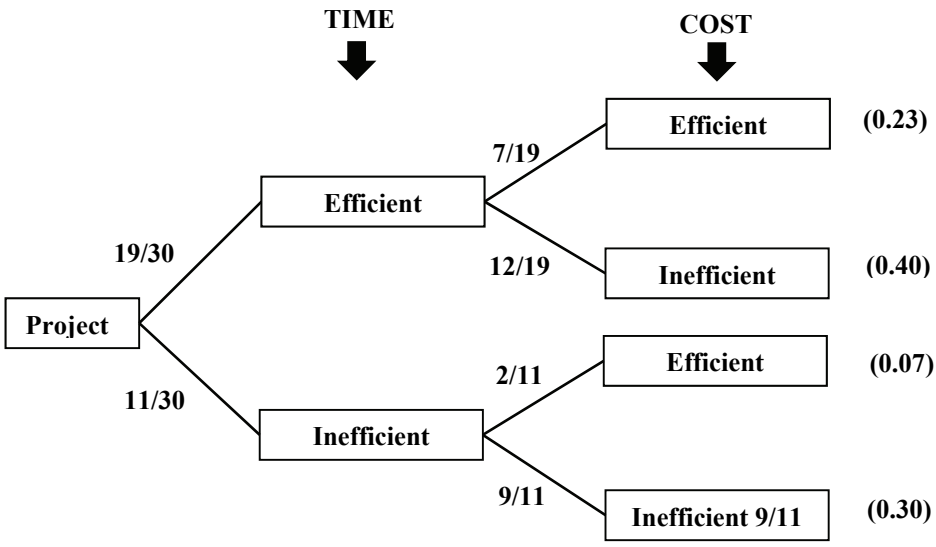

Figure 1 - Probability tree diagram of efficiency for time management criteria

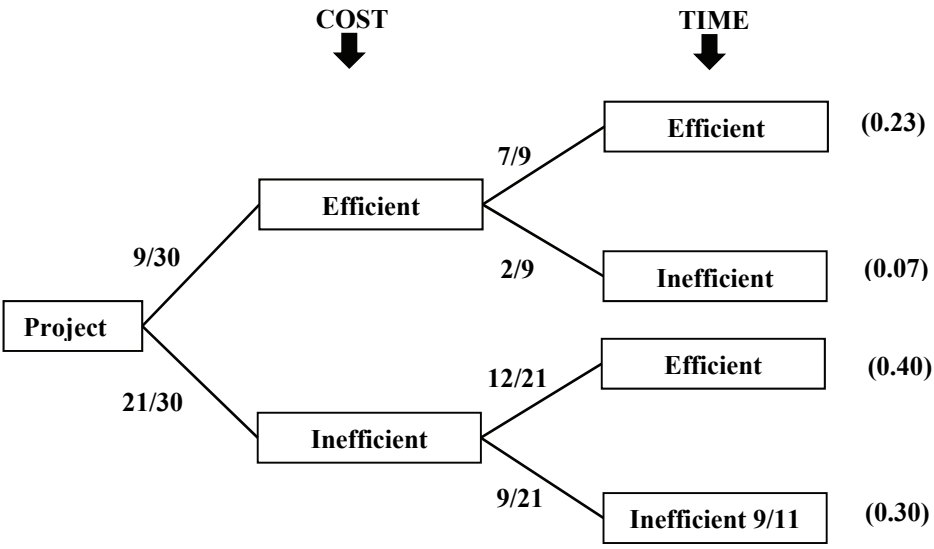

Figure 2 - Probability tree diagram of efficiency for cost management criteria

Based on Table 3 and 5, only 7 out of the total of 30 projects succeeded in managing both the time and cost criteria separately to achieve 100% efficiency. Projects 11 and 21 have inefficient management in terms of time and cost criteria, respectively. Figures 1 and 2 depict probability tree diagrams of the projects in terms of time and cost management efficiency.

Figure 1 plainly shows that, in the case of inefficient time management, the likelihood of inefficient cost management is approximately 4 times higher than that of efficient cost management. Therefore, time management is much more critical than cost management.

According to Figure 2, it can be concluded that the observed projects were mostly unsuccessful in terms of cost management efficiency. Moreover, efficient cost management is more likely to lead to efficient time management than to inefficient time management.

4.2. Impact of Different Elements of Project Management

It is believed that resulted cost and time overrun in the studied projects are a consequence of adverse causes that are rooted from other project management elements at the same time. Causes 3, 5, 8, 16, 24, 28, 45, 52 and 58 in Appendix 1 have direct relation with Communication Management, Contract Management, Quality Management, Procurement Management, Health and Safety Management, and Scope Management. Therefore, it can be concluded that not only time and cost management, but also existence of some other project management elements affects the time, and cost management efficiency. In other word, time and cost management efficiency is a portion of most of other project management elements combination.

5. CONCLUSIONS

The purpose of this article was to fill a gap in the literature concerning time and cost management efficiency for completed large transportation projects. By applying the CCR model in Data Envelopment Analysis, the authors have measured, scored, and benchmarked the schedule and budget supervisory efficiency of the studied projects. After benchmarking the efficient and inefficient projects in terms of time and cost management, a sensitivity analysis was conducted to examine the causes impacting these efficiencies.

The results obtained in this study reveal that design changes during the execution phase, delays in mobilization by the contractor, and poor project management have a significant effect on time management efficiency. Additionally, cost management efficiency is more sensitive to underestimated and inaccurate appraisals, changes in the exchange rate, and increases in the quantity of work. This article shows that this methodology can be widely and effectively applied to evaluate the managerial efficiency of project managers or project management teams in terms of time and cost or any other criteria. Moreover, using this methodology, the most significant causes impacting a project can be recognized, and these may be used as a guide for practitioners and decision makers to take the necessary countermeasures.

Another significant finding in this study is that inefficient time management of projects increases the chance of inefficient cost management to four times that of efficient cost management. Therefore, project managers should objectively pay more attention to controlling the time of the project.

The limitation of this investigation is that, this research was conducted based on projects implemented in Asia region. Also selected projects were among Asian Development Bank road projects. Moreover total number of studied projects were constrained by the number of projects that experienced time and cost overrun. Finally, the evaluated completion reports provides information, reason, and results of the problems for time and cost overrun.

It should be noted that, the obtained conclusions in this study are restricted to the selected project's data and considered criteria for those projects only.

Acknowledgements

The authors gratefully acknowledge the Asian Development Bank for providing the data used in this research through access to publicly disclosed Project Completion Reports. The data analysis phase detailed in this research would not have been possible without obtaining the data within these reports.

References

[1] Arditi, D., Akan, G. T., and Gurdamar, S., Cost overruns in public projects, International Journal of Project Management, 3, 4, 218-24, 1985.

[2] Flyvbjerg, B., Skamris Holm, M. K., and Buhl, S. L., How common and how large are cost overruns in transport infrastructure projects?, Transport Reviews, 23, 1, 71-88, 2003.

[3] Assaf, S. A., and Al-Hejji, S., Causes of delay in large construction projects, International Journal of Project Management, 24, 4, 349-57, 2006.

[4] Shane, J. S., Molenaar, K. R., and Schexnayder, C. Construction project cost escalation factors, Journal of Management in Engineering, 25, 4, 221-29, 2009.

[5] Ahsan, K., and Gunawan, I., Analysis of cost and schedule performance of international development projects, International Journal of Project Management, 28, 1, 68-78, 2010.

[6] Ahbab, C., and Celik, T., An investigation on delay, cost overrun, quality, and health and safety problems in construction projects, 10th International Congress on Advances in Civil Engineering, Ankara: Middle East Technical University, 2012.

[7] Cheng, Y.-M., An exploration into cost-influencing factors on construction projects, International Journal of Project Management, 32, 5, 850-860, 2014.

[8] Flyvbjerg, B., Holm, M. K. s., and Buhl, S. L., What Causes Cost Overrun in Transport Infrastructure Projects, Transport Reviews, 24, 1, 3-18, 2004.

[9] Love, P. E. D., Sing, C. P., Wang, X., Irani, Z., and Thwala, D. W., Overruns in transportation infrastructure projects, Structure and Infrastructure Engineering, 10, 2, 141-159, 2014.

[10] Shehu, Z., Endut, I. R., Akintoye, A., and Holt, G. D., Cost overrun in the Malaysian construction industry projects: A deeper insight, International Jouranl of Project Management, 32, 8, 1471-1480, 2014.

[11] Eliasson, J., and Fosgerau, M., Cost overruns and demand shortfalls – Deception or selection? Transportation Research Part B, 57, 105-113, 2013.

[12] Lock, D., Project Management, Hampshire: Gower Publishing Limited, 2007.

[13] Olsen, R. P., Can project management be defined?, Project Management Institute, 1971.

[14] Munns, A. K., and Bjeirmi, B. F., The role of project management in achieving project success, International Journal of Project Management, 14, 2, 81-87, 1996.

[15] Besner, C., and Hobbs, B., The Perceived Value and Potential Contribution of Project Management Practices to Project Success, Project Management Journal, 37, 3, 37-48, 2006.

[16] Chou, J.-S., and Yang, J.-G., Project Management Knowledge and Effects on Construction Project Outcomes An Empirical Study, Project Management Journal, 43, 5, 47-67, 2012.

[17] de Carvalho, M. M., Patah, L. A., and Bido, D. d. S., Project management and its effects on project success, Cross-country and cross-industry comparisons, International Journal of Project Management, 33, 7, 1509-1522, 2015.

[18] Joslin, R., and Müller, R., Relationships between a project management methodology and project success in different project governance contexts, International Journal of Project Management, 33, 6, 1377-1392, 2015.

[19] Thakor, A. V., and Boot, A. W., Handbook of Financial Intermediation and Banking, North Holland- Elsevier, 2008.

[20] The Value of Project Management, PMI-Project Management Institute, 2010. 2017, Retrieved from https://www.pmi.org/-/media/pmi/documents/public/pdf/white-papers/value-of-project-management.pdf

[21] Serrador, P., and Turner, R., The Relationship Between Project Success and Project Efficiency, Project Management Journal, 46, 1, 30-39, 2015.

[22] Iyer, K. C., and Banerjee, P. S., Measuring and benchmarking managerial efficiency of project execution schedule performance, International Journal of Project Management, 34, 2, 219-236, 2016.

[23] Markham, S., Parametric versus non-parametric, Monash University, 2016. 2017, Retrieved from http://users.monash.edu/~smarkham/resources/param.htm#param.

[24] Mester, L. J., Applying Efficiency Measurement Techniques to Central Banks, Wharton Financial Institutions Center, Wharton University of Pennsylvania, 2003. 2017, Retrived from http://fic.wharton.upenn.edu/fic/papers/03/0325.pdf

[25] El-Mashaleh, M. S., Rababeh, S. M., and Hyari, K. H., Utilizing data envelopment analysis to benchmark safety performance of construction contractors, International Journal of Project Management, 28, 1, 61-67, 2010.

[26] Trick, M., Michael Trick's Operations Research Page, Carnegie Mellon University, 1998. Retrieved from http://mat.gsia.cmu.edu/classes/QUANT/NOTES/chap12.pdf

[27] Guidelines for the Evaluation of Public Sector Operations, Asian Development Bank, 2016. 01-08-2016, Retrieved from

http://www.adb.org/sites/default/files/institutional-document/32516/guidelines-evaluation-public-sector.pdf.

[28] Charnes, A., Cooper, W. W., and Rhodes, E., Measuring the efficiency of decision making units, European Journal of Operational Research, 2, 6, 429-44, 1978.

[29] Banker, R. D., Charnes, A., and Cooper, W. W., Some Models for Estimating Technical and Scale Inefficiencies in Data Envelopment Analysis, Management Science, 30, 9, 1078-1092, 1984.

[30] Cooper, W. W., Seiford, L. M., and Tone, K., Data Envelopment Analysis, Springer US, 2007.

[31] Montoneri, B., Lin, T. T., Lee, C.-C., and Huang, S.-L., Application of data envelopment analysis on the indicators contributing to learning and teaching performance, Teaching and Teacher Education, 28, 3, 382-395, 2012.

[32] Daneshvar, S., Izbirak, G., and Javadi, A., Sensitivity analysis on modified variable returns to scale model in Data Envelopment Analysis using facet analysis, Computers & Industrial Engineering, 76, 32-39, 2014.

[33] Vartanian, T. P., Secondary Data Analysis: New York, Oxford University Press, 2011.

[34] Emrouzinejad, Ali, Thanassoulis, Emmanuel, PIM-DEA, PIM-DEA soft (Data Envelopment Analysis Software), 2017. Retrieved from http://deasoftware.co.uk/

[35] Cooper, W. W., Seiford, L. M., and Tone, K., Introduction to data envelopment analysis and its uses, with DEA-solver software and references, Springer Science & Business Media, 2006.

APPENDICES

Appendix 1. Full List of Causes Affecting Time & Cost Criteria and their Repetition in Studied Projects, respectively

Code	Affecting Cause	# Repetition	
		in Time	in Cost
1	Inadequate front-end planning of project	1	0
2	Inaccurate initial project scope and cost estimate	7	7
3	Inadequate communication between design and construction parties	1	1
4	Poor site management	1	0
5	Not communicating with all parties dealing with the budget	1	1
6	Owner interference in the project	1	1
7	Poor project management, construction management, and supervision	8	0
8	Poor contract management (inexperience of following contract condition)	2	1
9	Poor provision of information to project participants	1	1
10	Inflation	2	4
11	Failure to resolve change orders and prevent them from becoming claims/disputes	1	1
12	Too many construction activities going on at the same time	1	1
13	No financial incentive to contractor to finish the project ahead of schedule	1	1
14	Slowness of the owner's decision-making process (approval of activities)	10	1
15	Slow financial and payment procedures adopted by the client	4	2
16	Contract modifications and variations (replacement, addition, and change)	0	2
17	Delay in approval of feasibility study, drawings, and material	6	0
18	Financial difficulties of owner/client	5	0
19	Long period between time of bidding and contract award (initial delay)	16	2
20	Increase in quantity of work (additional works)	9	7
21	Design changes	10	10
22	Absence of consultant's staff on the project site	1	0

23	Lack of technical and managerial skills of consultant's staff (poor performance)	4	0
24	Lack of quality assurance, control	1	1
25	Poor documentation - incomplete drawings, poor drawings, design deficiencies	1	0
26	Slow inspection of completed works	1	1
27	Equipment and manpower shortage and bad distribution on site	4	0
28	Poor communication with consultant and owner	1	0
29	Financial difficulties of contractor	4	0
30	Low productivity of labour	0	2
31	Inadequate contractor experience (poor performance of contractor)	10	0
32	Rework and wastage of materials	1	1
33	Delay in mobilization by contractor	13	0
34	Inadequate and incompetent subcontractors	0	1
35	Slow or delayed material or equipment delivery to project site	7	2
36	Unavailability or shortage of required materials in the local market on time	5	21
37	Fluctuation and escalation in prices (materials, machinery, labour, equipment)	2	0
38	Monopoly of construction materials supply (steel, cement)	1	1
39	Equipment availability and failure	1	1
40	Lack of maintenance for the equipment	1	1
41	Skilled labour shortage	2	7
42	Poor and unforeseen site conditions (location, ground, geological, events, security)	5	1
43	Severe weather problems (heat, cold, snow, rain, cyclone)	12	1
44	Political issues, changes	5	0
45	Poor health and safety conditions on site	0	2
46	Changes in laws and regulations during the project, obstacles from government	1	13
47	Change in exchange rate	0	2
48	Inadequate design team experience	1	3
49	Extension of the construction phase (delay)	1	1
50	Complicated administrative and governmental procedures (institutional problems)	6	3

51	Damage of structure and equipment breakdown (flood, cyclone)	1	11
52	Increase or change in scope of the project	8	12
53	Underestimate and inaccurate appraisal (missing measures, cost adjustment)	2	2
54	Extension of consultant contract	0	1
55	Court cases (litigation)	2	3
56	Unexpected issues (public obstruction, earthquake, flood, security issues)	1	1
57	Quitting the work by contractor	3	1
58	Poor procurement procedure (longer period or procedures in bidding)	11	1
59	Change in quality of the work	1	1
60	Inaccurate estimation for duration of the project	0	6
61	Additional project management, consultancy, and administration costs	0	11
62	Increase in the amount of land acquisition, price, and compensation	0	0
63	Delay in land acquisition	8	0
64	Delay in appointment of consultant	7	0
65	Low contract bid	1	0
66	Repetition of tendering or bidding procedure	3	0

Appendix 2. Specifications of selected projects

Description /Project	Country	Estimated Cost $(Million)	Cost Overrun (%)	Estimated Duration (Months)	Time Overrun (%)
01	Bangladesh	15.60	10.71	624	92
02	New Guinea	15.34	29.20	528	41
03	Pakistan	178	-12.07	648	48
04	Laos	23.75	6.32	1369	49
05	Bangladesh	696	8.29	1581	0
06	Bangladesh	105.5	2.49	792	36
07	Nepal	50	-3	1613	7
08	Guinea	97	-57	1886	69

09	India	308.8	-2	1340	109
10	Tonga	12.5	6.48	1552	12
11	Nepal	16.9	-8	2190	33
12	Thailand	211	-30	2190	67
13	Viet Nam	237	-31	1742	20
14	Laos	44.8	101	1217	26
15	China	532	4	228	299
16	Sri Lanka	295.9	206	72	117
17	China	795.5	-8	2555	-7
18	Laos	50	21	60	80
19	China	360	-4	1490	49
20	Fiji	90	88	2283	148
21	Sri Lanka	123.3	48	1825	40
22	Cambodia	88.1	-1	40	65
23	China	345	-3.41	1798	40
24	China	770.3	28	1796	46
25	Cambodia	77.5	12	1200	58
26	Laos	37.5	-27	1551	47
27	Laos	39.2	26	96	-6
28	China	757	28	48	0
29	Sri Lanka	92.5	10	1824	15
30	India	378	21.80	1440	179
31	Pakistan	236	-17	2190	33
32	India	92	45	2371	62
33	China	582	32	1490	33
34	Bhutan	34.10	6	1825	35
35	Tajikistan	26.8	3	1460	29
36	China	455.2	2	1492	37
37	China	762	75	1643	50
38	China	611.8	41	1875	60
39	China	882	52	2010	36
40	China	2077	49	2190	0
41	India	649	53	1440	114

42	China	834	-3	1826	40
43	Tajikistan	23.6	-1	1216	28
44	China	726	11	1339	25
45	China	778.1	27	1825	-13
46	Mongolia	78.14	96	1642.5	122
47	Azerbaijan	93.2	47.64	1094	17
48	India	285.7	-1	1825	58
49	Pakistan	423.6	-29	1095	33
50	Kyrgyz	43.4	0	1065	18
51	China	745	49.03	1826	20
52	Afghanistan	80	3.11	940	114
53	India	400	-3.25	1186	54
54	China	1425	21.31	1642.5	0
55	China	519.51	73	2281	8
56	Tajikistan	64.5	-7.09	2100	13
57	China	524.55	2.60	1398	0
58	China	1566	27.60	1825	15
59	Afghanistan	140.9	24.41	1260	62
60	China	594	-4.97	1855	20
61	Kyrgyz	30.3	-30	1002	55
62	Kyrgyz	76.5	-7	2191	4
63	Honduras	64.6	26.47	1525	46

Teknik Dergi, 2019 8961-8985, Paper 530

Wage Determinants and Wage Inequalities - Case of Construction Engineers in Turkey

Serkan AYDINLI[1]
Mustafa ORAL[2]
Emel ORAL[3]

ABSTRACT

Unfair wage policies that fail to meet the needs of employees have been cited to be one of the most important reasons for high turnover rates of construction professionals. Despite, little research has been conducted related to the determinants of a fair wage, and industry-wide wage policies. Hence, a questionnaire survey was held in 2016 with 305 company/human resource managers and 410 construction engineers working in the Turkish construction industry, which is one of the largest in the world, to determine wage policies of the companies. Findings of the questionnaire survey are discussed within the frame of the literature findings related to the prerequisites of a fair wage. Wages of respondents are compared to the legal minimum wage requirements. Effects of some compensable variables like the level of education, experience, seniority in the company, foreign language skills, computer skills, the complexity of the project, the location of the project and the size of the company on the wage rates are examined by using Multinomial Logistic Regression Analysis and Self Organizing Maps. Lorenz Curves and Gini Coefficients are used to represent and analyze the wage distribution of the respondents. Multi-national comparisons are presented where possible.

The findings of the current research present a benchmark for further research related to the prevailing wages, wage inequalities, and the wage policies, not only for Turkish construction industry but also for the construction industry worldwide.

Keywords: Wage determinants, wage inequalities, construction engineer, construction industry, gini coefficient, lorenz curve, multinomial regression analysis, self-organizing maps.

Note:
- This paper has been received on January 15, 2018 and accepted for publication by the Editorial Board on October 09, 2018.
- Discussions on this paper will be accepted by May 31, 2019.
- https://dx.doi.org/10.18400/tekderg.378955

1 Cukurova University, Department of Civil Engineering, Adana, Turkey - saydinli@cu.edu.tr - https://orcid.org/0000-0002-2897-4144

2 Cukurova University, Department of Computer Engineering, Adana, Turkey - moral@cu.edu.tr - https://orcid.org/0000-0001-9127-8857

3 Cukurova University, Department of Civil Engineering, Adana, Turkey - eoral@cu.edu.tr - https://orcid.org/0000-0002-7477-7993

1. INTRODUCTION

Turkish construction industry is one of the largest in the world. More than 185 thousand construction companies employ around 1.8 million employees. In addition to domestic companies, there are 4418 foreign construction companies actively working in Turkey [1]. While about 67-77% of the construction investments is on building projects, around 23-33% is on infrastructure [2-3]. Although small to medium-sized companies dominate the domestic market, 40 Turkish construction companies are in the 'Top 250 International Contractors' list of ENR in 2016 which puts Turkey into second place after China in the international markets. In 2016, the growth rate of Turkish construction industry was about 7.4%. Meanwhile, the unemployment rate for construction engineers[†] was 11% [4]. The most important reason of such a high unemployment rate is the excessive number of graduates that join to the workforce each year (around ten thousand graduates annually which are nearly 10% of the total number of construction engineers) [5]. Supply/demand ratio works in the disadvantage of the engineers and as both the 'Demand and Supply Theory' by Marshall [6] and the 'Bargaining Theory of Wages' by Davidson [7] stress, it is inevitable that employers play a stronger role and wages, and job opportunities for the engineers tend to be low. Thus, it is vital for the job-seekers to be aware of the determinants that influence the employment opportunities and the wage policies in the industry. However, this is practically not easy to follow, as the employment is mainly project-based and, unionization, labor union agreements, and collective agreements are limited in the construction industry.

Wage policies in the industry should not be the concern of the job-seekers only; they should also be one of the primary concerns of the employers due to their effects on the employees' motivation, morale, group cooperation, efficiency, and employee turnover rates [8-29]. As 'Fair Wage Theory' by Akerlof [30] and Akerlof and Yellen [31], state that fairer an employee considers his/her wage, the harder he/she will work or vice versa.

Above discussion raises two critical issues to be resolved. First one is the definition and the constitutes of a fair wage for construction engineers, and the second one is the current situation in the industry regarding the wages of professionals, which engineers should consider while working out their wage expectations. Thus, the aim of the current research has been to; determine the constituents of a 'fair' wage for construction engineers, compare these with industry-wide applications and to present models that can be used to analyze the effect of different variables concerning level of wages. It is expected that findings will present guidance to; the academicians in determining course contents, company managers in establishing wage policies, construction engineers in gaining awareness related to the prevailing wages and the government bodies in both defining and implementing minimum wage regulations.

2. RESEARCH BACKGROUND AND LITERATURE REVIEW

International Labour Organization (ILO) describes wage as "payment which is made by the employers to the laborer for his services hired on the conditions of pay per hour, per day, per week, per fortnight or month" [32]. The ILO encourages its member states to implement

NOTE: In this context, Construction engineers are engineers/architects/technicians who undertake various responsibilities related with planning, coordination, organization, and control of work on construction projects.

minimum wage regulations to eliminate unduly low pay, reduce wage inequality and promote decent work. The ILO defines minimum wage as "the minimum amount of remuneration that an employer is required to pay wage earners for the work performed during a given period, which cannot be reduced by collective agreement or an individual contract" [33]. Minimum wage regulations change from country to country depending on the needs and choices. While some countries implement the same minimum wage rate to all of the employees, some enforce different standards according to the age or the occupation of the employee or according to the sector or the geographical region of work. [33].

Turkish minimum wage system is regulated under a constitutional guarantee and is fed from international contracts and the ILO's recommendations [34]. Minimum wage is set at the latest in every two years by the Minimum Wage Fixing Board by considering social and economic conditions of the country [35]. Inflation differentials are also reflected in the minimum wages every six months. Also, the minimum wages for engineers are regulated by a protocol signed between Union of Chambers of Turkish Engineers and Architects (UCTEA) and Presidency of Social Security Institution each year. The protocol states that wages of civil engineers/architects and city planners cannot be based on national minimum wages due to the nature of the responsibilities undertaken. Minimum gross wages that will be effective for the following year are publicized at the end of each year. Accordingly, in 2016, while the base minimum wage for all of the employees (disposable take-home pay, i.e., what remains after taxes, pensions, social security contributions, or other deductions) was set to be around 1.250TL/month*‡ the minimum wage for construction engineers (disposable take-home pay) was set to be around 2.500 TL/month*§ [36].

In addition to its recommendations with regard the implementation of minimum wages, the ILO emphasizes that for a wage system to be fair and effective, it should be transparent, it should reward employees according to the difficulty and quality of their work and it should ensure that the motivated workers can earn substantially more than the minimum wage [33].

The ILO's recommendations on wages, in general, are in parallel to the views of modern behavioral scientists like Simon [37], Robert Dubin [38] — who support the 'Behavioral Theory of Wages'. Behavioral Theory of Wages claims that wages are determined by factors like the size and the prestige of the company, the strength of the union, the employer's concern to maintain the workers, the social norms, the traditions, the customers prevalent in the organization, the psychological pressures on the management, the prestige attached to specific jobs in terms of social status and the wages paid for similar positions in other firms, etc. [39]. These views are also supported by construction management related literature stating that wages of construction professionals should;

(1) reflect the value of compensable variables like;

- level of education [40-46],
- computer and foreign language skills [47-50],
- experience and seniority [40],[41],[46],[51],[52] and,

‡ 417 USD/month (1 USD = 3.00 TL as an average in 2016) ,
§ 833 USD/month

(2) reward individual and collective performance [40],[41],[46] where; completion of work in estimated time/ cost/quality; low rate of rework, compliance with occupational health and safety requirements, customer satisfaction and, skills related with; not only decision making, but also problem solving, planning, coordination, communication with and motivating subordinates, personality characteristics like honesty, punctuality, attitude and fairness towards workers are the critical performance determinants of construction engineers. [53-55].

(3) reflect inflation rate [56-57],

(4) avoid undue disparities in wages within the company or concerning the prevailing wages in the industry [32],[40],[56],[57] and

(5) reflect the complexity of the project, project budget, project location, i.e., city, country, the distance between the construction site and the town center [58].

Above listed literature is overviewed below.

2.1. Level of Education and Foreign Language Knowledge

Effect of level of education on wages is one of the most studied topics related to the wage determinants in different industries (Table 1). Linear regression analysis is the mostly preferred statistical analysis method. Findings generally show a positive correlation between education levels and wages (see Table 1).

Table 1 - Literature review on the effect of level of education on wage rates

Author	Nation	Sector	Method	Result
Bhattarai & Wisnievski [40]	England	Private	Linear Regression Adj. R^2= 0,922	Wages of employees getting training certificates are 4.3% higher on average than others.
Boudarbat et al. [41]	Canada	Private	Linear Regression	There is a positive relationship between education level and wage.
Nestić [42]	Croatia	Private	Linear and Quantile Regression	There is a positive relationship between education level and wage.
Liu & Zhang [43]	China	Private	Linear Regression Adj. R^2= 0,506	There is a positive relationship between education level and wage.
Addabbo & Favaro [44]	Italy	Private	Quantile Regression Adj. R^2= 0,33	The level of education leads to the closure of the wage gap between men and women.
Yang & Mayston [45]	China	Private	Probit Regression	Employees with higher levels of education are more likely to find a better job.
Iriondo & Perez-Amaral [59]	Europe	Private	Linear Regression	There is no relationship between education level and wage.
Morikawa [46]	Japan	Public and Private	Quantile Regression Adj. R^2= 0,44	There is a positive relationship between education level and wage.

Among the researchers presented in Table 1, Yang & Mayston [45] are the only ones to investigate the effect of foreign language knowledge on wages. By using Probit Regression Analysis, they determined that as the level of English knowledge increases, the wage increases by an average of 4.3%.

2.2. Age and Experience

Literature related to the effects of age and experience on wage levels show that while wages mostly increase by age and experience, they tend to decrease after a certain age (which is around 45 to 55). Table 2 shows the findings of previous studies.

Table 2 - Literature review on the effect of age and experience on wage rates

Author	Nation	Sector	Method	Result
Bhattarai & Wisnievski [40]	England	Private	Linear Regression Adj. R^2= 0,922	The age at which the wage reaches the maximum level is 45.8.
Boudarbat et al. [41]	Canada	Private	Linear Regression	Employees with the highest wage are aged 46-55.
Nestić [42]	Croatia	Private	Linear and Quantile Regression	Experience (up to 30 years) causes wages to increase.
Liu ve Zhang [43]	China	Private	Linear Regression Adj. R^2= 0,506	The wage earned increases as the working age increases.
Morikawa [46]	Japan	Public and Private	Quantile Regression Adj. R^2= 0,44	Employees with the highest wage are aged 50-55.

2.3. Individual Performance

Researchers like Kagioglou et al. [53], Dainty et al. [54], Cox et al. [60], Cheng & Li [55], Samuel et al. [61] and Nassar & Abourizk [62] studied evaluation criteria for professional performance of construction professionals. Kagioglou et al. [53] and Cox et al. [60] determined the most significant measures as the customer satisfaction, completion of work on estimated time and cost, work accidents involved and rework. On the other hand, Dainty et al. [54] stated the personality characteristics like honesty, punctuality, attitude, motivating oneself, ability to work with different team members and fairness towards subordinates to be more significant than other factors as performance determinants of professionals. Analytical Hierarchy Process (AHP) has been the most commonly used method for determining the performance criteria [55][62].

2.4. Prevailing Wages

Babecký et al. [56] and Galuscak et al. [57] both studied the effect of prevailing wages on determining the wages of professionals by using Probit Regression analysis. Babecký et al. [56] concluded that prevailing wages in Czech construction industry was significant in determining the wages. Galuscak et al. [57] additionally stressed the fact that small-sized

European construction companies, rather than medium-large ones, considered prevailing wages while determining the wage levels of their employees.

2.5. City of Work and Size of the Company

Idson and Feaster [63] and Nestić [42] reached to similar results showing that employees working in large companies earn more than employees working in small companies. Wage differences reach up to 39%. In the meantime, Morikawa [46] determined that wages change around 40% between large cities and small towns.

3. RESEARCH MATERIAL AND METHODOLOGY

A questionnaire survey was undertaken in 2016, to determine industry-wide applications related to wage determinants of construction engineers and wage policies of construction companies in Turkey. Questionnaires were distributed to both the construction engineers and, the company/human resources managers who are the part of wage determination process of the companies. 410 construction engineers and 305 company/human resources managers participated in the survey which provided a statistically significant sample size within 95% confidence level [64].

The first part of the questionnaire consisted of questions related to the demographic characteristics of the respondents, attributes of their work and monthly wages earned (disposable take-home pay). Compensable variables and performance determinants were listed according to the literature findings discussed above and were questioned in the second part of the questionnaire. A 9 Point Likert Scale (1-strongly disagree to 9-strongly agree) was used for scaling questions.

Descriptive statistical analysis, Lorenz curve [65] and Gini coefficients, Multinomial Logistic Regression analysis and Self Organizing Maps (SOM) were used to derive results from the questionnaire findings. These methods were used complementarily to each other in discussing the results; Gini coefficients and Regression analysis provided statistical information for the discussion of the results, and SOM maps enabled to track and to analyze the results visually.

4. RESULTS AND DISCUSSION

4.1. Demographics of the Respondents

Table 3 shows age distribution of the respondents. It is observed that while most of the company managers are over 30 years old, construction engineers are at younger ages on the average. When the frequency of the construction engineers are compared with the frequency of the members of the Chamber of Civil Engineers (based on the list provided for the current research by the Chamber of Civil Engineers) it is observed that the sample represents active working population of engineers.

Table 3 - Age Distribution of the Respondents

Age Range	Frequency (%) Company Managers	Frequency (%) Construction Engineers	Frequency (%) Construction Engineers (Members of Chamber of Civil Engineers in 2017)
20-25	4.7	19.7	21.0
26-30	24.0	32.0	19.2
31-40	39.0	28.6	26.9
41-50	20.7	14.0	14.0
51-60	9.3	5.7	11.7
> 60	2.3	-	7.2

Table 4. shows the business areas of the respondents. Distribution of the respondents is in good agreement with the statistical data on Turkish construction industry showing that 67-77% of construction investments are on building projects and 23-33% are on infrastructure projects [2-3].

Table 4 - Business Areas of the Respondents

Business Area	% of Respondents	
	Company/Human Resources Managers	Construction Engineers
Building Projects	67.21	63.7
Infrastructure Projects	35.40	14.1
Prefabricated Production	17.04	5.6
Building Inspection	7.86	16.6

4.2. Wages and Wage Distribution Inequalities

Table 5 shows the answers of construction engineers related to their monthly wages in 2016. Results show that 0,73 % of the respondents do not even earn the national minimum wage of 1.250 TL/month. In total 24.87 % of the respondents earn less than 2.500 TL/ month, i.e., the disposable take-home pay value of the legal minimum monthly wage for construction engineers in 2016.

Figure 1 shows the Lorenz curve drawn according to the construction engineers' responses related to their monthly wages. The graph plots the percentiles of the cumulative population of the construction engineers on the x-axis, and their cumulative income (cumulative monthly wages) on the y-axis. The straight diagonal line represents perfect equality in income distribution (Gini coefficient equals to 0); the curve which lies under it (Lorenz curve) shows the actual distribution of wages according to the engineers' answers.

Table 5 - Monthly Wages of Construction Engineers in Turkey

Wage (TL/month)	Number of Respondents	% of respondents	Cumulative % of respondents
<1.250	3	0,73	0,73
1.250-2.500	99	24,14	24,87
2.501-4.000	210	51,22	76,09
4.001-6.000	49	11,95	88,04
6.001-8.000	36	8,78	96,82
8.001-10.000	8	1,95	98,77
>10.000	5	1,23	100
Total	410	100	100

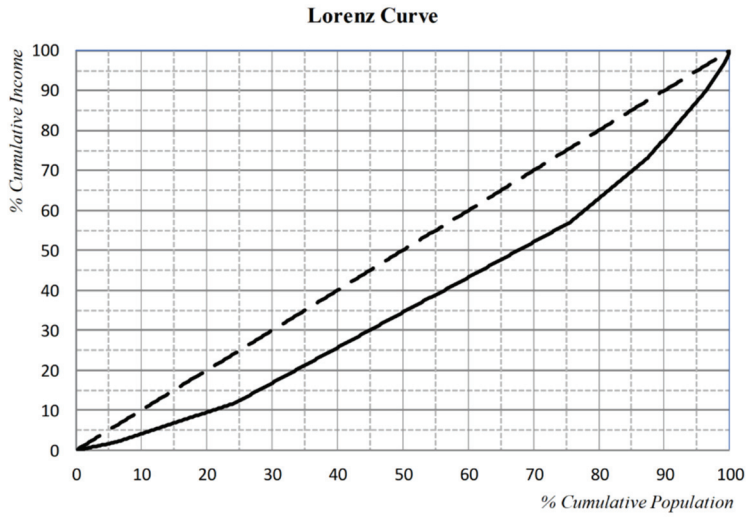

Figure 1 - Lorenz Curve for Wages of Construction Engineers in Turkey

Gini coefficient, which is a measurement of inequality, is expressed as the ratio of the area that lies between the line of perfect equality and the Lorenz curve to the total area under the line of perfect equality. Gini coefficient can range from 0 (perfect equality) to 1 (absolute inequality). Some Gini coefficients related to the wages of construction engineers were calculated by utilizing the following formula [66]. The Gini coefficient for the whole sample was determined to be 0,2526. Gini coefficients for different categories of the compensable variables that affect the wages were also calculated, and these are discussed in the following sections.

$$G = 1 - \sum_{i=1}^{N} [(X_i - X_{i-1})(Y_i + Y_{i-1})]$$

where;

G: Gini coefficient

X_i: Cumulative % of population corresponding to the i^{th} individual

Yi: Cumulative % of population income corresponding to the i^{th} individual

N: number of individuals

Statistics on income inequalities provided by international institutions like UN, World Bank, OECD or by governments are generally country or region based, and statistics on income inequalities amongst professionals is limited. Only one study related to the income distribution among construction professionals has been found during the literature review. Gini coefficient for Pakistani professionals was calculated to be 0,280 in that study [67] (see Table 6). Additionally, Gini coefficient for civil engineers working in the USA was roughly calculated to be 0,334 during the current research by using the data published by OECD [68] on civil engineers' incomes in the USA in 2016 (Table 6).

According to Turkish Statistical Institution figures [4], Gini coefficient for the working-age population between 18-65 in 2016 in Turkey is 0,40, and according to UNDP [69] figures it is around 0,40 for USA and 0,30 for Pakistan (Table 6). When Gini values of three countries are compared, it is observed that the income inequality for the construction professionals is the least in Turkey, income inequality for professionals in Pakistan is very close to their national average and, income inequality is not related to wealth.

Table 6 - Gini Coefficients for Working-Age Population and Construction Professionals in Turkey, USA and Pakistan

	Turkey	USA	Pakistan
Gini Coefficient for Working Age Population	0,40	0,40	0,30
Gini Coefficient for Construction Industry Professionals	0,2526	0,334	0,280

4.3. Effect of Inflation on Wages

As stated above, the inflation rate is a significant determinant of the amount of increase in minimum wages and is recommended to be reflected as an annual increase if the companies prefer to implement a fair wage policy. When Turkish construction engineers' answers related to the rate of increase in their wages between 2015 and 2016 are analyzed, it is observed that only 36% of them had an increase that is equal to or more than the official inflation rate of 8% (Table 7).

Table 7 - Increase % in the Wages of Construction Engineers Between 2015 and 2016

Increase %	Number of Respondents	% of Respondents	Cumulative % of Respondents
0 – 0.9	140	34.14	34.14
1 – 2.9	33	8.0	42.14
3 – 4.9	29	7.1	49.24
5 – 7.9	59	14.39	63.63
8 – 9.9	58	14.14	77.77
10 – 12.9	28	6.83	84.60
13 – 14.9	23	5.61	90.21
15 – 17.9	10	2.44	92.65
18 – 20.9	9	2.3	94.95
21 – 23.9	4	0. 9	95.85
24 – 25.9	3	0.73	96.58
26 – 28.9	3	0.73	97,31
29 – 30.9	3	0.73	98.04
>30.9	8	1.96	100.0
Total	410	100.0	

4.4. Effect of Compensable Variables on Wages and Wage Inequalities

Multinomial Logistic Regression analysis is preferred to examine the relationship between the independent and the dependent variables when the dependent variable includes three or more categories and when favouring one class of independent variables over another does not depend on the presence or absence of other irrelevant alternatives. Any category of the dependent variable is considered as the reference category, and other categories are analyzed concerning this category. For the current research, dependent variable ‘Monthly Wage' was represented by three categories which are ‘low,' ‘medium' and ‘high' (see Table 8). Independent variables were also categorized as shown in Table 8.

Variables ‘country of the project', ‘computer skills' and ‘travelling distance between the project site and the town centre' were excluded from the analysis due to the little variability and unsuitability for categorization. ‘Project size' was excluded due to the number of missing responses (which was around 40% of the responses). ‘Seniority' was excluded due to its high collinearity with the variable ‘experience.'

Pearson and Deviance significance values (greater than 0.05, see Table 9) show that model fit is statistically acceptable [70-71]. Additionally, Nagelkerke Pseudo R^2 Coefficient show that independent variables can explain 45.9% of the dependent variable ‘Monthly Wage' which is also statistically satisfactory.

Table 8 - Categories of Variables and Number of Respondents in Each Category

Variable	Category	Number of Respondents	% of Respondents
Monthly Wage	< 2500 TL (Low Wage)	102	24.88
	2500 – 4000 TL (Moderate Wage)	210	51.22
	> 4000 TL (High Wage)	98	23.90
Education	Associate Degree	22	5.36
	Undergraduate Degree	329	80.24
	Graduate Degree	59	14.40
Experience	0-2 years	77	18.78
	3-5 years	96	23.41
	6-10 years	87	21.22
	11-20 years	99	24.15
	> 20 years	51	12.44
Company Size	< 10	100	24.39
	11-50	162	39.51
	51-250	88	21.46
	> 250	60	14.64
Project Type	Prefabrication/Low Complexity	23	5.60
	Building Inspection/Low Complexity	68	16.58
	Building Construction /Medium Complexity	261	63.66
	Infrastructure Projects /High Complexity	58	14.16
City	1. Group Cities (İstanbul)	158	38.53
	2. Group Cities (Ankara – İzmir – Bursa)	82	20.01
	3. Group Cities (Others)	170	41.46
Foreign language	Scores by using Likert Scale 9.	410	100

Reference category of the dependent variable was determined by comparing the accuracy percentage between actual and estimated values for the three categories as shown in Table 10. Results show that accuracy of the model is 64.8%, which is very satisfactory for human resource management related studies. Results also indicate that the model works more accurately in comparisons between ‘low’ and ‘high’ wage categories rather than comparisons with 'medium'

wage categories. Thus, 'low' wage category was accepted as the reference category for further analysis (see Table 11).

Table 9 - Model-Fit Indicators

Model	Model-Fit Criteria	Likelihood Ratio Tests		
	-2 Log Likelihood	Chi-square	Df	Sig.
Constant	661.834			
Final Model	482.758	179.076	32	0.000
Pearson		497.282	524	0.794
Deviance		438.294	524	0.997
Nagelkerke Pseudo R^2		0.459		

Table 10 - Estimation Classification of Logistic Regression Model

Category/Actual	Category/Estimated			
	< 2500 TL	2500 – 4000 TL	> 4000 TL	Accuracy %
Low (< 2500 TL)	59	39	4	57,8
Medium (2500 – 4000 TL)	22	167	21	79,5
High (> 4000 TL)	3	39	56	57,1
Cumulative % Frequency	20,4	59,7	19,9	64,8

The exponential beta coefficient, Exp (B) in Table 11, represents the change in the dependent variable (i.e., monthly wage in the current research) which is associated with a one-unit change of the corresponding independent variable via the reference category. The Exp (B) results will be interpreted in the following paragraphs together with Gini coefficients and Self Organizing Maps (SOM).

SOM maps, given in Figure 2, were produced by using the SOM model developed by Oral and Oral [64]. SOM which is an unsupervised neural network algorithm converts complex, nonlinear statistical relationships between high-dimensional data items into simple geometric relationships on a low-dimensional display. It compresses information by preserving the primary topological and metric relationships of the primary data items on display. The SOM maps presented in this study display the relationships between wage and the level of education, experience, project type, size of the company and city categories. The relationship between the compensable variables and wage can be analyzed in detail if all the maps are evaluated together. To give an example; the low wage region on the upper right corner in Figure 2 (a) is due to the employees with six or more years' experiences that have either an associate or an undergraduate degree (Figure 2 (c)) and that is either a building construction engineer or a building inspector (Figure 2 (d)) in medium-sized companies (Figure 2 (e))

which is not located in Istanbul (Figure 2 (f)). Therefore, evaluation of all the maps given in Figure 2 enables observation of hidden relationships that may not be detected through statistical analysis.

Table 11 - Multinomial Logistic Regression Analysis Results

WAGE[a]		B	Std. Error	Wald	df	Sig.	Exp(B)	95% Confidence Interval for Exp(B)	
								Lower Bound	Upper Bound
Constant		-0.607	1.482	0.168	1	0.682			
Foreign Language**		0.157	0.095	2.705	1	0.100	1.170	0.970	1.410
Education	Associate degree	0b	.	.	0	.	.	.	.
	Undergraduate degree*	2.400	1.187	4.087	1	0.043	11.020	1.076	112.876
	Graduate degree*	3.917	1.343	8.511	1	0.004	50.234	3.616	697.905
Experience	0-2 years*	-1.805	0.770	5.499	1	0.019	0.164	0.036	0.744
	3-5 years	-0.509	0.692	0.541	1	0.462	0.601	0.155	2.333
	6-10 years	0b	.	.	0	.	.	.	.
	11-20 years*	1.296	0.654	3.925	1	0.048	3.656	1.014	13.181
	> 20 years	0.076	0.699	0.012	1	0.913	1.079	0.274	4.247
Building Construction /Medium Complexity		-0.527	0.642	0.674	1	0.412	0.591	0.168	2.077
Prefabrication */Low Complexity		-2.474	1.019	5.899	1	0.015	0.084	0.011	0.620
Building Inspection*/Low Complexity		-1.993	0.800	6.214	1	0.013	0.136	0.028	0.653
Infrastructure Projects /High Complexity		0b	.	.	0	.	.	.	.
City	İstanbul*	1.135	0.484	5.509	1	0.019	3.111	1.206	8.026
	2. Group**	0.961	0.530	3.291	1	0.070	2.614	0.926	7.379
	3. Group	0b	.	.	0	.	.	.	.
Company Size	< 10* (small)	-1.408	0.598	5.554	1	0.018	0.245	0.076	0.789
	11-50*(medium)	-1.614	0.560	8.313	1	0.004	0.199	0.066	0.596
	51-250 (large)	0b	.	.	0	.	.	.	.
	> 250 (very large)	-0.107	0.770	0.019	1	0.889	0.898	0.198	4.067

a. 'Low' wage is considered as the reference category.

b. Coefficients are calculated with reference to the reference categories.

* It is significant at the 95% confidence level.

** It is significant at the 90% confidence level

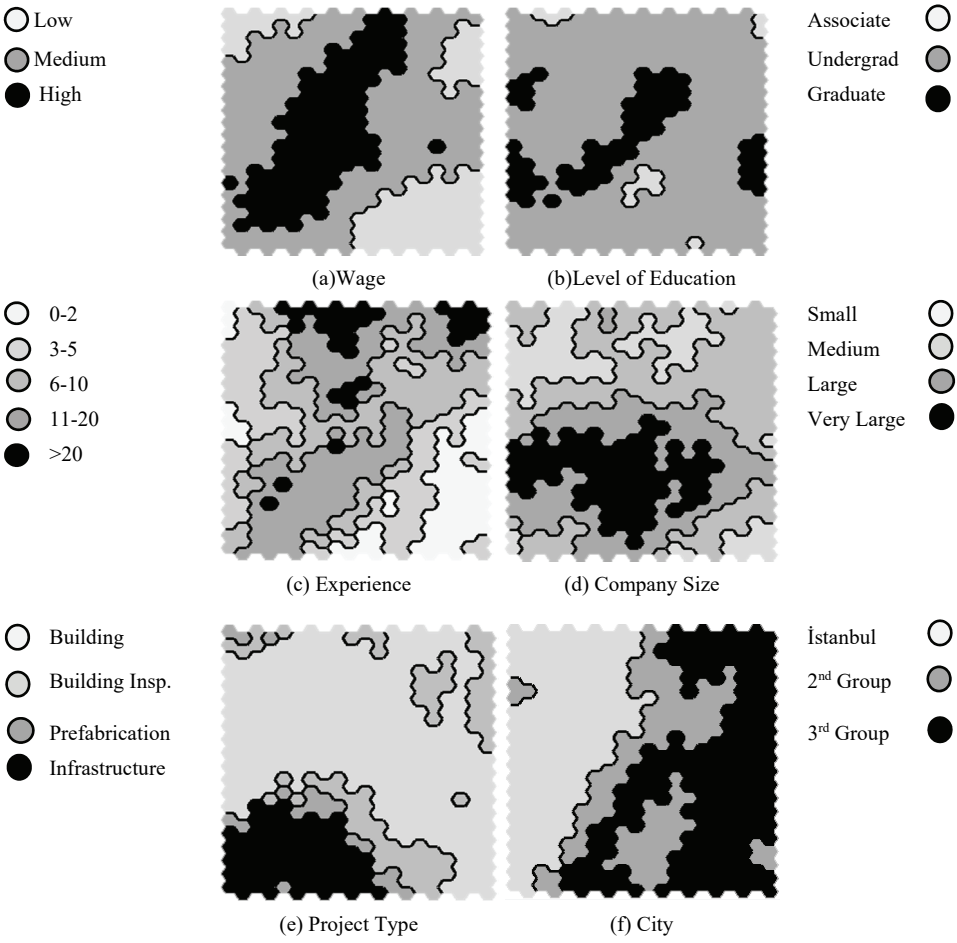

Figure 2 - SOM maps

Table 12 - Gini Coefficients for Compensable Variables

		Gini
	Overall	0.2526
Education	Associate degree	0.3814
	Graduate degree	0.2354
	Postgraduate degree	0.2685
Experience	0-2 years	0.2622
	3-5 years	0.1692
	6-10 years	0.1912
	11-20 years	0.2827

Table 12 - Gini Coefficients for Compensable Variables (continue)

		Gini
Company size	Overall	0.2526
	<10 employees (small)	0.2260
	11-50 (medium)	0.2206
	51-250 (large)	0.247
	>250 (very large)	0.4629
	>20 years	0.3205
Project Type	Building construction	0.2070
	Building inspection	0.2947
	Prefabrication	0.2596
	Infrastructure	0.2655

Finally, as informed previously, Gini coefficients were calculated for each category of the compensable variables to analyze the wage inequalities in the industry. The findings are presented in Table 12.

Based on the above-presented results, effects of compensable variables on wages of construction engineers in Turkey are discussed in the following paragraphs.

4.4.1. Level of Education

Results in Table 8 show that around 5% of respondents are construction technicians (Associate degree holders) by profession. They undertake the responsibilities of a construction engineer on site. It was indeed a widespread practice to employ experienced construction technicians to conduct the duties of site managers until an amendment in the related regulation [72] in 2014. Construction technicians were prohibited from undertaking legal responsibilities of construction projects by this amendment. Meanwhile, some construction companies have continued to work with these practitioners. The maps in Figures 2(a) and 2(b) show that none of these practitioners earns a 'high' wage. When the maps in Figure 2(b) and (d) are analyzed together, it is observed that all of these professionals who work in small-sized companies earn 'low' wages. Meanwhile, Gini coefficient being the highest for associate degree holders among the three categories of level of education is an indicator of the divergence between wages (Table 12). However, a few numbers of respondents with some outliers may be affecting the value of the Gini coefficient.

Results in Table 11 show that the odds to earn 'high' wages rather than 'low' wages for the engineers with undergraduate degrees or graduate degrees are respectively 11.020 and 50.234 times more than for associate degree holders. Meanwhile, a graduate degree provides 4.56 (= 50.234/11.020) times more chance to earn a 'high' wage rather than a 'low' wage than an 'undergraduate' degree. The map in Figure 2(b) supports these findings by showing that both

undergraduate and graduate degree holders earn 'high' wages, and the relative ratio of 'high' wages are higher for the graduate degree holders. These findings are in good agreement with the literature review findings presented in Table 1. As discussed by previous studies, there is a positive relationship between the wages paid to employees and their education levels. Like in many industries, the employers in the construction industry consider the benefits they can gain from the employees when determining the employee wages; resulting in the technical knowledge and the competencies that are acquired via academic degrees to be an important wage determinant.

4.4.2. Experience

The SOM maps in Figure 2(a) and 2(c) show that engineers with any experience may earn 'low' wages. However, the regression analysis results show that the odds of earning a 'high' wage rather than a 'low' wage for 11-20 years' experienced engineers are 22.29 (3.656/0.164) and 3.656 times more concerning engineers with experiences of 0-2 years and 6-10 years, respectively. Meanwhile, experience over 20 years does not guarantee a 'high' monthly wage. Gini coefficient being the highest for the most experienced group of engineers (Table 12) and literature findings given in Table 2. are in support of the regression analysis results showing that while some experienced engineers earn quite a lot, others earn quite a little. Such a deviation is because while some engineers at the retirement age continue to work in high positions in construction projects, others continue to work as senior building inspectors or in similar low profile positions, earning low wages after retirement. The variations between the wages of the experienced engineers are also observed in the map in Figure 2(c). The map additionally supports the regression analysis results by showing that 'high' wages are earned more by the 11-20 years' experienced engineers rather than others (Figure 2(c)). The map also shows that none of the least experienced engineers earn 'high' wages and engineers with 3-5 years' experience only earn 'high' wages if they work either in Istanbul or small-sized companies in other cities.

4.4.3. Company Size

Parallel to the results of Idson and Feaster [63] and Nestić [42], the map in Figure 2(d) shows that while the vast majority of engineers working in large and very large companies earn 'high' wages. Meanwhile, engineers with less than five years' experiences earn 'low' wages in these companies (Figure 2(c) and 2 (d)). The value of the Gini coefficient, being the highest (0.4629), additionally indicates that while the majority of engineers in very large companies earn 'high' wages, there exist engineers who work in these companies with extremely 'low' wages. Meanwhile, the results in Table 11 show that working in very large companies rather than large companies do not affect wages significantly. However, other company sizes affect the wages and the odds for an engineer working in a large-sized company to earn 'high' wage is 5.025 (=1/0.199) times more than for an engineer working in a medium-sized company, and 4.08 (=1/0.245) times more than for an engineer working in a small- sized company. Company size in construction industry is one of the important indicators of the company's ability to engage in large projects continuously and have higher turnovers. Thus, these companies are able to allocate higher budgets to human resources in order to keep their employees long term.

4.4.4. Project Type and Complexity:

The map in Figure 2(e) shows that vast majority of engineers working in infrastructure projects earn 'medium' or 'high' wages; only low (less than five years) experienced engineers earn 'low' wages. Meanwhile, engineers working in building inspection are more likely to earn 'low' or 'medium' wages. (Figure 2 (c) and 2(e)). Results in Table 11 additionally show a significant difference between the wages of construction engineers working in low complexity (i.e., building inspection and prefabrication) projects and the wages of the ones working in high complexity (infrastructure) projects. Results show that the odds to earn a 'high' wage rather than a 'low' wage for construction engineers when working in infrastructure projects are 7.35 (1/0.136), and 1.90 (=1/0.084) times more than working in building inspection, and in prefabrication projects, respectively. In the meantime, it is observed that wage inequalities for the four project complexity categories are similar as none of the Gini coefficients are distantly different than the others (see Table 12).

4.4.5. City of Work

'City of work' is categorized into three groups for regression analysis. The first group only includes Istanbul which has the highest cost of living in Turkey. The second group consists of Ankara, Izmir, and Bursa which follow Istanbul concerning the cost of living. The third group consists of other cities. The results show that the odds to earn 'high' wage rather than 'low' wage in Istanbul is 1.19 and 3.11 times more than the second group and the third group of cities, respectively. Statistical data provided by TSI [4] show that Gini coefficient for working population is 0.398 for Istanbul, which is the highest among all of the cities in Turkey. On the other hand, Gini coefficient for construction engineers is determined to be the lowest for Istanbul (Table 12). In support of the regression results, the map in Figure 2(f) shows that the vast majority of engineers working in Istanbul or second category of cities earn 'medium' or 'high' wages while 'low' wages dominate the cities in the third category. The analysis results show that cost of living is an important criterion in wage agreements as the wages are required to fulfill the needs of the employees.

4.4.6. Foreign Language Skills

Construction engineers were asked to rate their level of foreign language skills required for their occupation by using Likert Scale 9. Exp (B) value in Table 11which is 1.170 (within 90% confidence level) means that; the odds to earn a 'high' wage rather than a 'low' wage is 4.10 times more for an engineer who uses foreign language at a level of 9 out of 9 than the odds of an engineer who does not use any foreign languages at all. These results show that foreign language skills increase wage rates more in Turkish construction companies than in Chinese companies (as determined by Yang & Mayston [45]). The difference may be related to the differences between supply-demand balance of these two countries; as according to the English proficiency index (2017) by Education First, Turkey ranks 62th and China 36th between 80 countries [73]; which shows that English proficiency of the individuals is very low in Turkey and results foreign language skills increase wage rates more in Turkish construction companies than in Chinese companies.

4.4.7. Effect of Performance on Wages- Employee and Employer Perspectives

Only 6% of the construction engineers stated that their employer evaluated their performance and returned it as a bonus or as an increase in their wages. These engineers were then asked to choose the variables that were assessed by their employer during the performance appraisal. Their responses are presented in Table 13.

Results in Table 13 show that problem solving, planning, organization and coordination abilities related to the completion of tasks within a pre-determined schedule and quality specifications are the most frequently valued criteria during performance evaluation. Meanwhile, unlike the literature findings, level of compliance with health and safety rules and level of the number of accidents within the unit are not assessed as much as the other criteria, and that may be the result of two different approaches. First one is that complying with health and safety procedures and avoiding accidents is indispensable during construction works and should not be an issue to be considered during the performance appraisal. The second one is just the opposite; these issues are not of any concern for the Turkish construction companies.

Table 13 - Performance Indicators of Construction Engineers

Variable	% of Respondents	Rank
Problem-solving ability	5.66	1
Organization and coordination ability	5.66	1
On time completion of a task	4.58	2
Planning ability	4.58	2
Quality of work	4.58	2
Ability in finding construction faults	4.58	2
Productivity	4.31	3
Relations with customers	4.31	3
Level of compliance with health and safety rules	3.77	4
Social relationships with co-workers	3.77	4
Ability to motivate subordinates	2.16	5
Rate of rework	1.08	6
Number of accidents in his/her unit	0.81	7

Table 14 summarizes company/human resources managers' responses related to their wage evaluation criteria of construction engineers. Individual performance is the most significant wage determinant from the perspective of the employers. Experience, seniority, and level of education follow it. In contrary to regression analysis results foreign language skills is the least important criterion for the employers; although high coefficient of variation (V= 0.60) shows that there is not a good agreement amongst the employers related with the issue.

Table 14 - Employers' Preferences Related with Wage Determinants

Rank	Determinant	Mean Score	Std. Dev.	Coef. of Var. (V)
1	Individual performance	7.87	1.58	0.20
2	Experience	7.63	1.80	0.24
3	Seniority	7.05	2.11	0.30
4	Level of education	6.89	2.25	0.33
5	Computer skills	6.66	2.43	0.36
6	Inflation	6.59	2.58	0.39
7	Project complexity	6.45	2.47	0.38
8	Wages/salaries of other employees in company	6.38	2.45	0.38
9	Project budget	6.23	2.57	0.41
10	City	5.97	2.49	0.42
11	Distance between project and town centre	5.66	2.78	0.49
12	Wages/salaries of other employees in other companies	5.65	2.60	0.46
13	Country	5.45	2.98	0.55
14	Foreign language skills	4.22	2.83	0.60

5. CONCLUSIONS

Turkish construction industry which is one of the largest in the world faces two crucial problems regarding the employment of construction engineers. While on the one hand high numbers of engineers are unemployed; on the other hand, engineers with jobs are dissatisfied with what they earn. Although government policies are important determinants of the unemployment rates, awareness related to the compensation factors which affect the wages is an important issue on the individual basis in getting a job. In parallel, a fair wage policy is essential on company basis in keeping high motivation and low turnover of employees.

A wage system to be fair and adequate, it should reward employees according to the difficulty and quality of their work, and ensure that motivated and productive workers can earn substantially more than the legal minimum wage. In this approach, legal restrictions are the first constraints to be fulfilled. Unfortunately, current research on Turkish construction industry practices shows that nearly a quarter of construction engineers in Turkey do not earn the legal minimum wage that is set by the legislation each year for engineers and architects. Additionally, an annual increase in their wages is less than the official inflation rate, for most.

When it comes to ensuring fair wages to the motivated workers; employers claim that they give priority to performance evaluation during wage determination which is, according to engineers' claims, very rarely encountered in practice. Meanwhile, the difficulty of work is observed to be reflected on the wages of construction engineers; as engineers working in high

complexity projects or in the projects which require foreign language skills or higher levels of education are observed to earn more than their peers.

When wage inequalities are analyzed, it is observed that overall income inequality for construction engineers is not as high as the national average and the available international values. In the meantime, wage inequalities differ concerning the different categories of compensation variables.

In addition to presenting the constituents of a fair wage for construction engineers, findings of the current research will be beneficial to academicians, construction engineers, and company managers. By demonstrating the wage practices in the construction industry, determinants of wage rates, and the priorities of employers regarding the performance appraisals, the findings will help engineers, especially new graduates, in building realistic wage expectations. Findings will also be of use by the academicians as they reveal the necessity of the inclusion of practical issues in the course contents that would improve the problem solving, organization and coordination skills of the students. Finally, findings will be beneficial to construction company managers in implementing wage policies which would consider prevailing wages and industry-wide applications. In parallel, findings are expected to draw the attention of the government bodies, by presenting the deviations between legally expected and practically paid in the industry.

6. LIMITATIONS AND RECOMMENDATIONS FOR FUTURE WORK

While the current study focused on the determinants of construction engineers' wages and wage policies of Turkish construction companies only, its findings can be taken as a basis for further studies especially in developing countries. Larger sample sizes are recommended for these studies, as although the total number of respondents of the current study was statistically significant to derive conclusions, increasing number of respondents in each category of compensable variables would lead to the determination of more realistic Gini coefficient values.

The discussion in the current paper shows that the SOM maps help to interpret data by presenting the relationship between different variables in a simple visual format. In the meantime, SOM is a type of artificial neural network which can be utilized for prediction. Further developments of the current research, will focus on developing a SOM-based model that would help to predict wages of construction engineers under given conditions.

Finally, findings of the current survey can be used to create artificial intelligence based wage systems. Wages and salary increases can be more objectively and fairly determined using algorithms such as fuzzy logic and artificial neural networks. In this manner, contemporary intelligent wage systems can help for effective motivation and management of human resources in construction industry.

Acknowledgements

The first author of this study has been supported by TUBITAK (The Scientific and Technological Research Council of Turkey) with post graduate scholarship. The first author would like to express his thanks to TUBITAK for this support.

The authors would like to thank to Çukurova University, Scientific Research Project Funding (CU BAP) for their financial support [Project number: FBA-2016-5779].

References

[1] MET. Company Reports 2016. Ministry of Economy of Turkey, 2016.

[2] Buildecon. Turkey Construction Market Report 2012. Turkey, 2012.

[3] TSI. Construction Labor Input Indices 2016. Turkish Statistical Institute, [Online]. Available: http://www.turkstat.gov.tr/PreTablo.do?alt_id=1023, Accessed November 8, 2017, 2016.

[4] TSI. Construction Seasonally and Calendar Adjusted Gross Wages-Salaries Index and Percentage Changes (2010=100). Turkish Statistical Institute, [Online]. Available: http://www.turkstat.gov.tr/PreTablo.do?alt_id=1023, 2017, Accessed November 8, 2017.

[5] UCTEA. Member Information 2016. Union of Chambers of Turkish Engineers and Architects, [Online]. Available: https://www.tmmob.org.tr/icerik/tmmob-uye-sayisi-510-bini-asti, Accessed November 8, 2017.

[6] Marshall, A. Principles of political economy. Maxmillan, New York, 1890.

[7] Davidson, J. The Bargain Theory of Wages. New York; London: GP Putnam, 1898.

[8] Business Roundtable Integrating Construction Resources and Technology into Engineering, Report No. B-1A, Construction Industry Cost Effectiveness Project Report, New York, 1982.

[9] Abu-Hijleh, S. F., Ibbs, C. W. Schedule-based Construction Incentives. Journal of Construction Engineering and Management, 115(3), 430-443,1989.

[10] Huselid, M. A., The Impact of Human Resource Management Practices on Turnover, Productivity, and Corporate Financial Performance. Academy of Management Journal, 38(3), 635-672,1995.

[11] Igalens, J., & Roussel, P. A Study of The Relationships Between Compensation Package, Work Motivation and Job Satisfaction. Journal of Organizational Behavior, 1003-1025,1999.

[12] Fay, C. H., Thompson, M. A. Contextual Determinants of Reward Systems' Success: An Exploratory Study. Human Resource Management, 40(3), 213-226, 2001.

[13] Doloi, H. Analysis of Incentivised Remuneration Schemes in Construction Industries. 22st International Symposium on Automation and Robotics in Construction, 11-14 September, Ferrara, Italy, 2005.

[14] Gazioğlu, S., Tansel, A. Job Satisfaction in Britain: Individual and Job-Related Factors. Applied Economics, 38(10), 1163-1171, 2006.

[15] Brewster, C., Sparrow, P., Vernon, G. International Human Resource Management. 2nd ed., 2007.

[16] Enshassi A., Mohamed S., Abu Mustafa Z., & Mayer P. E. Factors Affecting Labour Productivity in Building Projects in The Gaza Strip. Journal of Civil Engineering and Management, 13(4), 245-254, 2007.

[17] Gooderham, P., Parry, E., Ringdal, K. The Impact of Bundles of Strategic Human Resource Management Practices on the Performance of European Firms. The International Journal of Human Resource Management, 19(11), 2041-2056, 2008.

[18] Randeree, K., Ghaffar Chaudhry, A. Leadership–Style, Satisfaction and Commitment: An Exploration in The United Arab Emirates' Construction Sector. Engineering, Construction and Architectural Management, 19(1), 61-85, 2012.

[19] Kazaz A., Manisalı E., Ulubeyli S. Effect of Basic Motivational Factors on Construction Workforce Productivity in Turkey. Journal of Civil Engineering and Management, 14(2), 95-106, 2008.

[20] Williams, M. L., Brower, H. H., Ford, L. R., Williams, L. J., & Carraher, S. M. A Comprehensive Model and Measure of Compensation Satisfaction. Journal of Occupational and Organizational Psychology, 81(4), 639-668, 2008.

[21] Arashpour, M., Arashpour, M. Important Factors Influencing Personnel Performance of Construction Companies. Economics, Business and Management, Vol.2., 32-37, 2011.

[22] Arumugam, V. C., Mojtahedzadeh, R. The Impact of Human Resource Management Practices on Financial Performance of Malaysian Industries. International Research Journal of Finance and Economics, 80, 49–54, 2011.

[23] Mudor, H., & Tooksoon, P. Conceptual Framework on The Relationship Between Human Resource Management Practices, Job Satisfaction, and Turnover. Journal of Economics and Behavioral Studies, 2(2), 41-49, 2011.

[24] Siems, F. U., Goelzner, H., Moosmayer, D. C. Reference Compensation: A Transfer of Reference Price Theory to Human Resource Management. Review of Managerial Science, 6(2), 103-129, 2012.

[25] Jarkas, A. M., Radosavljevic, M. Motivational Factors Impacting the Productivity of Construction Master Craftsmen in Kuwait. Journal of Management in Engineering, 29(4), 446-454, 2012.

[26] Gupta, N., Shaw, J. D. Employee Compensation: The Neglected Area of HRM Research. Human Resource Management Review, 24(1), 1-4, 2014.

[27] Chih, Y.Y., Kiazad, K., Zhou, L., Capezio, A. Li, M., Restubog, S.L.D. Investigating Employee Turnover in the Construction. Journal of Construction Engineering and Management, 142(6), 2016.

[28] Tanriverdi, H., Çakmak, C., Altindag, E. The Relationship of Organizational Culture and Wage Policies in Turkish Family Firms. Business Management Dynamics, 5(7), 1-16, 2016.

[29] Berber, N., Morley, M. J., Slavić, A., Poór, J. Management Compensation Systems in Central and Eastern Europe: A Comparative Analysis. The International Journal of Human Resource Management, 28(12), 1661-1689, 2017.

[30] Akerlof, G. A. Labor Contracts As Partial Gift Exchange. The quarterly journal of economics, 97(4), 543-569, 1982.

[31] Akerlof, G. A., & Yellen, J. L. The Fair Wage-Effort Hypothesis and Unemployment. The Quarterly Journal of Economics, 105(2), 255-283, 1990.

[32] ILO. "Definition of Wage" [Online]. Available: http://www.ilo.org/global/topics/wages/lang--en/index.htm, 2017, Accessed November 8, 2017.

[33] ILO, "General Survey concerning the Minimum Wage Fixing Convention, 1970 (No. 131), and the Minimum Wage Fixing Recommendation, 1970 (No. 135), Committee of Experts on the Application of Conventions and Recommendations". International Labour Organization. [Online]. Available: http://www.ilo.org/global/standards/WCMS_235303/lang--en/index.htm, Accessed November 7, 2017.

[34] Korkmaz, A., Avsallı, H. Türkiye'de Asgari Ücretin Hukuksal Yönü. Journal of Alanya Faculty of Business, 4(2), 2012.

[35] Labour Law 4857., [Online]. Available: http://turkishlaborlaw.com/turkish-labor-law-no-4857/19-4857-labor-law-english-by-article, Accessed November 8, 2017, 2003.

[36] UCTEA. "Meeting Decisions (19.12.2015)." Union of Chambers of Turkish Engineers and Architects, [Online]. Available: https://www.tmmob.org.tr/belgeler/toplanti-kararlari-28, 2015, Accessed November 8, 2017.

[37] Simon, H.A., "Behavioral economics. In: Eatwell, J., Millgate, M., Newman, P. (Eds.)", The New Palgrave: A Dictionary of Economics, Macmillan, London, 1987.

[38] Dubin, R. Theory building: Revised Ed. Free Press, 1978.

[39] Essays, UK. Economic and Behavioural Theories in Compensation Economics Essay. November 2013. [Online]. Available: https://www.ukessays.com/essays/economics/economic-and-behavioural-theories-in-compensation-economics-essay.php?vref=1 Accessed November 7, 2017.

[40] Bhattarai, K. R., Wisniewski, T. Determinants of Wages and Labour Supply in The UK. Chinese Business Review, 16(3), 126-140, 2002.

[41] Boudarbat, B., Lemieux, T., Riddell, W.C. Recent Trends in Wage Inequality and The Wage Structure in Canada. Dimensions of Inequality in Canada, University of British Columbia Press, Vancouver, Canada, 2006.

[42] Nestić, D. The Determinants of Wages in Croatia: Evidence From Earnings Regressions. 65th Anniversary Conference of the Institute of Economics, 18-19 November 2004, Zagreb, Croatia, 2005.

[43] Liu L., & Zhang C. Wages for Migrant Workers in The Pearl River Delta: Determining Factors. Social Sciences in China, 29(3), 104-120, 2008.

[44] Addabbo, T., Favaro, D. Gender Wage Differentials by Education in Italy. Applied Economics, 43(29), 4589-4605, 2011.

[45] Yang, J., & Mayston, D. Impact of Overeducation on Wages in China. Chinese Economy, 45(2), 65-89, 2012.

[46] Morikawa, M. A Comparison of The Wage Structure between the Public and Private Sectors in Japan. Journal of the Japanese and International Economies, 39, 73-90, 2016.

[47] Ginsburgh, V. A., Melitz, J., & Toubal, F. Foreign Language Learning: An Econometric Analysis. CEPR Discussion Paper No. DP10101, 2014.

[48] Di Paolo, A., & Tansel, A. Returns to Foreign Language Skills in a Developing Country: The Case of Turkey. The Journal of Development Studies, 51(4), 407-421, 2015.

[49] Ginsburgh, V. A., Melitz, J., Toubal, F. Foreign Language Learning, and Trade. Review of International Economics, 25(2), 320-361, 2017.

[50] Chen, Z., Ge, Y., Lai, H., & Wan, C. Globalization and Gender Wage Inequality in China. World Development, 44, 256-266, 2013.

[51] Dainty, A. R., Cheng, M. I., Moore, D. R. Competency-based Model for Predicting Construction Project Managers' Performance. Journal of Management in Engineering, 21(1), 2-9, 2005.

[52] Ogunlana, S., Siddiqui, Z., Yisa, S., & Olomolaiye, P. Factors and Procedures Used in Matching Project Managers to Construction Projects in Bangkok. International Journal of Project Management, 20(5), 385-400, 2002.

[53] Kagioglou, M., Cooper, R., and Aouad, G. Performance Management in Construction: A Conceptual Framework. Construction Management and Economics, 19(1), 85-95, 2001.

[54] Dainty, A. R., Cheng, M. I., Moore, D. R. Redefining Performance Measures for Construction Project Managers: An Empirical Evaluation. Construction Management and Economics, 21(2), 209-218, 2003.

[55] Cheng, E. W., & Li, H. Job Performance Evaluation for Construction Companies: An Analytic Network Process Approach. Journal of Construction Engineering and Management, 132(8), 827-835, 2006.

[56] Babecký, J., Dybczak, K., Galuščák, K. Survey on Wage and Price Formation of Czech Firms. Czech National Bank Working Paper Series, (12), 2008.

[57] Galuscak, K., Keeney, M., Nicolitsas, D., Smets, F., Strzelecki, P., Vodopivec, M. The Determination of Wages of Newly Hired Employees: Survey Evidence on Internal Versus External Factors. Labour Economics, 19(5), 802-812, 2012.

[58] EFBWW. "Wages in Construction" The European Federation of Building and Woodworkers. 2009. [Online]. Available: http://www.efbww.org/pdfs/1%20-%20CAO%20GB%20FINAL.pdf, Accessed November 7, 2017.

[59] Iriondo, I., & Pérez-Amaral, T. The Effect of Educational Mismatch on Wages in Europe. Journal of Policy Modeling, 38(2), 304-323, 2016.

[60] Cox, R. F., Issa, R. R., Ahrens, D. Management's Perception of Key Performance Indicators for Construction. Journal of construction engineering and management, 129(2), 142-151, 2003.

[61] Samuel, O. W., Omisore, M. O., & Atajeromavwo, E. J. Online Fuzzy Based Decision Support System for Human Resource Performance Appraisal. Measurement, 55, 452-461, 2014.

[62] Nassar, N., & AbouRizk, S. Practical Application for Integrated Performance Measurement of Construction Projects. Journal of Management in Engineering, 30(6), 04014027. 2014.

[63] Idson, T. L., & Feaster, D. J. A Selectivity Model of Employer-Size Wage Differentials. Journal of Labor Economics, 8(1, Part 1), 99-122, 1990.

[64] Oral E., Oral, M. Predicting Construction Crew Productivity by Using Self Organizing Maps. Automation in Construction, 19(6), 791-797, 2010.

[65] Lorenz, M. O. Methods of Measuring The Concentration of Wealth. Publications of The American Statistical Association, 9(70), 209-219, 1905.

[66] World Bank Group Inequality Measures, Poverty Manual, All, JH Revision of August 8, p. 218, 2005.

[67] Ahmad, M. Estimation of Distribution of Income Among Various Occupations/Professions in Pakistan. Pakistan Economic and Social Review, 119-134, 2001.

[68] OECD, Income inequality (indicator). [Online]. Available: https://data.oecd.org/inequality/income-inequality.htm, Accessed December 7, 2017.

[69] United Nations Development Programme (UNDP)) Human Development Reports [Online]. Available: http://hdr.undp.org/en/content/income-gini-coefficient , 2017, Accessed December 15, 2017.

[70] Tabachnick, B.G., Fidell L.S., Using Multivariate Statistics, 6th ed. Pearson, Boston, 2016.

[71] Peng, C. Y. J., Lee, K. L., Ingersoll, G. M. An Introduction to Logistic Regression Analysis and Reporting. The Journal of Educational Research, 96(1), 3-14, 2002.

[72] Regulation on the Records of Building Contractors and The Site Managers and Licenced Foremen (Yapı Müteahhitlerinin Kayıtları ile Şantiye Şefleri ve Yetki Belgeli Ustalar Hakkında Yönetmelik) [Online]. Available: http://www.resmigazete.gov.tr, Accessed December 7, 2017.

[73] EF. "Education First, English Proficiency Index" [Online]. Available: https://www.ef.com.tr/epi/, 2017, Accessed July 16, 2018.

Teknik Dergi, 2019 8987-9007, Paper 531

Static Analysis of Simply Supported Functionally Graded Sandwich Plates by Using Four Variable Plate Theory

Pınar Aydan DEMİRHAN[1]
Vedat TAŞKIN[2]

ABSTRACT

In this study, the static analysis of a simply supported square functionally graded sandwich plate is performed. The core of the sandwich plate is assumed to be isotropic and the face sheets functionally graded. The variations in the effective properties of functionally graded face sheets along the thickness are obtained by using Mori-Tanaka Micromechanical Model. Four variable plate theory is used for the displacement fields. The equation of sandwich plate under sinusoidal load is obtained using the virtual displacement principle. Closed form solution is obtained with Navier's approach. Parametric values are obtained for the core and face sheet thickness ratios. The numerical results are compared with the literature and a good agreement between the obtained results and other theories in the literature is observed.

Keywords: Sandwich plate, functionally graded plate, navier's solution, bending stress, shear stress

1. INTRODUCTION

Laminated composite materials are very popular and attractive for many application such as space, aircraft, automotive and sports etc. Since the laminates have different material properties, stress concentrations and delamination may occur in the layer interface. In order to overcome these problems, a new composite material type whose material properties varying gradually along a function was developed. Composition and structure of this functionally graded materials change gradually along the volume as a result of the change in the properties of materials. As the application areas of functionally graded structures expand, predicting the behavior of these materials under static and dynamic loads has become an important research area. Researchers have used existing theories or proposed new ones for

Note:
- This paper has been received on February 19, 2018 and accepted for publication by the Editorial Board on October 09, 2018.
- Discussions on this paper will be accepted by May 31, 2019.

• https://dx.doi.org/10.18400/tekderg.396672

1 Trakya University, Department of Mechanical Engineering, Edirne, Turkey – pinard@trakya.edu.tr - https://orcid.org/0000-0002-2618-4982

2 Trakya University, Department of Mechanical Engineering, Edirne, Turkey - vedattaskin@trakya.edu.tr - https://orcid.org/0000-0002-3013-2317

analysis of bending, buckling and vibration of functionally graded plates and beams [1,2]. Numerous studies using the classical plate theory [3, 4], which does not take into account the effects of shear deformation, the First-Order Shear Deformation Theory [3-6], which assumes shear deformation to be linear along the thickness, or High Order Shear Deformation Theories [7-16] can be seen in the literature. High Order Shear Deformation Theories can produce more accurate results, satisfying the condition where the shear stress at the boundary is zero. However, the calculating procedures of high order theories are considerably complex. Shimpi [17] developed a new theory for isotropic plates that separate transverse displacement as bending displacement and shear displacement. In addition to the computing process being very simple, the theory is accurate as a high order theory. Four Variable Plate Theory has been used by Mechab et al. [18] for the bending analysis of functionally graded materials and Houari et al. [19] for the thermoelastic bending analysis of functionally graded sandwich plates. The theory has been used in numerous studies for static and dynamic analysis of functionally graded plates due to its simplicity of calculation [20-30].

In the present study, static analysis of a square functionally graded sandwich plate is investigated by using the Four Variable Plate Theory. For the functionally graded face sheets, the effective properties of the material are varied through the thickness with a function which is derived by using Mori-Tanaka Micromechanical Model. The equations of the simply supported square plate are obtained through the virtual displacement principle. Navier's approach are used for the closed-form solution. Deflection, normal stress and shear stress values for varying ratios of core and face sheet thickness are obtained and compared with the literature.

2. EQUATIONS OF FUNCTIONALLY GRADED SANDWICH PLATE

A sandwich plate with a thickness of *h*, a length of *a* and a width of *b* is considered. For a square sandwich plate, *b* is equal to *a*. The face sheets of the sandwich plate are assumed to be of a functionally graded material and the core is assumed to be of homogeneous isotropic material. The outer parts of the plate are metal and the inner part gradually change from metal to ceramic. The interface between face sheets and the core is completely of ceramic.

The variation of the properties of the sandwich plate along the thickness is given in Figure 1. The section between h_1 and h_2 is referred to as bottom FG face sheet, the section between h_2 and h_3 is referred to as homogeneous core and the section between h_3 and h_4 is referred to as upper FG face sheet.

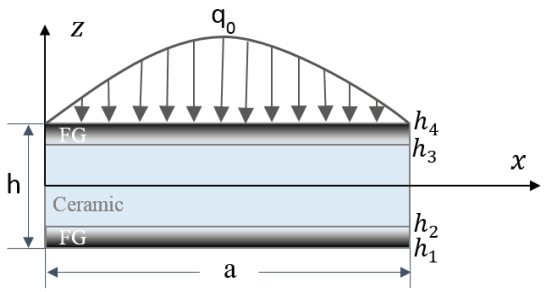

Fig. 1 - Transverse section of FG square sandwich plate with sinusoidal loading

The variation of the elasticity modulus of the functionally graded sandwich plate is given in Equation (1). Among the lower indices, bottom is used for lower sheet and top is used for upper sheet. The lower index of *c* represents ceramic and *m* represents metal. *p* is the power convention index and when it takes the value of zero, it represents the ceramic material. Increasing *p* values represent metal-rich material. Poisson's ratio is assumed to be constant along the thickness.

$$E(z) = \begin{cases} E_{bottom}(z) & for \quad h_1 \le z \le h_2 \\ E_c & for \quad h_2 < z < h_3 \\ E_{top}(z) & for \quad h_3 \le z \le h_4 \end{cases} \tag{1}$$

In Eqs. (2)-(5), V_c and V_m are the volume fractions of metal and ceramic materials for lower and upper face sheets.

$$V_{c_{bottom}}(z) = \left(\frac{z-h_1}{h_2-h_1}\right)^p \tag{2}$$

$$V_{c_{top}}(z) = \left(\frac{z-h_4}{h_3-h_4}\right)^p \tag{3}$$

$$V_{m_{bottom}}(z) = 1 - V_{c_{bottom}}(z) \tag{4}$$

$$V_{m_{top}}(z) = 1 - V_{c_{top}}(z) \tag{5}$$

In calculating the effective properties of composite materials composed of two different materials with different phases, Mori-Tanaka Micromechanical Model [30] is used. The change in the elasticity modulus of the lower and upper face sheets along the thickness is given by means of E_{bottom} and E_{top} functions. Equations (6)-(7).

$$E_{bottom}(z) = E_m + (E_c - E_m)\frac{V_{c_{bottom}}(z)}{1+V_{m_{bottom}}(z)\left(\frac{E_c}{E_m}-1\right)\frac{1+\nu}{3(1-\nu)}} \tag{6}$$

$$E_{top}(z) = E_m + (E_c - E_m)\frac{V_{c_{top}}(z)}{1+V_{m_{top}}(z)\left(\frac{E_c}{E_m}-1\right)\frac{1+\nu}{3(1-\nu)}} \tag{7}$$

Displacement components u, v and w respectively denote the displacements in the x, y, and z-axes. (Eqs. (8)-(10)) The lower index of b represents the bending coupling of transverse displacement and $_s$ represents the shear coupling of transverse displacement.

$$u = u_0 - z\frac{\partial w_b}{\partial x} + f(z)\frac{\partial w_s}{\partial x} \tag{8}$$

$$v = v_0 - z\frac{\partial w_b}{\partial y} + f(z)\frac{\partial w_s}{\partial y} \tag{9}$$

$$w = w_b + w_s \tag{10}$$

Eqs. (11)-(16) give the relationships between strain and displacement.

$$\varepsilon_x = \frac{\partial u}{\partial x} - z\frac{\partial^2 w_b}{\partial x^2} + f(z)\frac{\partial^2 w_s}{\partial x^2} \tag{11}$$

$$\varepsilon_y = \frac{\partial v}{\partial y} - z\frac{\partial^2 w_b}{\partial y^2} + f(z)\frac{\partial^2 w_s}{\partial y^2} \tag{12}$$

$$\varepsilon_z = 0 \tag{13}$$

$$\gamma_{xy} = \frac{\partial u}{\partial y} + \frac{\partial v}{\partial x} - 2z\frac{\partial^2 w_b}{\partial x\,\partial y} + 2f(z)\frac{\partial^2 w_s}{\partial x\,\partial y} \tag{14}$$

$$\gamma_{yz} = g(z)\frac{\partial w_s}{\partial y} \tag{15}$$

$$\gamma_{xz} = g(z)\frac{\partial w_s}{\partial x} \tag{16}$$

The f(z) and the g(z) functions are described in Equations (17)-(18).

$$f(z) = z\left(\frac{1}{4} - \frac{5}{3}\frac{z^2}{h^2}\right) \tag{17}$$

$$g(z) = 1 + \frac{df(z)}{dz} \tag{18}$$

The constitutive relationships for functionally graded sandwich plate can be derived as follows. (Eqs. (19)-(20).

$$\begin{Bmatrix}\sigma_x\\ \sigma_y\\ \tau_{xy}\end{Bmatrix} = \begin{bmatrix}Q_{11} & Q_{12} & 0\\ Q_{12} & Q_{22} & 0\\ 0 & 0 & Q_{66}\end{bmatrix}\begin{Bmatrix}\varepsilon_x\\ \varepsilon_y\\ \gamma_{xy}\end{Bmatrix} \tag{19}$$

$$\begin{Bmatrix}\tau_{yz}\\ \tau_{xz}\end{Bmatrix} = \begin{bmatrix}Q_{44} & 0\\ 0 & Q_{55}\end{bmatrix}\begin{Bmatrix}\gamma_{yz}\\ \gamma_{xz}\end{Bmatrix} \tag{20}$$

Rigidity expressions along the thickness can be written as follows. (Eq. (21))

$$Q_{11} = Q_{22} = \frac{E(z)}{1-\nu^2}$$

$$Q_{12} = \frac{\nu E(z)}{1-\nu^2} \tag{21}$$

$$Q_{44} = Q_{55} = Q_{66} = \frac{E(z)}{2(1+\nu)}$$

Governing equations can be obtained by using virtual displacement principle. Where U is the strain energy and W is the work done by external force:

$$\delta(U - W) = 0 \tag{22}$$

$$U = \int_{-h/2}^{h/2} \int_{\Omega} (\sigma_x \varepsilon_x + \sigma_y \varepsilon_y + \tau_{xy}\gamma_{xy} + \tau_{yz}\gamma_{yz} + \tau_{xz}\gamma_{xz})\, d\Omega dz \tag{23}$$

$$W = \int_{\Omega} q w d\Omega \tag{24}$$

$$\delta(U - W) = \int_{\Omega} \left[N_x \delta\left(\frac{\partial u}{\partial x}\right) + N_y \delta\left(\frac{\partial v}{\partial y}\right) + N_{xy} \delta\left(\frac{\partial u}{\partial y} + \frac{\partial v}{\partial x}\right) - M_x^b \delta\left(\frac{\partial^2 w_b}{\partial x^2}\right) - M_y^b \delta\left(\frac{\partial^2 w_b}{\partial y^2}\right) - M_{xy}^b \delta\left(\frac{\partial^2 w_b}{\partial x\, \partial y}\right) - M_x^s \delta\left(\frac{\partial^2 w_s}{\partial x^2}\right) - M_y^s \delta\left(\frac{\partial^2 w_s}{\partial y^2}\right) - M_{xy}^s \delta\left(\frac{\partial^2 w_s}{\partial x\, \partial y}\right) + S_{yz}^s \delta\left(\frac{\partial w_s}{\partial y}\right) + S_{xz}^s \delta\left(\frac{\partial w_s}{\partial x}\right) \right] d\Omega - \int_{\Omega} q(\delta w_b + \delta w_s) d\Omega = 0 \tag{25}$$

Force and moment components are obtained as follows:

$$N_x = \int_{-\frac{h}{2}}^{\frac{h}{2}} \sigma_x dz$$

$$N_y = \int_{-\frac{h}{2}}^{\frac{h}{2}} \sigma_y dz \tag{26}$$

$$N_{xy} = \int_{-h/2}^{h/2} \tau_{xy} dz$$

$$M_x^b = \int_{-\frac{h}{2}}^{\frac{h}{2}} \sigma_x z dz$$

$$M_y^b = \int_{-\frac{h}{2}}^{\frac{h}{2}} \sigma_y z dz \tag{27}$$

$$M_{xy}^b = \int_{-\frac{h}{2}}^{\frac{h}{2}} \tau_{xy} z dz$$

$$M_x^s = \int_{-\frac{h}{2}}^{\frac{h}{2}} \sigma_x f(z) dz$$

$$M_y^s = \int_{-\frac{h}{2}}^{\frac{h}{2}} \sigma_y f(z) dz \tag{28}$$

$$M_{xy}^s = \int_{-\frac{h}{2}}^{\frac{h}{2}} \tau_{xy} f(z) dz$$

$$S_{xz}^s = \int_{-\frac{h}{2}}^{\frac{h}{2}} \tau_{xz} g(z) dz$$

$$S_{yz}^{s} = \int_{-h/2}^{h/2} \tau_{yz} g(z) dz \tag{29}$$

The rigidity matrix can be written as follows.

$$\begin{Bmatrix} N_x \\ N_y \\ M_x^b \\ M_y^b \\ M_x^s \\ M_y^s \end{Bmatrix} = \begin{bmatrix} A_{11} & A_{12} & B_{11} & B_{12} & B_{11}^s & B_{12}^s \\ A_{12} & A_{22} & B_{12} & B_{22} & B_{12}^s & B_{22}^s \\ B_{11} & B_{12} & D_{11} & D_{12} & D_{11}^s & D_{12}^s \\ B_{12} & B_{22} & D_{12} & D_{22} & D_{12}^s & D_{22}^s \\ B_{11}^s & B_{12}^s & D_{11}^s & D_{12}^s & H_{11}^s & H_{12}^s \\ B_{12}^s & B_{22}^s & D_{12}^s & D_{22}^s & H_{12}^s & H_{22}^s \end{bmatrix} \begin{Bmatrix} \partial u/\partial x \\ \partial v/\partial y \\ -\partial^2 w_b/\partial x^2 \\ -\partial^2 w_b/\partial y^2 \\ -\partial^2 w_s/\partial x^2 \\ -\partial^2 w_s/\partial y^2 \end{Bmatrix} \tag{30}$$

The stiffness coefficients are given in Eq. (31) collectively.

$$\left\{A_{ij}, A_{ij}^s, B_{ij}, B_{ij}^s, D_{ij}, D_{ij}^s, H_{ij}^s\right\} = \int_{-\frac{h}{2}}^{\frac{h}{2}} \{1, g, z, f, z^2, fz, f^2\} Q_{ij} dz \qquad (i, j = 1,2,4,5,6) \tag{31}$$

Eqs. (32)-(35) are plate equilibrium equations.

$$\frac{\partial N_x}{\partial x} + \frac{\partial N_{xy}}{\partial y} = 0 \tag{32}$$

$$\frac{\partial N_{xy}}{\partial x} + \frac{\partial N_y}{\partial y} = 0 \tag{33}$$

$$\frac{\partial^2 M_x^b}{\partial x^2} + 2\frac{\partial M_{xy}^b}{\partial x\,\partial y} + \frac{\partial^2 M_y^b}{\partial y^2} + q = 0 \tag{34}$$

$$\frac{\partial^2 M_x^s}{\partial x^2} + 2\frac{\partial M_{xy}^s}{\partial x\,\partial y} + \frac{\partial^2 M_y^s}{\partial y^2} + \frac{\partial N_{xz}^s}{\partial x} + \frac{\partial N_{yz}^s}{\partial y} + q = 0 \tag{35}$$

The differential equations of the plate (Eqs. (36)-(39)), are obtained by using the force and moment components in Eq.(30) by inserting in Eqs. (32)-(35).

$$A_{11}\frac{\partial^2 u}{\partial x^2} + A_{66}\frac{\partial^2 u}{\partial y^2} + (A_{12} + A_{66})\frac{\partial^2 v}{\partial x\,\partial y} - B_{11}\frac{\partial^3 w_b}{\partial x^3} - (B_{12} + 2B_{66})\frac{\partial^3 w_b}{\partial x\,\partial y^2} - B_{11}^s\frac{\partial^3 w_s}{\partial x^3} - (B_{12}^s + 2B_{66}^s)\frac{\partial^3 w_s}{\partial x\,\partial y^2} = 0 \tag{36}$$

$$(A_{12} + A_{66})\frac{\partial^2 u}{\partial x\,\partial y} + A_{66}\frac{\partial^2 v}{\partial x^2} + A_{22}\frac{\partial^2 v}{\partial y^2} - (B_{12} + 2B_{66})\frac{\partial^3 w_b}{\partial x^2\,\partial y} - B_{22}\frac{\partial^3 w_b}{\partial y^3} - (B_{12}^s + 2B_{66}^s)\frac{\partial^3 w_s}{\partial x^2\,\partial y} - B_{22}^s\frac{\partial^3 w_s}{\partial y^3} = 0 \tag{37}$$

$$B_{11}\frac{\partial^3 u}{\partial x^3} + (B_{12} + 2B_{66})\frac{\partial^3 u}{\partial x\,\partial y^2} + (B_{12} + 2B_{66})\frac{\partial^3 v}{\partial x^2\,\partial y} + B_{22}\frac{\partial^3 v}{\partial y^3} - D_{11}\frac{\partial^4 w_b}{\partial x^4} - 2(D_{12} + 2D_{66})\frac{\partial^4 w_b}{\partial x^2\,\partial y^2} - D_{22}\frac{\partial^4 w_b}{\partial y^4} - D_{11}^s\frac{\partial^4 w_s}{\partial x^4} - 2(D_{12}^s + 2D_{66}^s)\frac{\partial^4 w_s}{\partial x^2\,\partial y^2} - D_{22}^s\frac{\partial^4 w_s}{\partial y^4} + q = 0 \tag{38}$$

$$B_{11}^{s}\frac{\partial^3 w_s}{\partial x^3}+(B_{12}^{s}+2B_{66}^{s})\frac{\partial^3 u}{\partial x\,\partial y^2}+B_{22}^{s}\frac{\partial^3 v}{\partial y^3}-D_{11}^{s}\frac{\partial^4 w_b}{\partial x^4}-D_{22}^{s}\frac{\partial^4 w_b}{\partial y^4}+(B_{12}^{s}+2B_{66}^{s})\frac{\partial^3 u}{\partial x^2\,\partial y}-$$
$$H_{11}^{s}\frac{\partial^4 w_s}{\partial x^4}-H_{22}^{s}\frac{\partial^4 w_s}{\partial y^4}-2(D_{12}^{s}+2D_{66}^{s})\frac{\partial^4 w_b}{\partial x^2\,\partial y^2}-2(H_{12}^{s}+2H_{66}^{s})\frac{\partial^4 w_s}{\partial x^2\,\partial y^2}+A_{55}^{s}\frac{\partial^2 w_s}{\partial x^2}+$$
$$A_{44}^{s}\frac{\partial^2 w_s}{\partial y^2}+q=0 \tag{39}$$

Boundary conditions for the simply supported functionally graded sandwich plate are given in Eq.(40).

$$v(0,y)=w_b(0,y)=w_s(0,y)=\frac{\partial w_b}{\partial y}(0,y)=\frac{\partial w_s}{\partial y}(0,y)=0$$
$$v(a,y)=w_b(a,y)=w_s(a,y)=\frac{\partial w_b}{\partial y}(a,y)=\frac{\partial w_s}{\partial y}(a,y)=0$$
$$N_x(0,y)=M_x^b(0,y)=M_x^s(0,y)=N_x(a,y)=M_x^b(a,y)=M_x^s(a,y)=0 \tag{40}$$
$$u(x,0)=w_b(x,0)=w_s(x,0)=\frac{\partial w_b}{\partial x}(x,0)=\frac{\partial w_s}{\partial x}(x,0)=0$$
$$u(x,b)=w_b(x,b)=w_s(x,b)=\frac{\partial w_b}{\partial x}(x,b)=\frac{\partial w_s}{\partial x}(x,b)=0$$
$$N_y(x,0)=M_y^b(x,0)=M_y^s(x,0)=N_y(x,b)=M_y^b(x,b)=M_y^s(x,b)=0$$

For the analytical solution of the simply supported plate, Navier's procedure is used. The external force applied is written in double series expansion according to the Navier's approach.

$$q(x,y)=\sum_{m=1}^{\infty}\sum_{n=1}^{\infty}q_{mn}\sin(\alpha x)\sin(\beta y) \tag{41}$$

where $\alpha=\frac{m\pi}{a}$, $\beta=\frac{n\pi}{b}$. For sinusoidal loading, *m*, *n*, and q_{mn} are defined as follows.

$$m=n=1,\qquad q_{11}=q_0 \tag{42}$$

The displacement components fulfilling the boundary conditions according to the Navier's solution procedure are considered to be as follows:

$$\begin{Bmatrix}u\\v\\w_b\\w_s\end{Bmatrix}=\sum_{m=1}^{\infty}\sum_{n=1}^{\infty}\begin{Bmatrix}U_{mn}\cos(\alpha x)\sin(\beta y)\\V_{mn}\sin(\alpha x)\cos(\beta y)\\W_{bmn}\sin(\alpha x)\sin(\beta y)\\W_{smn}\sin(\alpha x)\sin(\beta y)\end{Bmatrix} \tag{43}$$

U_{mn}, V_{mn}, W_{bmn}, W_{smn} are unknown coefficients. When K is the coefficients matrix and F is the applied external force, the unknown coefficients are obtained by solving the Eq. (44).

$$K\Delta=F \tag{44}$$

$$\Delta^T = \{U_{mn},\ V_{mn},\ W_{bmn},\ W_{smn}\} \tag{45}$$

$$F^T = \{0,\ 0,\ -q_{mn},\ -q_{mn}\} \tag{46}$$

$$K = \begin{bmatrix} K_{11} & K_{12} & K_{13} & K_{14} \\ K_{12} & K_{22} & K_{23} & K_{24} \\ K_{13} & K_{23} & K_{33} & K_{34} \\ K_{14} & K_{24} & K_{34} & K_{44} \end{bmatrix} \tag{47}$$

the coefficients of K matrix are given in Eq. (48)

$$\begin{aligned} K_{11} &= A_{11}\alpha^2 + A_{66}\beta^2 \\ K_{12} &= \alpha\beta(A_{12} + A_{66}) \\ K_{13} &= -\alpha[B_{11}\alpha^2 + (B_{12} + 2B_{66})\beta^2] \\ K_{14} &= -\alpha[B^s_{11}\alpha^2 + (B^s_{12} + 2B^s_{66})\beta^2] \\ K_{22} &= A_{66}\alpha^2 + A_{22}\beta^2 \\ K_{23} &= -\beta[(B_{12} + 2B_{66})\alpha^2 + B_{22}\beta^2] \\ K_{24} &= -\beta[(B^s_{12} + 2B^s_{66})\alpha^2 + B^s_{22}\beta^2] \\ K_{33} &= D_{11}\alpha^4 + 2(D_{12} + 2D_{66})\alpha^2\beta^2 + D_{22}\beta^4 \\ K_{34} &= D^s_{11}\alpha^4 + 2(D^s_{12} + 2D^s_{66})\alpha^2\beta^2 + D^s_{22}\beta^4 \\ K_{44} &= H^s_{11}\alpha^4 + 2(H^s_{12} + 2H^s_{66})\alpha^2\beta^2 + H^s_{22}\beta^4 + A^s_{55}\alpha^2 + A^s_{44}\beta^2 \end{aligned} \tag{48}$$

3. RESULTS

Some results are presented for the Navier's solution of the functionally graded square sandwich plate which is under sinusoidally distributed load and simply supported in all edges. The properties of the material used for obtaining the numerical results are defined as follows:

Ceramic (ZrO_2)	$E_c = 151$ GPa,	$\nu = 0.3$
Metal (Al)	$E_m = 70$ GPa,	$\nu = 0.3$

In order to compare the values with those in the literature, the following non-dimensional expressions are used.

$$\overline{W} = \frac{10hE_0}{q_0a^2}W\left(\frac{a}{2},\frac{b}{2}\right),\ \overline{\sigma_x} = \frac{10h^2}{q_0a^2}\sigma_x\left(\frac{a}{2},\frac{b}{2},\frac{h}{2}\right),\ \overline{\tau_{xz}} = \frac{h}{q_0a}\tau_{xz}(0,\frac{b}{2},0) \tag{49}$$

where $E_0 = 1\ GPa$. For the comparison of numerical results, plate thickness ratios found in the literature are used. Four symmetric and two non-symmetric ratios are used.

(1-0-1) FG sandwich plate: The plate without a core. h_2=0 and h_3=0

(1-1-1) FG sandwich plate: The thickness of the core and face sheets are equal. h_2=-h/6 and h_3=h/6

(1-2-1) FG sandwich plate: The functionally graded face sheets have half the thickness of the core. h_2=-h/4 and h_3=h/4

(2-1-2) FG sandwich plate: The core has half the thickness of the functionally graded face sheets. h_2=-h/10 and h_3=h/10

(2-1-1) FG sandwich plate: The thickness of the lower face sheet is twice as much as the thickness of the core and upper face sheet. h_2=0 and h_3=h/4

(2-2-1) FG sandwich plate: The upper face sheet has half the thickness of the core and lower face sheet h_2=-h/10 and h_3=3h/4

The results are presented in the Tables 1-3 and in the Figs. 3-7.

In the Figure 2, the variation of elasticity modulus along the thickness for symmetric and non-symmetric sandwich plates is given. The plate, which is metal in the outer surfaces, turns into a ceramic-rich form as it gets closer to the midplane. The change in the elasticity modulus diverges from being linear with the increasing power law index and shows parabolic distribution.

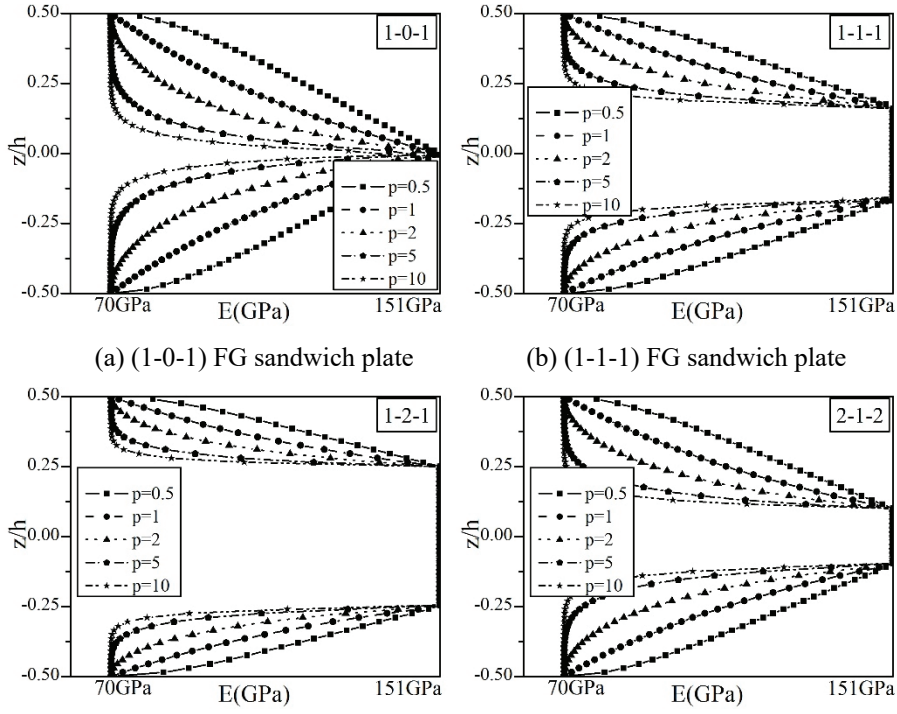

(a) (1-0-1) FG sandwich plate

(b) (1-1-1) FG sandwich plate

(c) (1-2-1) FG sandwich plate

(d) (2-1-2) FG sandwich plate

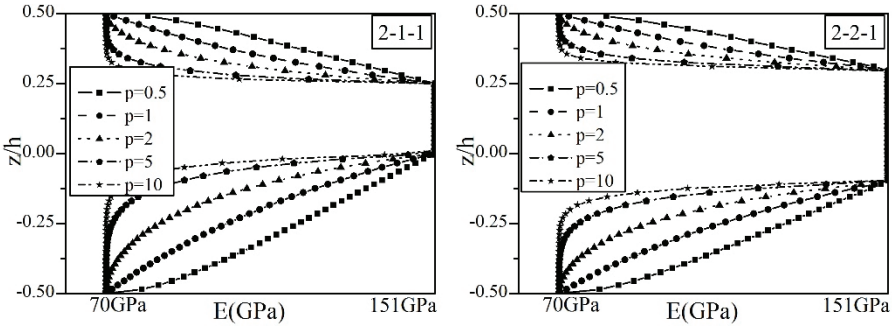

(e) (2-1-1) FG sandwich plate (f) (2-2-1) FG sandwich plate

Fig.2 - Elasticity modulus function with different p values (Ec=151GPa, Em=70GPa, a/h=10)

Tables 1, 2 and 3 respectively display the values for non-dimensional deflection, normal stress and shear stress. Results obtained based on a polynomial four variable refined plate theory in this study is compared with those given by Zenkour (2005) based on first [3a] and third [3b] order plate theory, Bessaim et al. (2013) based on high-order shear and normal deformation theory, Nguyen et al. (2014) based on an inverse trigonometric shear deformation theory, Thai et al. (2016) based on a simple four-unknown shear and normal deformations theory. In Table 1, it is seen that the lowest deflection value is obtained with the p=0 where the plate is completely ceramic. Its metallic properties increase with the increase in the p and thus, the deflection increases. Different thickness ratios reveal that the highest deflection value is observed in the (1-0-1) FG sandwich plate where there is no core. The deflection value decreases as the core-to-plate thickness ratio increases. The lowest deflection value is obtained in (1-2-1) FG sandwich plate. Non-dimensional normal stress values are listed in Table 2 with different p values for different thickness ratios. Non-dimensional shear stress values are listed in Table 3. In the table, obtained results are over-assumed compared to the references.

Table 1 - Non-dimensional center deflections of Al/ZrO_2 square sandwich plates.

P	Theory	1-0-1	2-1-2	2-1-1	1-1-1	2-2-1	1-2-1
0	[3a]	0.19607	0.19607	0.19607	0.19607	0.19607	0.19607
	[3b]	0.19606	0.19606	0.19606	0.19606	0.19606	0.19606
	[30]	-	0.19486	0.19486	0.19486	0.19486	0.19486
	[14]	0.19597	0.19597	0.19597	0.19597	0.19597	0.19597
	[31]	0.19490	0.19490	0.19490	0.19490	0.19490	0.19490
	Present	0.19606	0.19606	0.19606	0.19606	0.19606	0.19606
1	[3a]	0.32484	0.30750	-	0.29301	0.28168	0.27167

Table 1 - Non-dimensional center deflections of Al/ZrO_2 square sandwich plates.(continue)

P	Theory	1-0-1	2-1-2	2-1-1	1-1-1	2-2-1	1-2-1
	[3b]	0.32358	0.30632	-	0.29199	0.28085	0.27094
	[30]	-	0.30430	0.29448	0.29007	0.27874	0.26915
	[14]	0.32348	0.30622	0.29666	0.29191	0.28077	0.27086
	[31]	0.32000	0.30280	-	0.28870	0.27780	0.26830
	Present	0.34539	0.32677	0.31494	0.31032	0.29665	0.28519
2	[3a]	0.37514	0.35408	-	0.33441	0.31738	0.30370
	[3b]	0.37335	0.35231	-	0.33289	0.31617	0.30263
	[30]	-	0.35001	0.33495	0.33068	0.31356	0.30060
	[14]	0.37322	0.35221	0.33769	0.33279	0.31608	0.30255
	[31]	0.36890	0.34740	-	0.32830	0.31190	0.29900
	Present	0.38650	0.36655	0.35030	0.34653	0.32763	0.31366
5	[3a]	0.41120	0.39418	-	0.37356	0.35123	0.33631
	[3b]	0.40927	0.39183	-	0.37145	0.34960	0.33480
	[30]	-	0.38934	0.36981	0.36902	0.34649	0.33255
	[14]	0.40911	0.39170	0.37295	0.37134	0.34950	0.33472
	[31]	0.40530	0.38630	-	0.36580	0.34450	0.33040
	Present	0.41291	0.39706	0.39760	0.37727	0.35452	0.33994
10	[3a]	0.41919	0.40657	-	0.38787	0.36395	0.34996
	[3b]	0.41772	0.40407	-	0.38551	0.36215	0.34824
	[30]	-	0.40153	0.38111	0.38303	0.35885	0.34591
	[14]	0.41754	0.40398	0.38430	0.38540	0.36202	0.34815
	[31]	0.41450	0.39890	-	0.38010	0.35740	0.34430
	Present	0.41900	0.41295	0.39248	0.39482	0.37041	0.35683

Table 2 - Non-dimensional normal stress of Al/ZrO_2 square sandwich plates.

P	Theory	1-0-1	2-1-2	2-1-1	1-1-1	2-2-1	1-2-1
0	[3a]	1.97576	1.97576	1.97576	1.97576	1.97576	1.97576
	[3b]	2.04985	2.04985	2.04985	2.04985	2.04985	2.04985
	[30]	-	1.99524	1.99524	1.99524	1.99524	1.99524
	[14]	1.99482	1.99482	1.99482	1.99482	1.99482	1.99482
	[31]	2.00480	2.00430	-	2.00400	2.00340	2.00360
	Present	1.95721	1.95721	1.95721	1.95721	1.95721	1.95721

Table 2 - Non-dimensional normal stress of Al/ZrO_2 square sandwich plates.(continue)

P	Theory	1-0-1	2-1-2	2-1-1	1-1-1	2-2-1	1-2-1
1	[3a]	1.53245	1.45167	-	1.38303	1.27749	1.28096
	[3b]	1.57923	1.49587	-	1.42617	1.32062	1.32309
	[30]	-	1.46131	1.35053	1.39243	1.28274	1.29030
	[14]	1.54441	1.46297	1.35703	1.39406	1.28852	1.29174
	[31]	1.56760	1.48570	-	1.41520	1.30280	1.30970
	Present	1.62848	1.54457	1.41548	1.46713	1.33792	1.34633
2	[3a]	1.77085	1.67496	-	1.58242	1.42528	1.43580
	[3b]	1.82167	1.72144	-	1.62748	1.47095	1.47988
	[30]	-	1.68472	1.52101	1.59170	1.42887	1.44497
	[14]	1.78383	1.68682	1.52988	1.59393	1.43693	1.44707
	[31]	1.81230	1.71730	-	1.62320	1.45640	1.47210
	Present	1.82102	1.73586	1.56265	1.64304	1.46762	1.48584
5	[3a]	1.93576	1.86479	-	1.76988	1.56401	1.59309
	[3b]	1.99272	1.91302	-	1.81580	1.61181	1.63814
	[30]	-	1.87516	1.66856	1.77919	1.56627	1.60203
	[14]	1.95031	1.87709	1.67895	1.78159	1.57620	1.60459
	[31]	1.97620	1.91190	-	1.81800	1.60150	1.63830
	Present	1.93514	1.87915	1.67627	1.79068	1.57722	1.61390
10	[3a]	1.96780	1.92165	-	1.83754	1.61645	1.65844
	[3b]	2.03036	1.97126	-	1.88376	1.66660	1.70417
	[30]	-	1.93266	1.71835	1.84705	1.61792	1.66754
	[14]	1.98382	1.93431	1.72890	1.84933	1.62840	1.67019
	[31]	2.00410	1.96840	-	1.88820	1.65820	1.70990
	Present	1.95453	1.91930	1.71255	1.84092	1.61617	1.66440

Figure 3 shows the non-dimensional deflection of the symmetric sandwich plates with different thickness ratios. In each of four symmetric ratios, the lowest maximum deflection value is obtained for p=0 as expected. It is observed that, maximum deflection is increased along with increasing power convention index. When all the four symmetric ratios are compared, it is seen that, the highest maximum deflection value is obtained in the (1-0-1) FG sandwich plate. The second largest maximum deflection after the (1-0-1) FG sandwich plate occurs in the (2-1-2) FG sandwich plate, which is the condition where face sheet thickness is the highest as compared to the core thickness. In the (1-1-1) and (1-2-1) FG sandwich plates whose face thicknesses are equal, it is observed that the maximum deflection value decreases with the increase in the thickness of the core. Also, the non-dimensional deflection of the

non-symmetric sandwich plates with two different thickness ratios are given in the Figure 3. In the (2-2-1) FG sandwich plate where the core is thicker, the maximum deflection has a lower value. In the (2-1-1) FG sandwich plate, it is observed that the maximum deflection rapidly increases with increase in the p value.

Table 3 - Non-dimensional shear stress of Al/ZrO_2 square sandwich plates.

P	Theory	1-0-1	2-1-2	2-1-1	1-1-1	2-2-1	1-2-1
0	[3a]	0.19099	0.19099	0.19099	0.19099	0.19099	0.19099
	[3b]	0.23857	0.23857	-	0.23857	0.23857	0.23857
	[30]	-	0.23794	0.23794	0.23794	0.23794	0.23794
	[14]	0.23581	0.23581	0.23581	0.23581	0.23581	0.23581
	[31]	0.19510	0.19510	-	0.19510	0.19480	0.19510
	Present	0.23852	0.23852	0.23852	0.23852	0.23852	0.23852
1	[3a]	0.26099	0.24316	-	0.23257	0.22762	0.22057
	[3b]	0.29203	0.27104	-	0.26117	0.25951	0.25258
	[30]	-	0.27050	0.27017	0.26060	0.25890	0.25196
	[14]	0.28953	0.26882	0.26852	0.25906	0.25736	0.25054
	[31]	0.29810	0.28050	-	0.26820	0.25910	0.25190
	Present	0.30078	0.26934	0.26824	0.25440	0.25222	0.24166
2	[3a]	0.29731	0.26752	-	0.25077	0.24316	0.23257
	[3b]	0.32622	0.28838	-	0.27188	0.26939	0.25834
	[30]	-	0.28792	0.28742	0.27138	0.26885	0.25776
	[14]	0.32336	0.28607	0.28569	0.26982	0.26731	0.25645
	[31]	0.34090	0.31520	-	0.29750	0.28410	0.27420
	Present	0.34187	0.28911	0.28651	0.26543	0.26153	0.24566
5	[3a]	0.34538	0.29731	-	0.27206	0.26009	0.24596
	[3b]	0.38634	0.31454	-	0.28643	0.28265	0.26512
	[30]	-	0.31419	0.31293	0.28606	0.28217	0.26463
	[14]	0.38250	0.31182	0.31087	0.28420	0.28047	0.26327
	[31]	0.38260	0.34920	-	0.32660	0.30900	0.29690
	Present	0.40619	0.31798	0.31239	0.28156	0.27490	0.25209
10	[3a]	0.37277	0.31316	-	0.28299	0.26998	0.25257
	[3b]	0.43206	0.33242	-	0.29566	0.29080	0.26895
	[30]	-	0.33210	0.32959	0.29534	0.29036	0.26850
	[14]	0.42744	0.32936	0.32732	0.29326	0.28854	0.26705
	[31]	0.40020	0.36680	-	0.33960	0.32040	0.30770
	Present	0.44818	0.33540	0.32754	0.29172	0.28274	0.25611

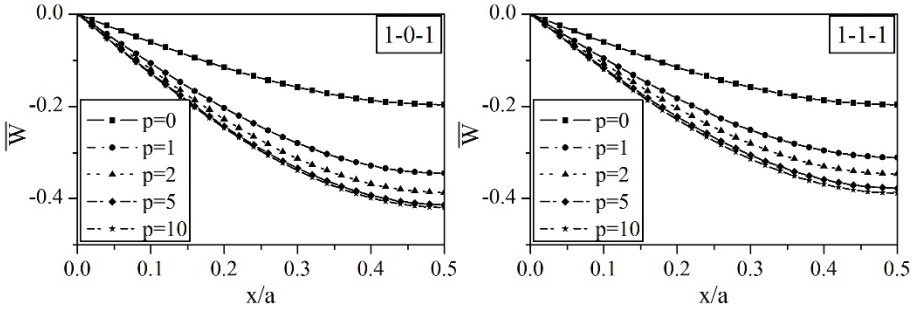

(a) (1-0-1) FG sandwich plate (b) (1-1-1) FG sandwich plate

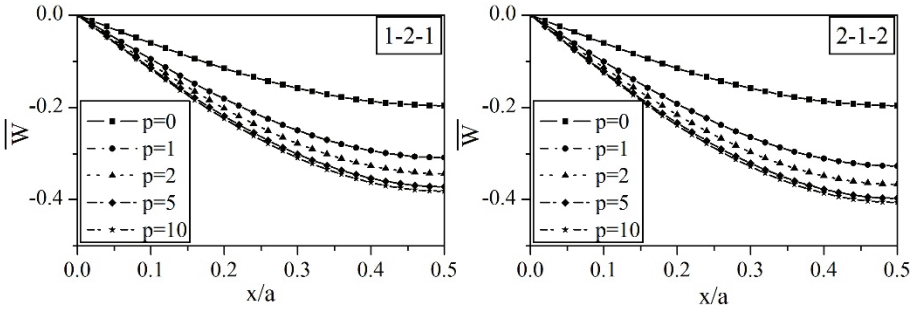

(c) (1-2-1) FG sandwich plate (d) (2-1-2) FG sandwich plate

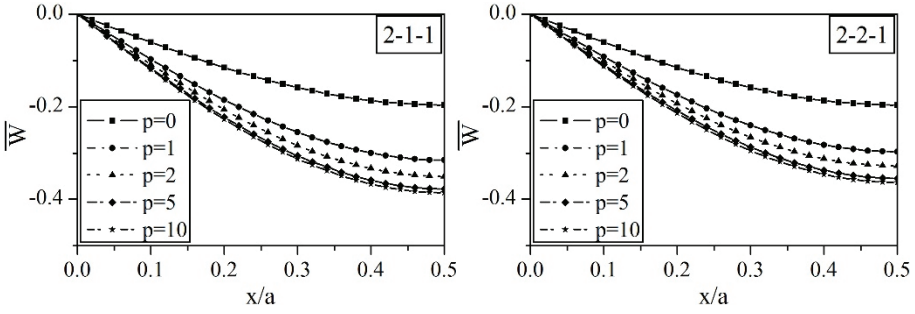

(e) (2-1-1) FG sandwich plate (f) (2-2-1) FG sandwich plate

Fig.3 - Nondimensional deflection of the symmetric and nonsymmetric square sandwich plates with varying thickness combinations

In the Figure 4, non-dimensional normal stress distributions of the symmetric sandwich plates along the thickness are given. In the (1-0-1) FG sandwich plate, the normal stress shows a linear distribution for p=0 and a parabolic distribution with the increase in p, and the values for maximum tensile and compressive stress decrease. In the (1-1-1) FG sandwich plate, which has core and face sheets thicknesses of equal value, it is observed that the local extreme stress, which occurs between the face and the core, is lower than the (2-1-2) FG plate. Nevertheless, it is clear that the highest local extreme stress occurs in the (1-2-1) FG

sandwich plate. For all thickness ratios, maximum tensile stress and compressive stress values decrease with the increase in the power convention index. Figure 4 also presents the non-dimensional normal stress distributions of the non-symmetric sandwich plates along the thickness. The normal stress distribution of the core appears to be linear for both plates, and the stress, which occurs between the face sheet and the interface of the core in the (2-1-1) FG sandwich plate is lower. The stress value decreases in the thinner face sheet with the increase in p. In the (2-2-1) FG sandwich plate, it is observed that the normal stress, which occurs between the thin face and core interface, is higher in comparison with the (2-1-1) FG sandwich plate.

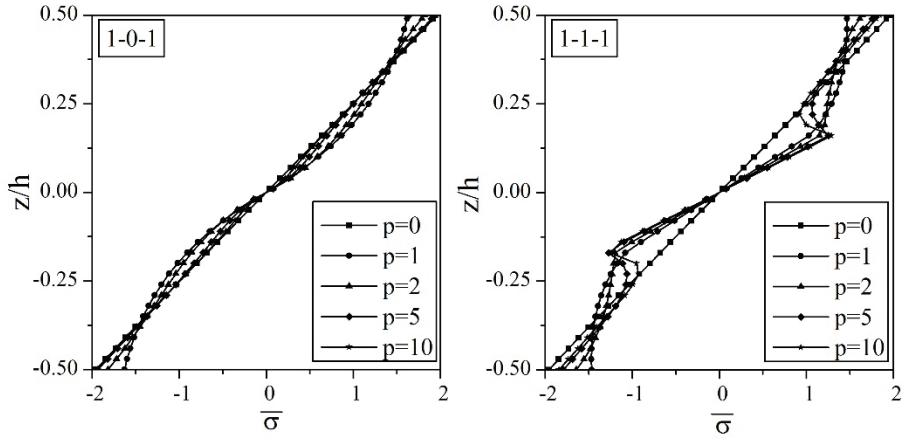

(a) (1-0-1) FG sandwich plate (b) (1-1-1) FG sandwich plate

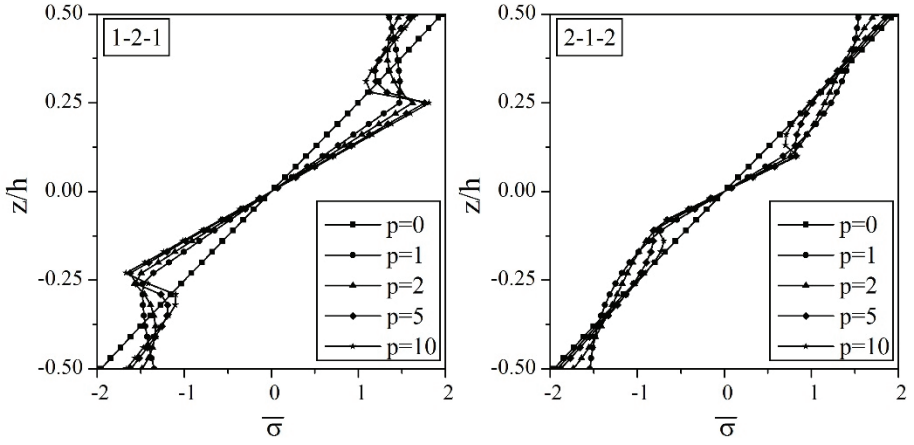

(c) (1-2-1) FG sandwich plate (d) (2-1-2) FG sandwich plate

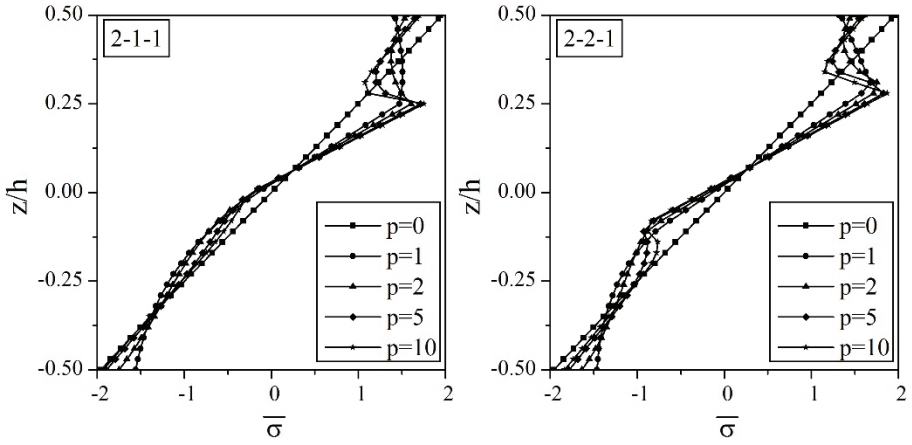

(e) (2-1-1) FG sandwich plate (f) (2-2-1) FG sandwich plate

Fig.4 - Non-dimensional Normal Stress for different p values for symmetric and non-symmetric square sandwich plates.

Figure 5 shows the normal stress distributions along the thickness direction for different ratios of core and face sheet thickness values. Figure 5(a) demonstrates p=1 and Figure 5(b) demonstrates p=5. The highest normal stress values are seen at the interface of the core and face sheets in (1-2-1) FG sandwich plate for both p=1 and p=5. For p=5, local extreme stresses are observed at the interfaces.

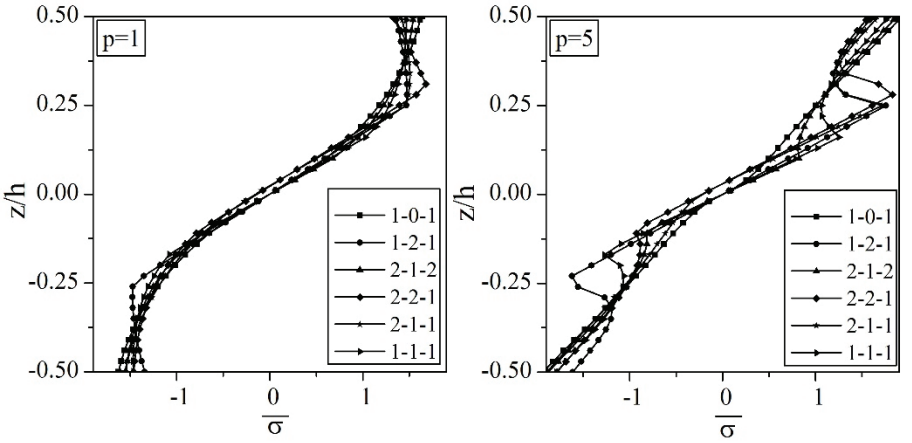

Fig.5 - Dimensionless Normal Stress for different type of square sandwich plates.

Shear stress distributions of the symmetric sandwich plates along the thickness direction for different power law index values are seen in Figure 6. In (1-0-1) FG sandwich plate, which does not contain a core, shows that the maximum, stress which occurs in the interface between lower and upper face sheets, rapidly increases with the increase in the p-value. In

the (1-1-1) FG sandwich plate, in which the thickness of the core and the face are equal, it is observed that the shear stress value in the face sheets decreases, but the shear stress value at interface of the core and the face sheets, and the maximum shear stress increases with increasing p-value. With the increase in the p-value in the (1-2-1) FG sandwich plate, in which the thickness of the core is higher than that of the face sheets, the shear stress value decreases in the face sheets, but the same value slightly increases in the core. In the (2-1-2) FG sandwich plate, which has the smallest core-to-face thickness ratio, the shear stress decreases with the increasing p-value, but the shear stress values of the core and the interface increase rapidly. Shear stress distributions of the non-symmetric sandwich plates along the thickness direction for the power convention index values can be seen in Figure 6. In both combinations, the shear stress of the core has a non-symmetric distribution. The shear stress, which occurs in the interface between the core and the thicker face sheet is considerably higher than the other interface. In the shear stress distribution that occurs in the face sheets it can be seen that the thin face sheet is less severely affected by the power convention index, and the stress distribution of the thicker face sheet decreases with the increasing p-value in both conditions.

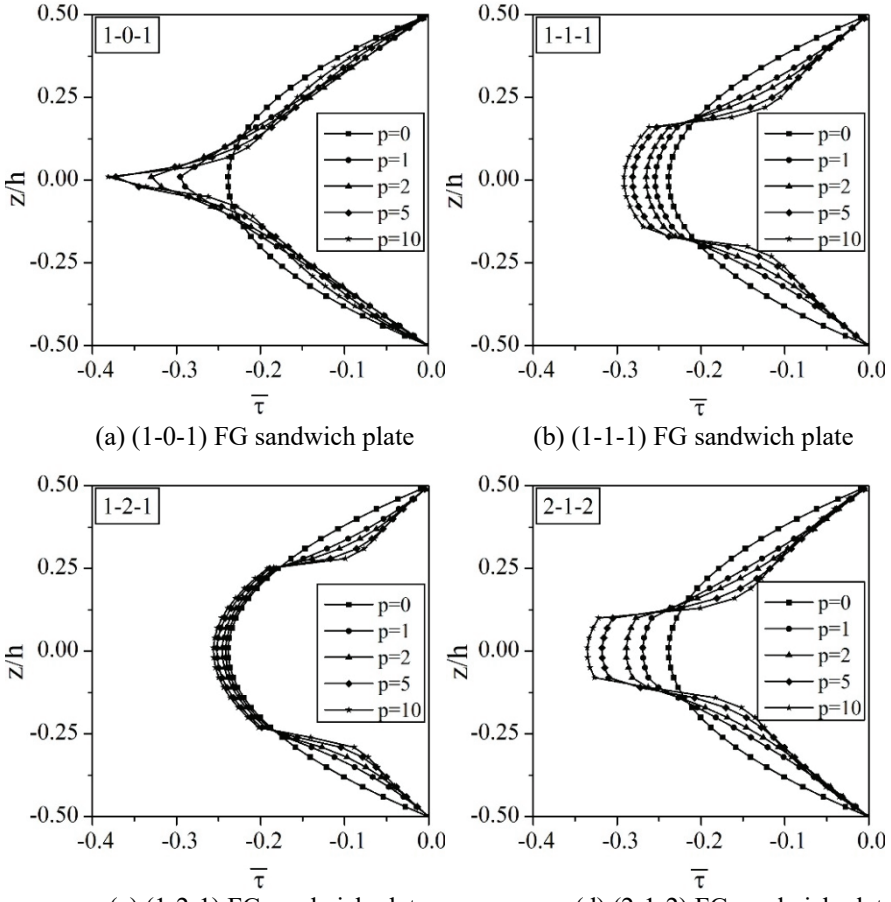

(a) (1-0-1) FG sandwich plate (b) (1-1-1) FG sandwich plate

(c) (1-2-1) FG sandwich plate (d) (2-1-2) FG sandwich plate

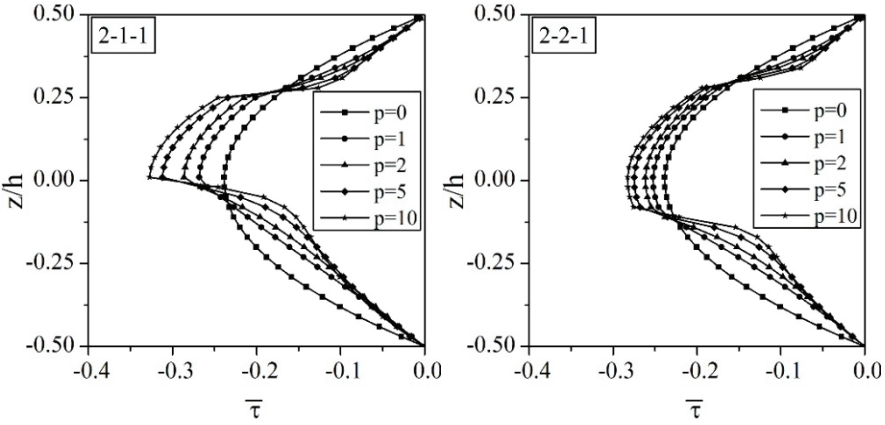

(e) (2-1-1) FG sandwich plate (f) (2-2-1) FG sandwich plate

Fig.6 - Non-dimensional Shear Stress for different p values for symmetric and non-symmetric square sandwich plates.

Figure 7 gives the shear stress distributions along the thickness direction for different ratios of core and face sheet thickness values. Figure 7(a) demonstrates p=1 and Figure 7(b) demonstrates p=5. The shear stress in all ratios increases with the increase in the p-value. In the shear stress distribution of the (1-0-1) FG sandwich plate for p=5, it is observed that the shear stress rapidly increases in the section closer to the interfaces, and it takes values that are very similar to the p=2 condition in the areas closer to the face sheets. The stress distributions remain in the same form with the increase in the p-value and they are shifted towards higher values. The analysis of the shear stress distributions of the sandwiches with symmetric combinations reveals that as the core-to-face thickness ratio increases, the maximum shear stress and the shear stress which occurs in the interfaces decrease.

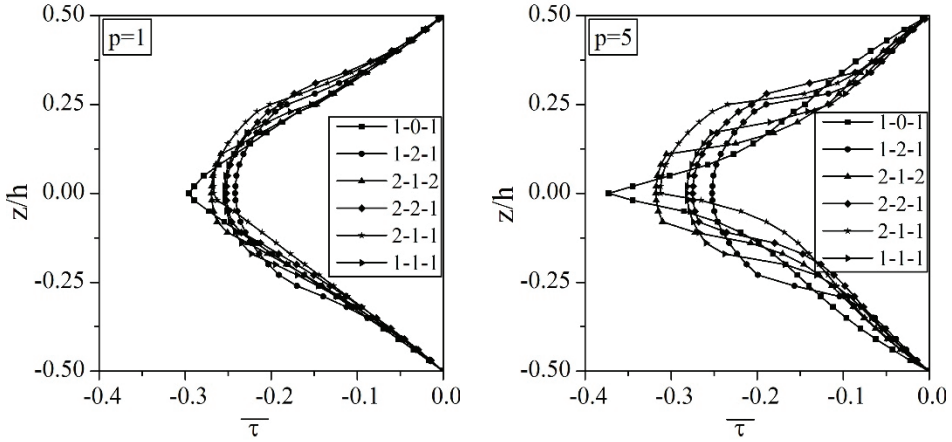

Fig.7 - Dimensionless transverse shear stress for different type of square sandwich plates.

4. CONCLUSION

Static analysis of a functionally graded square sandwich plate is studied in this paper. The effective properties of the functionally graded face sheets are varied through thickness direction with the Mori-Tanaka Micromechanical Model. For displacement fields, the Four Variable Plate Theory is used. The theory separates the bending and shear coupling of vertical displacements, so it is very simple and accurate. The equations of the simply supported square plate are obtained through the virtual displacement principle. Navier's approach is used for the closed-form solution. Numerical results are obtained for Al-ZrO_2 square sandwich plate with sinusoidal loading. Non-dimensional deflection, normal stress and shear stress values for different core and face sheet thickness ratios are obtained and compared with the references. It is seen that obtained results are sufficiently in agreement with the other theories.

References

[1] Reddy, J.N., Wang, C.M., An overview of the relationships between solutions of the classical and shear deformation plate theories. Composites Science and Technology, 60, 2327-2335, 2000.

[2] Thai, H.T., Kim, S.E., A review of theories for the modeling and analysis of functionally graded plates and shells. Composite Structures. 128, 70-86, 2015.

[3] Zenkour, A.M., A comprehensive analysis of functionally graded sandwich plates: Part 1-Deflection and stresses. International Journal of Solids and Structures, 42, 5224-5242, 2005.

[4] Zenkour, A.M., Alghamdi, N.A., Bending analysis of functionally graded sandwich plates under the effect of mechanical and thermal loads. Mechanics of Advanced Materials and Structures, 17, 419–432, 2010.

[5] Thai, H.T., Choi, D.H., A simple first-order shear deformation theory for the bending and free vibration analysis of functionally graded plates. Composite Structures, 101, 332-340, 2013.

[6] Thai, H.T., Nguyen, T.K., Vo, T.P., Lee, J., Analysis of functionally graded sandwich plates using a new first-order shear deformation theory. European Journal of Mechanics A/Solids, 45, 211-225, 2014.

[7] Kim, J., Reddy, J.N., Analytical solutions for bending, vibration, and buckling of FGM plates using a couple stress-based third-order theory. Composite Structures, 103, 86-98, 2013.

[8] Tounsi, A., Houari, M.S.A., Benyoucef, S., Bedia, E.A.A., A refined trigonometric shear deformation theory for thermoelastic bending of functionally graded sandwich plates. Aerospace Science and Technology, 24, 209-220, 2013.

[9] Reddy, J.N., Analysis of functionally graded plates. International Journal for Numerical Methods in Engineering, 47, 663-684, 2000.

[10] Mantari, J.L., Oktem, A.S., Soares, C.G., Static and dynamic analysis of laminated composite and sandwich plates and shells by using a new higher-order shear deformation theory. Composite Structures, 94, 37-49, 2011.

[11] Abdelaziz, H.H., Atmane, H.A., Mechab, I., Boumia, L., Tounsi, A., Abbas, A.B.E., Static analysis of functionally graded sandwich plates using an efficient and simple refined theory. Chinese Journal of Aeronautics, 24, 434-448, 2011.

[12] Mantari, J.L., Granados, E.V., Thermoelastic analysis of advanced sandwich plates based on a new quasi-3D hybrid type HSDT with 5 unknowns. Composites: Part B, 69, 317-334, 2014.

[13] Brischetto, S., Leetsch, R., Carrera, E., Wallmersperger, T., Kröplin, B., Thermo-mechanical bending of functionally graded plates. Journal of Thermal Stresses, 31, 286-308, 2008.

[14] Nguyen, V.H., Nguyen, T.K., Thai, H.T., Vo, T.P., A new inverse trigonometric shear deformation theory for isotropic and functionally graded sandwich plates. Composites: Part B, 66, 233-246, 2014.

[15] Li, X.F., Wang, B.L., Han, J.C., A higher-order theory for static and dynamic analyses of functionally graded beams. Archive of Applied Mechanics, 80, 1197-1212, 2010.

[16] Akavci, S.S., Tanrikulu, A.H., Static and free vibration analysis of functionally graded plates based on a new quasi-3D and 2D shear deformation theories. Composites Part B, 83, 203-215, 2015.

[17] Shimpi, R.P., Refined Plate Theory and Its Variants. AIAA JOURNAL, 40, 137-146, 2002.

[18] Mechab, I., Atmane, H.A., Tounsi, A., Belhadj, H.A., Bedia, E.A.A., A two variable refined plate theory for the bending analysis of functionally graded plates. Acta Mechanica Sinica, 26, 941-949, 2010.

[19] Houari, M.S.A., Benyoucef, S., Mechab, I., Tounsi, A., Bedia, E.A.A., Two-variable refined plate theory for thermoelastic bending analysis of functionally graded sandwich plates. Journal of Thermal Stresses, 34(4), 315-334, 2011.

[20] Benachour, A., Tahar, H.D., Atmane, H.A., Tounsi, A., Ahmed, M.S., A four variable refined plate theory for free vibrations of functionally graded plates with arbitrary gradient. Composites Part B-Engineering, 42(6), 1386-1394, 2011.

[21] Hadji, L., Atmane, H.A., Tounsi, A., Mechab, I., Bedia, E.A., Free vibration of functionally graded sandwich plates using four-variable refined plate theory. Applied Mathematics and Mechanics, 32(7), 925-942, 2011.

[22] Bouiadjra, M.B., Houari, A.M.S., Tounsi, A., Thermal buckling of functionally graded plates according to a four-variable refined plate theory. Journal of Thermal Stresses, 35(8), 677-694, 2012.

[23] Demirhan, P.A., Taskin, V., Levy solution for bending analysis of functionally graded sandwich plates based on four variable plate theory. Composite Structures, 177, 80-95, 2017. https://doi.org/10.1016/j.compstruct.2017.06.048.

[24] Thai, H.T., Choi, D.H., A refined shear deformation theory for free vibration of functionally graded plates on elastic foundation. Composites Part B-Engineering, 43(5), 2335-2347, 2012.

[25] Thai, H.T., Uy, B., Levy solution for buckling analysis of functionally graded plates based on a refined plate theory. Proceedings of The Institution of Mechanical Engineers Part C-journal of Mechanical Engineering Science, 227(12), 2649-2664, 2013.

[26] Thai, H.T., Choi, D.H., Improved refined plate theory accounting for effect of thickness stretching in functionally graded plates. Composites: Part B, 56, 705–716, 2014.

[27] Demirhan, P.A., Taskin, V., Static analysis of simply supported foam core sandwich plate, Materials, Methods & Technologies, ISSN 1314-7269, Volume 10, 2016.

[28] Thai, H.T., Choi, D.H., Levy solution for free vibration analysis of functionally graded plates based on a refined plate theory. KSCE Journal of Civil Engineering 18(6), 1813-1824, 2014.

[29] Rouzegar, J., Abad, F., Free vibration analysis of FG plate with piezoelectric layers using four-variable refined plate theory. Thin-Walled Structures, 89, 76-83, 2015.

[30] Bessaim, A., Houari, M.S.A., Tounsi, A., Mahmoud, S.R., Bedia, E.A.A., A new higher-order shear and normal deformation theory for the static and free vibration analysis of sandwich plates with functionally graded isotropic face sheets. Journal of Sandwich Structures and Materials, 15(6), 671–703, 2013.

[31] Thai, C.H., Zenkour, A.M., Wahab, M.A., Nguyen-Xuan, H., A simple four-unknown shear and normal deformations theory for functionally graded isotropic and sandwich plates based on isogeometric analysis. Composite Structures, 139, 77–95, 2016.

Teknik Dergi, 2019 9009-9027, Paper 532

Effect of Unsaturated Soil Properties on the Intensity-Duration Threshold for Rainfall Triggered Landslides

Melih Birhan KENANOĞLU[1]
Mohammad AHMADI-ADLI[2]
Nabi Kartal TOKER[3]
Nejan HUVAJ[4]

ABSTRACT

Rainfall triggered landslides are one of the most common natural hazards in many countries throughout the world, as well as in Turkey. This study investigates the effect of unsaturated soil properties on landslide-triggering rainfall intensity-duration threshold. In addition to the time to failure, the suction (negative pore water pressure) distribution in the slope, the shape and depth of the failure surface are also evaluated. Properties of soil-water characteristic curve which affect the distribution of suction in the soil in response to changes in water content are varied in a parametric study. Effects of air entry value (relates to particle size), desaturation rate (relates to uniformity of particle size distribution), saturated volumetric water content (relates to void ratio) and residual volumetric water content (relates to fines content and characteristics) are evaluated by determining the intensity-duration threshold numerically by carrying out infiltration and slope stability calculations, using finite element and limit equilibrium methods, respectively. The variation of unsaturated soil properties is found to significantly alter the landslide mechanism/the cause of failure (ranging from mere surface erosion to groundwater level rise in response to complete infiltration), and consequent intensity-duration thresholds for the same slope geometry. Among the parameters considered, air entry value appears to be the most influential parameter. The effects of the slope angle and initial moisture condition on threshold rainfall intensity-duration are also investigated. This study could be useful for creating the basis and mechanical understanding for future research on early warning systems for rainfall triggered landslides.

Note:
- This paper has been received on April 12, 2018 and accepted for publication by the Editorial Board on October 09, 2018.
- Discussions on this paper will be accepted by May 31, 2019.

• https://dx.doi.org/10.18400/tekderg.414884

1 Middle East Technical University, Civil Engineering Department, Ankara, Turkey - melih.kenanoglu@metu.edu.tr - https://orcid.org/0000-0001-7453-2286

2 Islamic Azad University, Tehran, Iran - ahmadiadli@gmail.com - https://orcid.org/0000-0003-3240-7756

3 Middle East Technical University, Civil Engineering Department, Ankara, Turkey - toker@metu.edu.tr - https://orcid.org/0000-0001-8858-0510

4 Middle East Technical University, Civil Engineering Department, Ankara, Turkey - nejan@metu.edu.tr - https://orcid.org/0000-0002-0909-1135

Keywords: Unsaturated soil, rainfall triggered landslide, intensity-duration threshold, soil water characteristic curve, suction.

1. INTRODUCTION

Slope instability in unsaturated soils is very common in many parts of the world. The rainfall is the major triggering factor, however, the slope topography, geology, hydrology and material characteristics all contribute to development of such instability. In fact, extreme and/or prolonged rainfall events frequently cause landslides in many parts of the world [1-12]. A rainfall triggered landslide develops due to wetting of an unsaturated soil, by which moisture content increases and suction in the ground decreases. Accordingly, weight of the soil increases while its shear strength decreases and deformations in the soil develop. Modelling of rainfall infiltration and slope instability is quite complex for unsaturated soils, since it is controlled by many variables such as the characteristics of the rainfall and the nonlinear hydraulic and constitutive properties of the soil.

One of the mitigation methods for rainfall triggered landslides is early warning. By using landslide early warning systems, alarms can be set up to warn and evacuate people, and to close the roads and railways near the slopes. In the literature, available methods to predict rainfall-triggered landslides are based on two approaches. The first approach is using physically-based models considering infinite slope mechanism [5-10]. Such physically-based models require an understanding of the physical mechanism which controls seepage and slope stability. Slope stability is evaluated by means of static limit equilibrium for a potential failure surface using infinite slope stability analysis assuming a planar slip surface parallel to the ground surface. Pore pressures are assumed or obtained by simple rainfall infiltration models. These methods generally oversimplify unsaturated soil behaviour.

The second approach relies on empirical studies to define (global, regional or national) rainfall intensity (I) and duration (D) threshold. This threshold is defined as the threshold, or the limit value, of the pair of rainfall intensity and rainfall duration, at or above which the total amount of water infiltrating into the unsaturated soil slope would trigger landslides. This threshold is first introduced by [11] as an intensity versus duration (I-D) plot and it is commonly obtained by statistically evaluating the records of past rainfall events that triggered landslides 11-16] (Fig. 1). Only for the sake of examples and visualizing the shape of the rainfall intensity-duration thresholds, in Figure 1, thresholds for different parts of the world proposed by different researchers are presented. In Figure 1, it can be seen that both high intensity-short duration rainfalls and low intensity-long duration rainfalls can trigger landslides (high intensity can be considered as rainfall intensities greater than 50 mm/hr in Figure 1). However, a rainfall with very small intensity might not cause failure even if it rains for a prolonged duration. Statistically-developed empirical thresholds (such as the ones in Figure 1) may be limited by some of the shortcomings of the raw data. For example, archived records of rainfall and slope instability may not be available, the data may not be complete, it may not be precise, or it may have a bias. In some countries such data may not be available, or can be very limited to be able to carry out a statistical evaluation. The data may have a bias such that the rainfalls that caused slope instability may have been recorded more frequently but the rainfalls which did not cause any landslides may not have been recorded. Landslide events which cause damages in urban areas are often recorded but landslides in

unpopulated areas (for example, in different geological formations and slope angles) are typically not recorded. Moreover different landslide types (for example rockfalls, shallow landslides in unsaturated soils, mudflows, debris flows, deep landslides etc.) are typically not treated separately in the database, while different mechanisms control each of these landslide types [17].

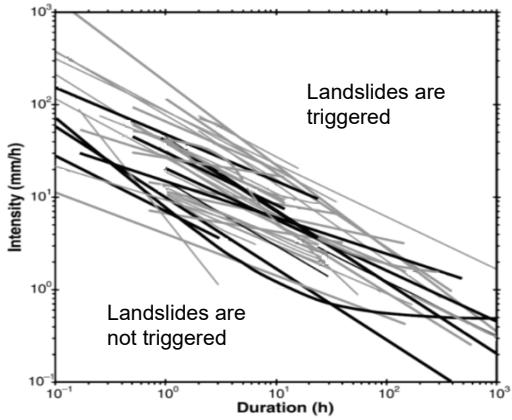

Figure 1 - Rainfall intensity-duration thresholds that are proposed by different researchers for different parts of the world, modified after [15]).

Obtaining a rainfall threshold that triggers a landslide on a particular slope is possible by performing a number of numerical analyses with different rainfall intensity-duration combinations (applying constant rainfall intensity in each analyses until failure) and calculating the factor of safety (F.S.) of the slope. Then a boundary (a threshold) can be generated between "landslide" (F.S. equal to or less than 1.00) and "no landslide" (F.S. equal greater than 1.00) cases. This study investigates the effect of unsaturated soil properties (such as the properties of soil water characteristic curve, SWCC, and the hydraulic conductivity function, HCF) on the distribution of suction in the slope, the shape of the failure surface, failure time, and rainfall intensity-duration threshold. In order to study the effects of changes in characteristics of SWCC, hypothetical soils are needed so that each parameter can be controlled and its effect on the results can be identified individually. SWCC of these soils are generated by changing one of the characteristic parameters (AEV, θ_s, DSR, θ_r) while keeping others constant. We considered SWCC of a sand (Edosaki sand from [4, 18] as starting point and we generated SWCCs with different air entry values (AEV - the suction corresponding to the border of saturated and unsaturated states of the soil); saturated volumetric water contents (θ_s); desaturation rates (DSR - defined as the rate of change of volumetric water content (θ) with matric suction (Ψ)) and residual volumetric water contents (θ_r) as defined in Fig. 2 [19].

These hypothetical soils' properties are then used in a 2D numerical model that has been defined in Geo-Slope 2007 software package (SEEP/W and SLOPE/W) [20] for simulation of seepage and slope stability in 7 m tall finite slopes. Suction distribution in the slope, the

shape of the slip surface, time to failure and slope instability-triggering rainfall intensity-duration threshold were investigated by performing staged seepage (equalization and rainfalling) and limit equilibrium slope stability calculations. Although this general topic has been studied in the literature, the novelties in this study are (i) modeling seepage and slope stability numerically without the assumption of infinite slope, (ii) considering the equalization and rainfall stages using the drying and wetting unsaturated properties of the soils separately (i.e. considering hysteresis in SWCC); (iii) characterizing SWCC through independent physical soil properties, rather than curve fitting parameters, (iv) demonstrating the effects of unsaturated soil properties on the I-D threshold.

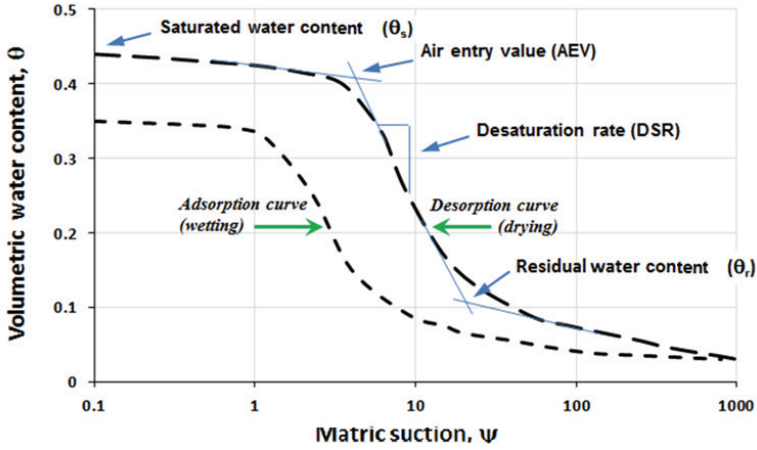

Figure 2 - Drying and wetting soil-water characteristic curve and their key parameters [19].

2. PARAMETRIC STUDY

In this study SWCC is defined in terms of four parameters: AEV (air entry value), θ_s (saturated volumetric water content), DSR (desaturation rate) and θ_r (residual volumetric water content) (Fig. 2). Each of these parameters has a physical meaning. AEV represents the gradation of the soil, e.g. a soil with a higher AEV is a finer grained soil. Saturated volumetric water content, θ_s, represents the density (a soil with a higher θ_s value is a denser soil). DSR is related to the uniformity of the material, e.g. the higher the DSR the more uniform grain size distribution curve is. Residual volumetric water content, θ_r, is related to the fines content such that, as the fines content of a soil increases, θ_r increases. The parameters are different from the curve fitting parameters of the equations that describe SWCC in the literature (such as the parameters *a*, *m* and *n* of [21]). In the following sections the effect of changes in any of these parameters on suction distribution, failure surface, time to failure and I-D plots have been investigated.

2.1. Generation of Hypothetical Soils

Although some measured SWCC curves of real soils are available in the literature, with corresponding grain size distribution curves, they were not sufficient for the purposes of this study. Because, for example, in order to study the effects of fines content, we would like to have SWCC curves of soil with different fines content (as the fines content increases, residual volumetric water content θ_r increases, and SWCC curve changes), however these were not available in the literature in a systematic way. Therefore, in order to study the effects of changes in SWCC characteristics in a controlled manner, generation of hypothetical soils was necessary.

Estimation of SWCC curve from particle size is possible [e.g. 22, 23, 24]. However the existing methods are computationally cumbersome for a full grain size distribution curve covering many different particle sizes. Obtaining SWCC curves by scaling, e.g. by multiplying the suction values with the same number that is used to multiply the grain sizes, is a reasonable and practical approach used in this study [22-25].

As a starting point, a sand from the literature (Edosaki sand from Japan) whose grain size distribution, wetting and drying SWCC's were measured [4, 18] is used. Edosaki sand is classified as silty sand (SM) according to Unified Soil Classification System. The specific gravity of solids and maximum and minimum void ratios of the soil were reported as 2.75, 1.59, and 1.01, respectively, by [4, 18]. Figure 3(a) includes drying and wetting soil water characteristic data for Edosaki sand which has been obtained using Tempe Pressure Cell method for a sample of the same dry density as that in the flume, 1.22 g/cm^3 [4, 18] Appropriate curves have been fitted to these data using the equation proposed by [22]. In addition, drying hydraulic conductivity of this soil has been measured as a function of suction by using a permeameter by [4, 18]. Wetting hydraulic conductivity for Edosaki sand was not measured. Therefore, we deduced it from measured drying hydraulic conductivity data points through drying and wetting SWCCs, assuming there is a negligible hysteresis in HCF when plotted against volumetric water content [26, 27]. In Figure 3(b) HCF data for Edosaki sand are plotted with respect to volumetric water content. These data are compared to some HCF predictions. The method proposed [21], which was found to predict hydraulic conductivity function for this material successfully.

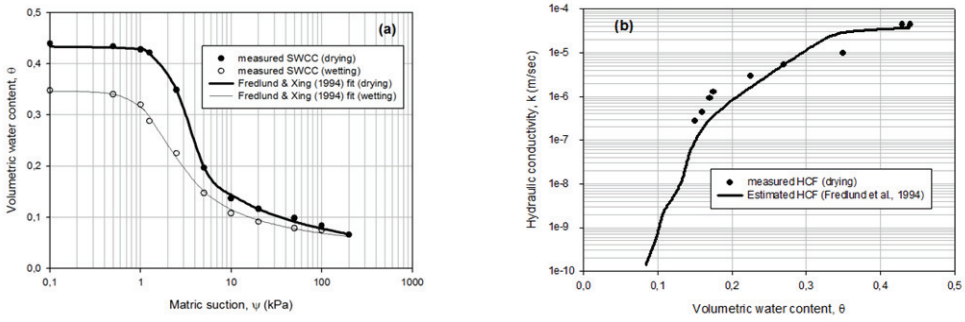

Figure 3 - (a) Soil-water characteristic curves and (b) hydraulic conductivity function (data from [4, 18]).

Air Entry Value: Grain size distribution directly controls the pore size distribution (not only the pore size) [22-25]. Therefore, three hypothetical soils with different AEVs are generated by multiplying grain size distribution data of Edosaki sand by 0.5, 2.0 and 4.0 (Fig. 4). Because AEV of a soil is a measure of its pore size, SWCCs of four hypothetical soils are obtained by scaling the suction values of Edosaki sand SWCC by 0.5, 2.0 and 4.0, whereas volumetric water content values data remain constant. Obviously air entry value in these soils is 0.5, 2.0 and 4.0 times that of Edosaki sand (1.75 kPa), respectively. These hypothetical soils/SWCCs are designated as "AEV=0.88", "AEV=3.5", "AEV=7.0", all values having the unit of kPa (Fig. 5a). Names of the soils according to Unified Soil Classification System (USCS), mean particle size (D_{50}), and fines content (% smaller than 0.074 mm) are given in Table 1. In order to generate hydraulic conductivity functions of four hypothetical soils, saturated hydraulic conductivity (k_s) values are needed as input in the method proposed by [21]. Saturated hydraulic conductivity is assumed to be proportional to the square of particle or pore size, based on pipe flow equations and empirical correlation between permeability and effective grain size (equation 1) by [28]

$$k = C \cdot (D_{10})^2 \quad (1)$$

Where k is the permeability in cm/sec, D_{10}, effective particle size in mm, represents a grain diameter for which 10% of the sample will be finer than it, and coefficient C can be taken as 1.0. Particle, or pore sizes, are assumed to be inversely proportional to AEV, based on capillary tube analogy as well as correlations by [29, 25]. Hence the original saturated hydraulic conductivity value of Edosaki sand is multiplied by 4, 1/4, 1/16 and 1/36 for respective AEV values. These values are then used as an input in the method proposed by [21] which was used to predict hydraulic conductivity functions. Figure 5 shows SWCCs of generated hypothetical soils and their predicted HCFs.

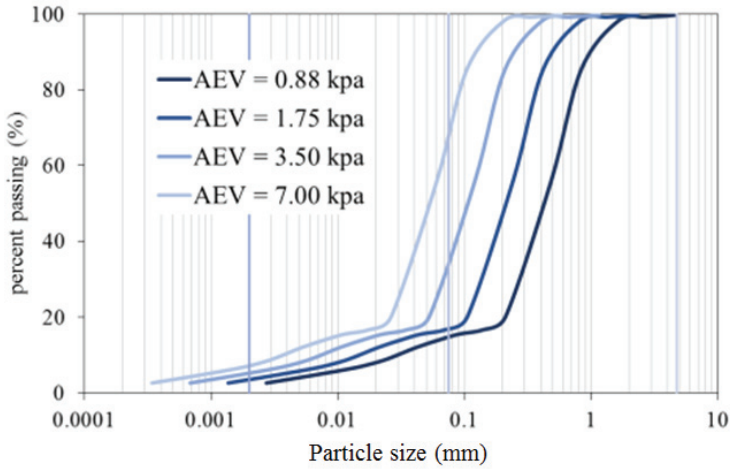

Figure 4 - Grain size distribution curves of soils with different AEVs (grain size distribution data for AEV 1.75 kPa is taken from measured data of [4, 18]).

Table 1 - Specification of generated hypothetical soils with different AEVs.

Soil name	AEV (kPa)	USCS Classification*	D_{50} (mm)	Fines content (%)	C_u	C_c
AEV=0.88	0.88	SM	0.44	15	17.7	3.9
AEV=1.75	1.75	SM	0.22	17		
AEV=3.5	3.5	SM	0.11	32		
AEV=7.0	7.0	ML	0.06	66		

* in USCS classification, plasticity index of the soils would be needed. The soils in this study are considered non-plastic.

Desaturation Rate: As the soil becomes more uniform, desaturation rate (defined in Fig. 2) increases. To obtain soils with different rates of desaturation, DSR of Edosaki sand (0.06) is multiplied by 0.5, 2.0, 4.0 and 8.0. These hypothetical soils / SWCCs are designated as "DSR=0.03", "DSR=0.12", "DSR=0.24" (Fig. 5c). It is assumed that changes in DSR of a soil have no significant effect on its k_s.

Saturated Volumetric Water Content: Another set of four hypothetical soils with different θ_S are generated by varying saturated volumetric water content values of Edosaki sand SWCC (which is 0.44) by increments/decrements of 0.04; thus, θ_S values in the range of 0.36 to 0.52 are obtained (Fig. 5e). Physical interpretation of this action is increasing and decreasing dry density of hypothetical soil. A soil with a higher θ_S value is a looser soil. Saturated hydraulic conductivity of these newly generated soils, to be used as an input in HCF estimation at SEEP/W, are deduced from permeability of Edosaki sand considering density of each hypothetical soil. Pipe flow equation and volume mass relations are used to derive a relation between k_S and volumetric water content.

Residual Volumetric Water Content: Soils with increased and decreased residual water content are generated from original SWCC data set of Edosaki sand (which is 0.135). To do so, volumetric water contents of data at residual/tail part of SWCC (with suction higher than 10 kPa) are increased and decreased by 0.01 (Fig. 5g).

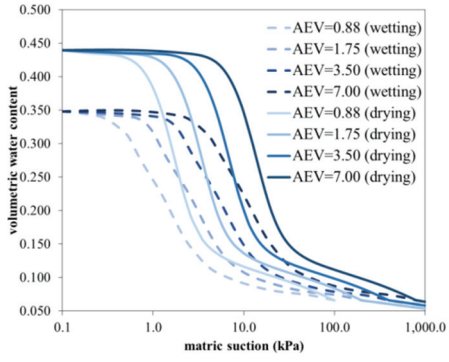

(a)

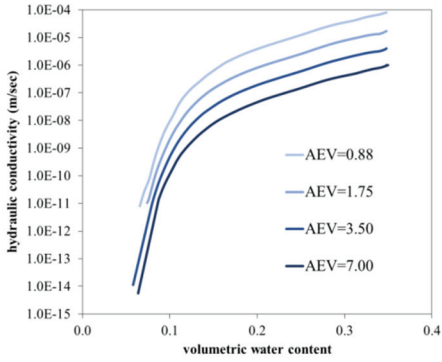

(b)

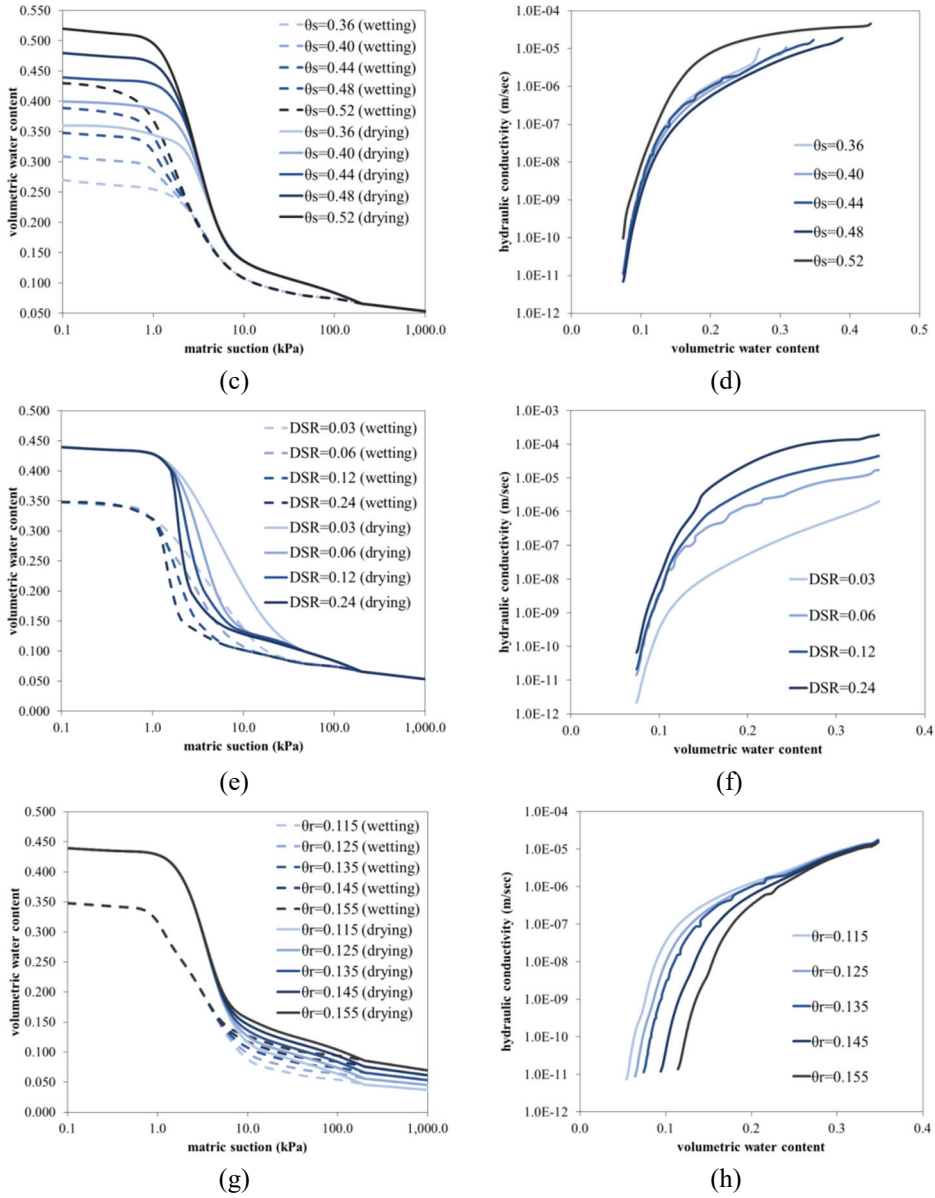

Figure 5 - SWCC's of hypothetical soils with different (a) AEV's, (c) θ_s values, (e) DSR's and (g) θ_r values. HCF's of hypothetical soils (since the hydraulic conductivity curves are plotted with volumetric water content drying-wetting hysteresis effect would not be seen) for different (b) AEV's, (d) θ_s values, (f) DSR's and (h) θ_r values.

3. NUMERICAL SIMULATIONS

3.1. Geometry and Boundary Conditions of the Finite Slope

The numerical approach is first validated by predicting the triggering rainfall-intensity duration for a well-instrumented laboratory slope model test on Edosaki sand by [4, 18] in [30, 31]. The numerical model is defined in GeoStudio 2007 software (SEEP/W and SLOPE/W) (Figure 4a). SEEP/W can model both saturated and unsaturated flows and SLOPE/W can model stability of slopes considering variable pore-water pressure conditions using limit equilibrium method [31, 32]. As part of the current study, unsaturated seepage and slope stability study were performed over a hypothetical finite slope. A 10-m-high, 15-m-wide model that includes a 7 m high, 45-degree slope is defined and then the entire spectrum of hypothetical soils were assigned to it (Figure 6a). In the finite element model, boundary conditions are considered as "no-flow" boundaries at the bottom and on the left-side of the model, since no water flow is allowed through these boundaries (Figure 6a). Other boundaries are "unit flux" boundaries since rainfall is infiltrating at a defined rate (Figure 6a).

Initial sensitivity analyses were performed to determine the required width of the model, in order to see whether a wider model geometry would give different results. Based on the sensitivity analyses, it was concluded that the results are not influenced by the boundary conditions, and that, a 15m wide model was sufficient for the purposes of this study. Similarly, different heights of the model did not influence the suction values, the failure mechanisms and the failure surfaces in this study, therefore a 10m high model was found to be sufficient.

A seepage analysis is carried out in two time-dependent (transient) stages at SEEP/W. These stages are;

- **Equilibration stage** which is a 30-day period of waiting, during which suction equilibration took place. Time period for this stage is selected so long to eliminate the effect of different drying hydraulic conductivities on equalibration of suctions.
- **Rainfalling stage** during which rainfall is applied and slope stability analyses are carried out.

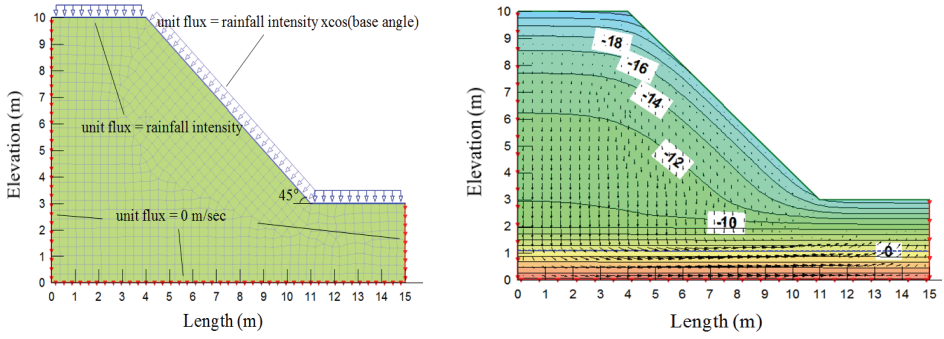

Figure 6 - (a) Geometry and boundary conditions of the finite slope model, (b) initial suction values in the slope before the rainfall application.

The initial suction value (before equalization stage) is needed in the analyses. A constant initial volumetric water content, instead of constant initial suctions, are assumed in four hypothetical soils in Figure 4a. This is a realistic assumption, because the finer-grained soils would have higher initial suction values. For example, let's compare the suction values corresponding to volumetric water content of 0.148 for AEV=7.0 kPa soil and for AEV=0.88 kPa soil in Figure 4a, in their wetting curves. AEV=7.0 kPa soil is a finer-grained soil and has higher initial suction value. The initial volumetric water content should be a low value, but not as low as to be in the range of residual water content zone of each hypothetical soil. The reason for choosing this number as a low value is that, with the initial suction values, for the given slope angle and slope geometry, slopes should be initially stable in each of the four hypothetical soils [31]. Therefore, SWCC's of four hypothetical soils given in Figure 4a are considered when choosing the initial volumetric water content value of 0.148 for all soils (and this value corresponds to different initial suction values for each of the four hypothetical soils in Figure 4a).

After equalization stage, the values of suction that satisfy hydraulic equilibrium throughout the slope are obtained (Fig. 6b) and are taken as the initial suction values for rainfall stage. The pore water pressure distributions obtained for each time increment of seepage analysis are used in stability analyses to determine the factor of safety of the slope using SLOPE/W. For stability analyses, the pore water pressure obtained from numerical seepage analyses are used to determine the factor of safety of the slope by Morgenstern and Price (1965)'s limit equilibrium method [33]. In order to interpret shear strength of soils in unsaturated state, the method proposed by [34] is used as in equation (2)

$$\tau = c' + (\sigma_n - u_a)\tan\phi + (u_a - u_w)\tan\phi\left(\frac{\theta - \theta_r}{\theta_s - \theta_r}\right) \tag{2}$$

where τ denotes shear strength of unsaturated soil, c' is effective cohesion of saturated soil; ϕ' is internal friction angle, σ_n is total normal stress on the plane of failure, θ is the volumetric water content, θ_r is the residual volumetric water content, θ_s is the saturated volumetric water content, u_a and u_w are pore air and water pressures, respectively. This equation is available in SLOPE/W software.

3.2. Seepage and Stability Analyses

By using unsaturated hydraulic properties (SWCC & HCF) of hypothetical soils seepage and stability analyses of the model are performed under constant rainfall intensity values between 5 and 80 mm/hr rainfall. Examples of pore water pressures and slip surfaces calculated at the time of failure (F.S.=1.00) are demonstrated in Fig. 7 through Fig. 10. It should be noted that, in this study, the effects of the surface vegetation/roots on infiltration and slope stability (and hence on I-D threshold) is not considered, however, it is anticipated that these would influence the results.

Before starting to study the effects of changes in SWCC of the soils, in order to decide on initial pore water pressure in any of numerical models, preliminary analyses were carried out on a single model with different initial water contents. The results showed that initial suction

in the soil body can significantly affect the behavior of the slope. In all of the cases with different initial suctions, failure modes are observed to be very similar (at the time of failure). On the other hand, assuming constant initial suctions for all models (models with different SWCCs) leads to different initial water contents. Slopes with higher initial suctions require more water volume to reach failure and lower initial suctions make slopes eligible for earlier failure. Therefore, in different models, we decided to assume constant water content instead of constant suctions at the initial state. Consequently, in all analyses initial suction is set to correspond to 0.148 volumetric water content. In this way, in the models with finer soil type (e.g. higher AEVs), initial suctions (onset of analyses) are set to higher values, but they require the same volume of infiltration to reach saturation.

Air Entry Value – After analysis of the set of models with different AEVs, we observed that pore water pressure values within the soil vary from -26 to +26 kPa for different soil types (Fig. 7). Suction remains high in the depths of slopes with finer soil types while it is reduced only at the surface, even after a period of rainfall long enough to reach failure. This is because lower hydraulic conductivity at high suctions prevents infiltration more than a few meters beyond the surface. Therefore, only shallow failures occur in slopes composed of finer material.

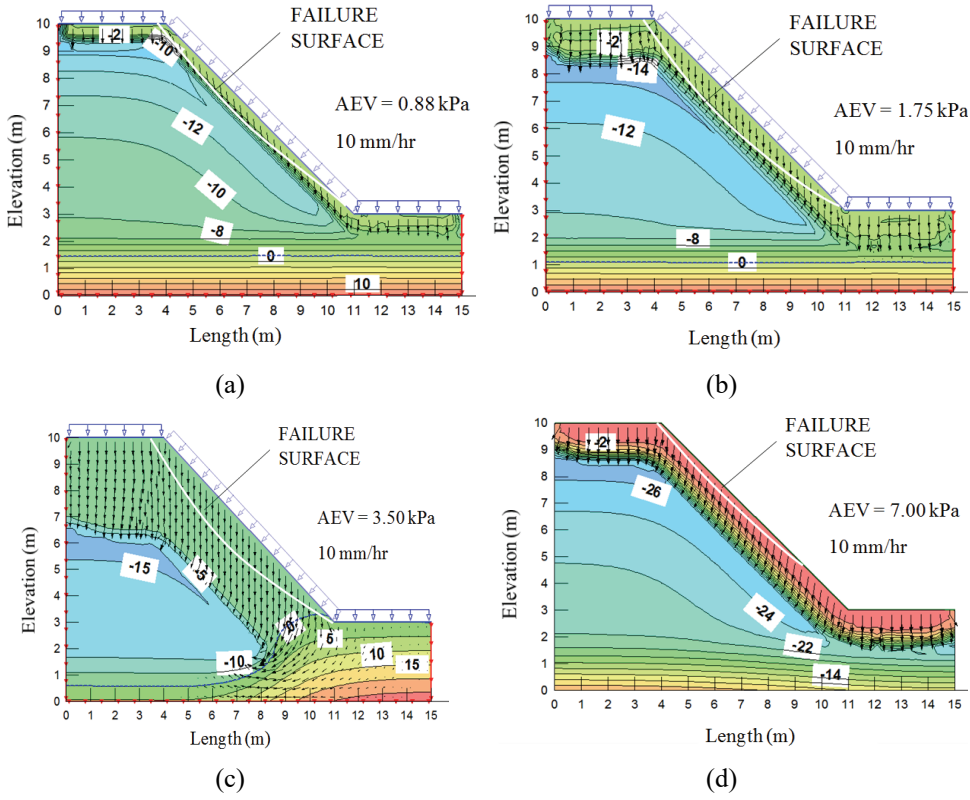

Figure 7 - Pore water pressure distribution and failure mode of slopes of hypothetical soils with different AEVs: (a) 0.88 kPa, (b) 1.75 kPa, (c) 3.50 kPa, (d) 7.00 kPa.

Saturated Volumetric Water Content – Soils with higher θ_s values represent looser soils. However, this does not significantly change suction distribution and failure surface at the time of failure for the slopes composed of these soils. Numerical analyses show that for denser soils (lower θ_s) water table at the time of failure is deeper (Fig. 8) and slip surface is slightly shallower. However, this analysis does not consider the increase in friction angle of the soil, ϕ, due to greater density.

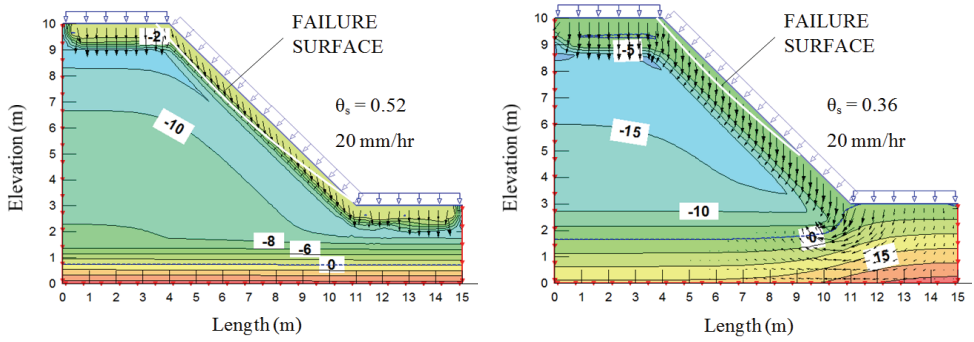

Figure 8 - Pore water pressure and failure mode of slopes composed of hypothetical soils with highest and lowest θ_s values: (a) 0.52, (b) 0.36.

Desaturation rate – Desaturation rate is mostly controlled by uniformity of the grain sizes of soil. Pore water pressure distribution for highest and lowest DSR values, 0.24 and 0.03, respectively, are demonstrated in Fig. 9. In non-uniform soils (lower DSR) due to higher initial suction values and consequently lower hydraulic conductivities, less infiltration occurs.

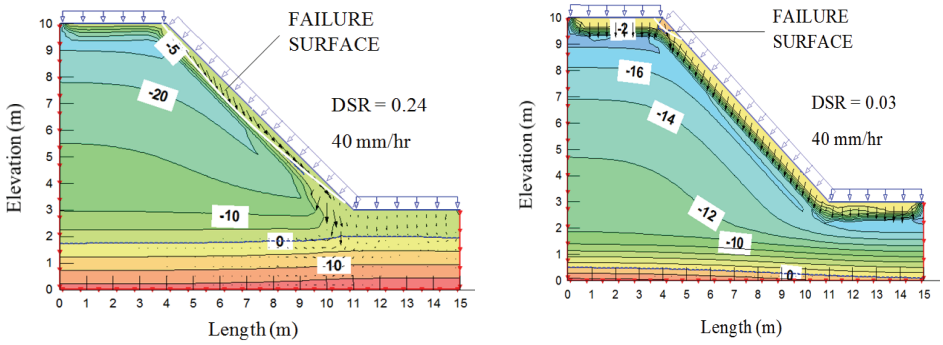

Figure 9 - Pore water pressure and failure mode of slopes composed of hypothetical soils with highest (a) and lowest (b) DSR values.

Residual Volumetric Water Content – Changes in fines content cause significant changes in the shape of SWCC but this does not affect suction distribution in the slope of this soil. Suction distribution and the shape of slip surface in slopes with soils of different θ_r values are very similar to those of Edosaki sand (Fig. 10). Water tables at the time of failure in these analyses are very similar despite the differences in θ_r. However differences would arise if the initial water contents were smaller.

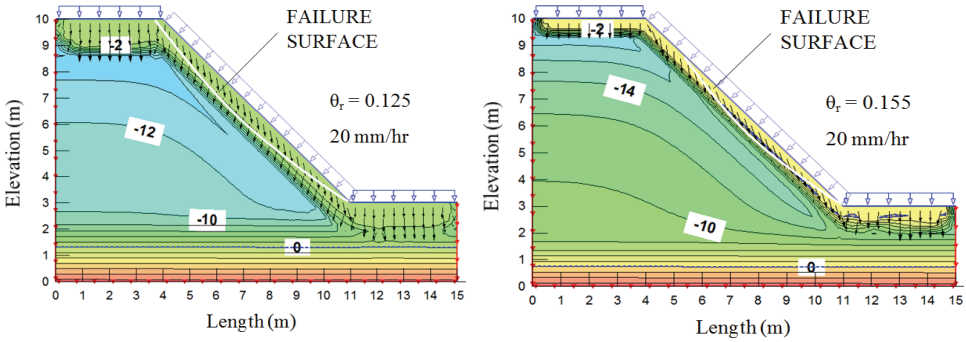

Figure 10 - Pore water pressure and failure mode of slopes composed of hypothetical soils with highest (a) and lowest (b) θ_r values.

It is observed that, in all of the analyses carried out in this study, the failures can be considered as "shallow landslides", i.e. the depth of failure surface is small as compared to the length of the landslide. The failure mechanisms (or causes of failure) that are observed in this study can be grouped into three categories: (A) surface erosion, (B) failure due to suction decrease, (C) positive pore water pressure development. In type (A), the surface erosion type, the failure surfaces are very shallow, i.e. less than 30 cm deep and suction values in the soil are high, e.g. the failure surface for AEV=7.0 in Fig. 7. Type (A) failure mechanism is shown by red colored data points in Fig. 11 and 12, which are mostly occurring at high intensity rainfall events. In cause of failure Type (B), infiltrating water progresses downward in a profile similar to a wetting front parallel to the slope surface, suctions in this zone decrease in response and lead to failure (e.g. the failure surface for AEV=0.88 and 1.75 in Fig. 7). Type (B) failure events are represented by blue data points on the I-D thresholds in Figures 11 and 12, generally reaching failure with lower cumulative amounts of rainfall. Type (C) failure happens in cases where the rainfall is very slow relative to the permeability (or permeability is large relative to rainfall), the water percolates all the way down to the groundwater level without causing too much decrease in suctions in the unsaturated zone. This results in a rise in groundwater level and development of positive pore pressures at the lower part of the failure arc (e.g. the failure surface for AEV=3.5 in Fig. 7). Type (C) failure events are represented by green data points in Figures 11 and 12.

3.3. Rainfall Intensity-Duration (I-D) Thresholds

Intensity and duration are primary rainfall properties controlling the infiltration into a slope and instability. We investigated the effects of slope angle, in the range of 41 to 49 degrees, on the I-D threshold for given soil properties (Edosaki sand) and given initial moisture state (volumetric water content of 0.148) (Fig. 11a). It is observed that for relatively high intensity rainfalls (greater than 50 mm/hr) the changes in the slope angle did not influence the I-D threshold significantly. The reasoning behind this can be, at high intensity rainfalls, the rainfall does not have time to infiltrate into the ground, rather, the most of the rainfall moves down in the form of surface runoff. For rainfalls having less than 50 mm/hr intensity, the I-D thresholds differ dramatically, e.g. at a given rainfall intensity, the steeper slopes require less duration of rainfall to develop landslides, which can be expected, due to initial higher shear stresses existing in the ground before the rainfall. At a given slope angle (45 degrees), the changes in the initial moisture state affected the I-D thresholds, only slightly, for the given soil, and given initial moisture conditions (Fig. 11b).

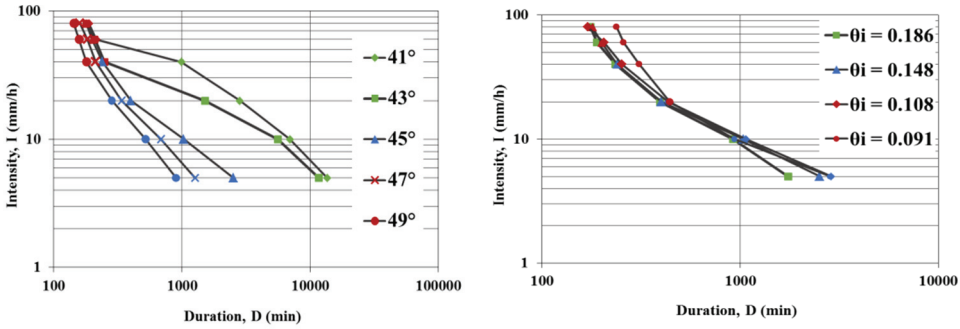

(a) (b)

Figure 11 - Changes in I-D threshold for a given soil, (a) for a given initial moisture state, at different slope angles, (b) for a given 45 degree slope angle at different initial moisture states

I-D thresholds for different hypothetical soils and the effects of SWCC characteristics for a finite slope are shown in Fig. 12. In Figure 12, each data point corresponds to a new analysis for rainfall intensities in the range of 5 to 80 mm/hr, and each data point corresponds to the time of failure. Changes in AEV (i.e. grain size) of a soil appears to have a significant effect on I-D threshold (Fig. 12a). For a given rainfall intensity, longer duration is required to fail a slope composed of finer soil in comparison to a slope composed of coarser soil. As the soil gets finer, the difference between the durations required to trigger a landslide for high-intensity and low-intensity rainfalls decreases (i.e. the slope of the I-D threshold line on a log-log plot increases). In other words, a high-intensity rainfall may trigger a landslide in a coarser soil in shorter duration in comparison to a finer soil. The exception to this is if the soil is very coarse, then failure is unreachable with a rainfall that has a low intensity since the water can freely be drained through the soil by gravity, never increasing the degree of saturation.

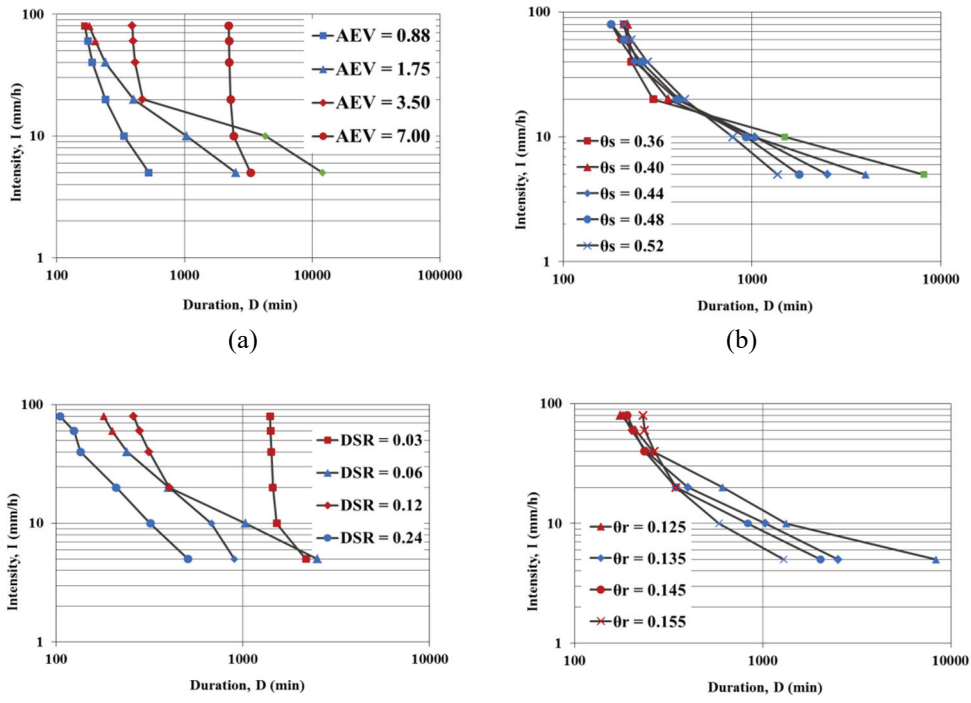

Figure 12 - I-D thresholds for soils of different AEV, θ_s, DSR and θ_r values.

Saturated volumetric water content does not seem to affect the I-D threshold significantly, as compared to other parameters studied. As the saturated volumetric water content, θ_s, of the soil changes (i.e. dry density), the durations on the I-D threshold change but its inclination remains constant (Fig. 12b). For a given rainfall duration, for greater θ_s (looser soil) higher intensity rainfalls are needed to make the slope fail. In other words, for a given rainfall intensity, longer duration rainfall is needed to cause failure as the soil gets denser. It must be noted that at lower intensities no significant difference is observed for different values of θ_s.

Increasing of desaturation rate, DSR, (i.e. uniformity) can also affect I-D plot. Slopes of soils with more uniform particle size distribution (higher DSR) tend to fail in shorter time for a given rainfall intensity (Fig. 12c). This is probably because a greater amount of water infiltrates the uniform soils faster and consequently suction is reduced sooner, reducing shear strength. In soils with non-uniform particle size distribution (low DSR) there seems to be no significant changes in stability due to DSR changes.

Value of θ_r (i.e. fines content) also affect I-D threshold offset slightly. Soils composed of higher percent of fine particles may fail in shorter time while soils with less fine content do not tend to fail at low rainfall intensities. This has been shown in Fig. 12(d) that in low rainfall intensities (less than 20 mm/hr) no failure (data point) has been observed in slopes of soils with less fine content (low θ_r value).

4. CONCLUDING REMARKS

Understanding the effects of wetting/drying SWCC and HCF on I-D thresholds is a necessary first-step towards an integrated early warning system for rainfall triggered landslides that considers the physical mechanism of the problem and natural variability of soils.

The intensity-duration threshold that triggers a landslide can be computed given that the unsaturated hydraulic and shear strength properties of the soil are known.

The results indicate that different unsaturated soil properties lead to different intensity-duration thresholds for the same slope geometry. Unsaturated soil properties such a SWCC and HCF play a critical role in the behavior of unsaturated slopes and in rainfall-triggering of landslides. Current study is focused on the effects of changes in controlling parameters of SWCC, namely the air entry value (AEV), saturated water content (θ_s), desaturation rate (DSR) and residual water content (θ_r) on the landslide development. Among the parameters considered, air entry value (which is related to grain size) seems to be the most influential parameter on the rainfall threshold.

In coarse-grained soils, for a given rainfall intensity, as the particle size gets smaller (i.e. AEV gets larger) time to failure becomes longer due to the existence of higher suctions and slower infiltration. In other words longer duration of rainfall is needed to cause failure, and shallower slip surfaces are expected. It is observed that θ_s (the density of the soil) does not significantly change the failure surface, suction distribution at the time of failure. For a given rainfall intensity, a looser soil (with larger θ_s) requires slightly longer duration rainfalls to cause the slope to fail. In soils with uniform particle size distribution (i.e. greater DSR) infiltration occurs more quickly and failure occurs in shorter time as compared to a soil with lower DSR. Changes in θ_r (i.e. fines content) cause significant changes in the shape of SWCC but this does not affect suction distribution at the time of failure, unless the slope is initially very dry. θ_r also offsets the I-D threshold slightly without changing its inclination.

Both “high intensity short duration” rainfalls and “low intensity long duration” rainfalls can cause landslides in unsaturated soils, as characterized by I-D thresholds. Based on the analyses carried out in this study for rainfall intensities between 5 - 80 mm/hr it is observed that I-D threshold that triggers a landslide is nonlinear in a log-log plot. As the soil gets finer, the difference between the durations required to trigger a landslide for high-intensity and low-intensity rainfalls decreases (i.e. the slope of the I-D threshold line on a log-log plot increases). In other words, a high-intensity rainfall may trigger a landslide in a coarser soil in shorter duration in comparison to a finer soil. For finer grained soils, time to failure is independent of rainfall intensity above a certain level. This is because above that certain intensity, only surface runoff increases and infiltration into the soil does not change.

Three distinct failure mechanisms (or causes of failure) are observed in this study: (A) surface erosion, (B) failure due to suction decrease, (C) positive pore water pressure development. Cause of failure type (A) mostly occurs at high intensity rainfall events, cause of failure type (B) generally at lower cumulative amounts of rainfall, and type (C) in cases where the rainfall is very slow relative to the permeability and a rise in groundwater level and development of positive pore pressures at the lower part of the failure arc.

The novelties in this study, as compared to the previous physically-based models, are (i) modeling seepage and slope stability using the drying and wetting unsaturated properties of

the soils separately for evaporation and precipitation stages respectively (i.e. considering hysteresis in SWCC; (ii) characterizing SWCC through independent physical soil properties, rather than curve fitting parameters; (iii) demonstrating the effects of unsaturated soil properties on I-D threshold.

Acknowledgements

Funding for this research was provided by the Scientific and Technological Research Council of Turkey (TUBITAK) research project No. 109M635.

References

[1] Alonso, E., Gens, A., and Delahaye, C.: Influence of rainfall on the deformation and stability of a slope in over consolidated clays: a case study, Hydrogeology Journal, 11(1), 174-192, 2003.

[2] Chen, H., Dadson, S., and Chi, Y.: Recent rainfall induced landslides and debris flow in northern Taiwan, Geomorphology, 77, 112-125, 2006.

[3] Guzzetti, F., Peruccacci, S., Rossi M., and Stark, C.P.: The rainfall intensity–duration control of shallow landslides and debris flows: an update, Landslides, 5, 3-17, 2008.

[4] Gallage, C. P. K., and Uchimura, T: Investigation on parameters used in warning systems for rain-induced embankment instability. In Kwok, Charles (Ed.) Proceedings from the 63rd Canadian Geotechnical Conference (GEO2010), GEO2010 Calgary, Calgary, Alberta, 1025-1031, 2010.

[5] Montgomery, D.R., and Dietrich, W.E.: A physically based model for the topographic control of shallow landsliding, Water Resources Research, 30(4), 1153–1171, 1994.

[6] Wilson, R.C., and Wieczorek, G.F.: Rainfall thresholds for the initiation of debris flow at La Honda, California, Environ. Eng. Geosci., 1(1), 11–27, 1995.

[7] Wu, W., and Sidle, R.C.: A distributed slope stability model for steep forested basins, Water Resour. Res., 31, 2097–2110, 1995.

[8] Iverson, R.M.: Landslide triggering by rain infiltration, Water Resources Research, 36(7), 1897-1910, 2000.

[9] Crosta, G. B., and Frattini, P.: Distributed modelling of shallow landslides triggered by intense rainfall, Nat. Hazards Earth Syst. Sci., 3, 81-93, doi:10.5194/nhess-3-81-2003, 2003.

[10] Eichenberger, J., Ferrari, A., and Laloui, L.: Early warning thresholds for partially saturated slopes in volcanic ashes, Computers and Geotechnics, 49, 79-89, 2013.

[11] Caine, N.: The rainfall intensity-duration control of shallow landslides and debris flows, Geogr. Ann., 62 A(1-2), 23-27, 1980.

[12] Reichenbach, P., Cardinali, M., De Vita, P., and Guzzetti, F.: Regional hydrological thresholds for landslides and floods in the Tiber River Basin (central Italy), Environmental Geology, 35(2&3), 146-159, 1998.

[13] Corominas, J.: Landslides and climate, in: Proceedings of the 8th International Symposium on Landslides, edited by: Bromhead, E., Dixon, N., and Ibsen, M. L., A. A. Balkema, Cardiff, 4, 1–33, 2000.

[14] Aleotti, P.: A warning system for rainfall-induced shallow failures, Eng. Geol., 73, 247-265, 2004.

[15] Guzzetti, F., Peruccacci, S., Rossi M., and Stark, C.P.: Rainfall thresholds for the initiation of landslides in central and southern Europe, Report, Istituto di Ricerca per la Protezione Idrogeologica, Perugia, Italy, 48 pp., 2007.

[16] Lu, N., and Godt, J.W.: Hillslope Hydrology and Stability, Cambridge University Press, Cambridge, UK, 2013.

[17] Cornforth, D.H., Landslides in Practice: Investigation, Analysis, and Remedial/Preventative Options in Soils, Wiley, 624 pages, 2005.

[18] Gallage, C., Kodikara, J., Uchimura, T.: Laboratory measurement of hydraulic conductivity functions of two unsaturated sandy soils during drying and wetting processes, Soils and Foundations, V.53(3), p. 417-430, 2013.

[19] Fredlund, D.G., Rahardjo, H., Fredlund, M.D.: Unsaturated Soil Mechanics in Engineering Practice, Wiley, 926 pages, 2012.

[20] GEO-SLOPE, SEEP/W, GEO-SLOPE International Ltd., Calgary, Alberta, Canada, 2007.

[21] Fredlund, D.G., Xing, A., and Huang, S.Y.: Predicting the permeability function for unsaturated soils using the soil water characteristic curve, Canadian Geotechnical Journal, Vol. 31, No. 4, 533-546, 1994.

[22] Arya, L.M. and Paris, J. F.: Physicoempirical model to predict the SMC from particle size distribution and bulk density data, Soil Science Society of America Journal, Vol.45, 1023-1030, 1981.

[23] Fredlund, D.G., Wilson, G.W. and Fredlund, D.G.: Use of grain size distribution for estimation of the soil-water characteristic curve. Canadian Geotechnical Journal, 39, 1103-1117, 2002.

[24] Shoarian Sattari, A. and Toker, N.K.: Obtaining soil-water characteristic curves by numerical modeling of drainage in particulate media. Computers and Geotechnics Journal, Vol. 74, 196-210, 2016.

[25] Toker, N.K.: Improvements and reliability of MIT tensiometers and studies on soil moisture characteristic curves, M.S. Thesis, Massaschusets Institute of Technology Civil Engineering Department, Boston, USA, 143 p., 2002.

[26] Fredlund, D.G. and Rahardjo, H.: Soil mechanics for unsaturated soils, John Wiley and Sons Inc. New York, 1993.

[27] Lu, N. and Likos, W.J.: Unsaturated Soil Mechanics, John Wiley & Sons, NJ, 2004.

[28] Hazen, A.: Water Supply, In American Civil Engineers Handbook. John Wiley & Sons, New York, p.1444-1518, 1930.

[29] Sjoblom, K.J.: The mechanism involved during the desaturation process of a porous matrix, Ph.D. Thesis, Massaschusets Institute of Technology Civil Engineering Department, Boston, USA, 2000.

[30] Ahmadi-adli, M., Huvaj, N., and Toker, N. K.: Rainfall triggered landslides in unsaturated soils: a numerical sensitivity analysis, in Proceedings of 10th International Congress on Advances in Civil Engineering, Middle East Technical University, Ankara, Turkey, 17-19 October 2012, Article 1179, 2012.

[31] Ahmadi-adli, M.: Shallow landslides triggered by rainfall in unsaturated soils, Ph.D. Thesis, Middle East Technical University, Civil Engineering Department, Ankara, Turkey, 2014.

[32] Ahmadi-adli, M, Huvaj, N. and Toker, N.K.: Prediction of seepage and slope stability in a flume test and an experimental field case, Procedia Earth and Planetary Science, v.9, p.189-194, 2014.

[33] Morgenstern, N.R., and Price, V.E.: The analsis of the stability of general slip surfaces, Geotechnique, Vol. 15, pp. 79-93, 1965.

[34] Vanapalli, S.K., Fredlund, D.G., Pufahl, D.E., and Clifton, A.W.: Model for the prediction of shear strength with respect to soil suction". Canadian Geotechnical Journal, 33(3), 379-392, 1996.

Teknik Dergi, 2019 9029-9051, Paper 533

Flood Analysis Using Adaptive Hydraulics (ADH) Model in the Akarcay Basin

Halil Ibrahim BURGAN[1]
Yilmaz ICAGA[2]

ABSTRACT

Every year, thousands of people are loosing their lives and significant financial losses occur because of flood disasters. Floods stem from basin characteristics. Floods can occur due to effects of snow melts and erratic rainfall because of shallow rivers even in summer months in the Akarcay Basin. In this study, Adaptive Hydraulics (AdH) model and The Finite Element Surface Water Modeling System (FESWMS) were used to generate a hydraulic model. Consequently, many settled areas would not face flood risk, but especially agricultural lands in some regions near the banks of streams can experience damages after floods.

Keywords: Flood damages, hydraulic modeling, shallow rivers, surface water.

1. INTRODUCTION

Flood disaster on a hydrological basin can be predicted by scientific methods. Various modeling techniques are used for the prediction and the prevention studies of flood disaster. These studies covered mathematical, visualization (as 2D/3D mapping etc.) and statistical methods. Also, new Geographic Information System (GIS) technologies are used while producing flood risk maps. Although, hydrological models provide a foresight about flood risk magnitude of a basin, detailed flood risk maps of a basin can be produced by hydraulic models after assessment of the hydrological models. It can be said that hydrological models can be used at basin scale applications and hydraulic models can be used at local scale applications.

Various hydraulic models are used to assess flood risks. Widely used models are exemplifyed as (HEC-RAS, AdH, RMA2 or 4, TUFLOW, MIKE, FLO-2D, IDRISI, SOBEK, FloodWorks, LISFLOOD-FP, TELEMAC-2D, etc.). Surface Water Modeling System (SMS) software comprehends riverine models (*e.g.* AdH, FESWMS, RMA, TUFLOW) and coastal

Note:
- This paper has been received on April 17, 2018 and accepted for publication by the Editorial Board on October 09, 2018.
- Discussions on this paper will be accepted by May 31, 2019.
- https://dx.doi.org/10.18400/tekderg.416067

1 Istanbul Technical University, Department of Civil Engineering, Istanbul, Turkey - burgan@itu.edu.tr - https://orcid.org/0000-0001-6018-3521

2 Afyon Kocatepe University, Dep. of Civil Engineering, Afyonkarahisar, Turkey - yicaga@aku.edu.tr - https://orcid.org/0000-0001-9347-4683

models (*e.g.* ADCIRC, CGWAVE, CMS, TUFLOW). In this study for the aim of assessing flood risk of the Akarcay Basin, Turkey, AdH and FESWMS models developed by Coastal and Hydraulics Laboratory [1] of US Army Corps of Engineers (USACE) – Engineer Research and Development Center (ERDC) and Brigham Young University (BYU), respectively, were used as the SMS software.

Flood estimations studies can be made by statistical methods as well as visualization methods (as 2D/3D mapping etc.). Statistical methods cover regional flood frequency analysis [2], with a region of influence (ROI) approach and seasonality [3, 4, 5], with two-component extreme value distribution [6], with historical data [7], with copula method [8] and asymmetric copula [9], Gumbel mixed model [10], classification with basin characteristics [11]. Basically, the statistical modeling occurs by regionalization of gauging stations, the definition of homogenous/similar catchments or transfer of gauged flow data to the catchments which have similar hydrological, meteorological or morphological characteristics. Then, frequency analysis can be used to determine flood discharge corresponding to any return period after the best fit distribution selection of the data and the calculation of selected distribution parameters.

Visualization methods are based on the solutions of 2D or 3D hydrodynamic models, and they are preferable in terms of the presentation of comparable and interpretable results. The usage of them can be in the basin scale as well as local scale. Substantial data with high resolution is required for local scale hydrodynamic modeling. For example, higher than 1:5000 scale digital elevation model (DEM) data is required to be able to extract cross sections of a river. Detailed topography of the watershed was used for the definition of flood risky areas near River Meuse in The Netherlands with a length of 35 km, 100 m width for river with floodplain bed of the river and 3 km width per cross section [12]. Horritt & Bates (2002) compared three hydrodynamic models to assess flood risk of Severn River, UK [13]. Sanders (2007) used different on-line DEMs to evaluate flood inundation risks [14]. The acquisition of local DEM data is difficult and also-costly. Besides, the global DEM is freely and easily accessible. Therefore, global DEM as Advanced Spaceborne Thermal Emission and Reflection Radiometer (ASTER), Shuttle Radar Topography Mission (SRTM) and newly Multi-Error-Removed Improved-Terrain (MERIT) with high accuracy, not high resolution by Yamazaki *et al.* (2017) is widely used in flood risk mapping studies [15].

Shallow waters and lowlands can be affected by flash floods rapidly. Some indices as topographic wetness index or SAGA wetness index or hydrological models can be used for determination of flash flood prone areas. The area of interest of this study is shallow waters and low-lands, so the basin responds in the form of flash floods rapidly to extreme rainfall in winter or snow melts in spring. The investigations support this information for other basins of hydrological similarity. Ciervo *et al*. (2015) used FLATModel for shallow waters with 1:500 scale topographic maps [16]. Also, Bradford & Sanders (2002) used Riemann solver for shallow water equations [17]. de Almeida *et al*. (2016) performed shallow water model with extremely fine-resolution (10 cm) terrain data for an urban area [18]. Falter *et al*. (2016) used FLEMOps+r damage model for shallow water areas[19].

There are many applications of FESWMS model. The applications are mostly hydrodynamic models around weir structures and some models for simulation of flow [20], scour analysis [21, 22] comparison of HEC-RAS/FESWMS flood risk boundaries [23], habitat restoration and sediment transport [24, 25, 26], park restoration [27], sedimentation and scour in small urban lakes [28], habitat model [29], river bifurcation analysis [30].

The second hydrodynamic model was used as AdH model in this study. The AdH model is newly developed and is shared openly with users. The model has a very wide range of usage, and leads to very innovative applications and satisfactory results. Some of the applications are modeling of floating objects [31], surge overtopping of a levee [32], groundwater [33], the effects of shoreline sensitivity on oil spill trajectory [34], complex river–lake interactions [35], the effects of the surge protection structure on Gulf Intracoastal Waterway [36], habitat restoration and flood control protection [37], navigation lock filling system and mass conservation [38, 39], transient simulation [40], hydrologic model at watershed scale [41], dam and levee breach [42].

Peak flood discharge or flood hydrograph is required as an input in the hydraulic model. It can be acquired from observed flow data of gauging station on the stream. However most of the time, it is not possible to find gauging stations on the river. In this case, synthetic hydrograph methods can be used. In this study, for the observed flow data from State Hydraulic Works in Turkey, Mockus method, SCS method and linear regression between rainfall and discharge data were used to acquire peak flood discharge.

2. METHODS

In the first step of this work, the determination of peak flood discharges, which were used in the models, consisted of three methods. Firstly, observed monthly flow data (hydrographs) from gauging stations was assessed. Then, Synthetic methods, SCS & Mockus, to estimate peak flood discharges were used. Finally, rainfall-runoff relationship was investigated using observed monthly total precipitation data.

In the final step, hydrodynamic models, AdH and FESWMS models were run using peak flood discharge and DEM data. The most important advantage of the selected hydrodynamic models is that they provide good results in shallow water modeling as in the case of Akarcay Basin rivers.

2.1. SCS Method

SCS method has very simple and easy methodology to estimate peak flood discharge based on basin morphological parameters. The method provides close results to the observations. The required parameters basically were calculated. The time of concentration, t_c (h) is found by Kirpich equation:

$$t_c = 0.066 \left(\frac{L^2}{S}\right)^{0.385} \quad (1)$$

In which L is the length of the drainage channel (km), S is average slope of drainage area (%). The total duration of rainfall, is D (h):

$$D = 0.133 t_c \quad (2)$$

Time of peak, t_p (h):

$$t_p = \frac{D}{2} + 0.6t_c \quad (3)$$

Then Curve Number (CN) is found according to soil moisture capacity from SCS-CN table. The potential maximum retention, S' (mm):

$$S' = \frac{1000}{CN} - 10 \quad (4)$$

The maximum flow height, h_e (mm):

$$h_e = \frac{(h_a - 1)^2}{(h_a - 1 + S')} \quad (5)$$

where h_a is annual rainfall depth of selected return period (mm). Then, peak discharge, Q_p (m^3/s):

$$Q_p = 0.2083 \frac{A}{t_p} h_e \quad (6)$$

where drainage area, A (km^2).

2.2. Mockus Method

Triangular hydrograph is produced by the Mockus method. It can be applied easily for defining flood hydrograph. Also this method considers the basin shape factor, R_d:

$$R_d = \frac{A}{A'} \quad (7)$$

where A' (km^2) is the smallest circle area which covers drainage boundary. The time of concentration, t_c (h) is calculated by the Kirpich formula (Eq. 1) if R_d is between 0.6-0.7 then the basin shape is assumed to be circular. Time of peak, t_p (h):

$$t_p = \sqrt{t_c} + 0.6t_c \quad (8)$$

The unit peak discharge, q_p (m^3/s mm):

$$q_p = 0.208 \frac{A}{t_p} \quad (9)$$

Peak discharge, Q_p (m^3/s):

$$Q_p = q_p h_a \quad (10)$$

where annual rainfall depth of selected return period, h_a (mm).

2.3. Rainfall-Runoff Relationship for Peak Flood Discharge

The nonlinear regression method is applied to monthly peak discharge, Q_p (m^3/s), drainage area, A (km^2) and monthly total precipitation data, P (mm). The regression equation for peak discharge, Q_p (m^3/s):

$$Q_p = 3.7141(A.P)^{0.1358} \quad (11)$$

3. STUDY AREA

Akarcay Basin is located between 30°-32° east longitudes (240000-400000 UTM) and 38°-39° north longitudes (4210000-4330000 UTM). The basin is the second large closed basin in Turkey with 7340 km^2 drainage area. The basin has boundaries with the Aegean, Mediterranean and Central Anatolia geographical regions of Turkey. Due to its geographical location, it has characteristics of depression plain and impermeable soil layer. In the basin, erratic rainfall causes extreme events. In consequence of this erratic rainfall, increasing amount of water can cause flash floods in some rivers during winter and some rivers can run dry due to the decreasing amount of water during summer months. There are two natural lakes Lake Eber and Aksehir (Figure 1). They have rich living species. Hydrological studies have great importance because source of income where local people lives is provided by agriculture and animal husbandry. Also, the closed basin is fed by groundwater resources. Gazligol and Afyonkarahisar which have main settlements developed due to thermal water (SPA's) and health tourism [43].

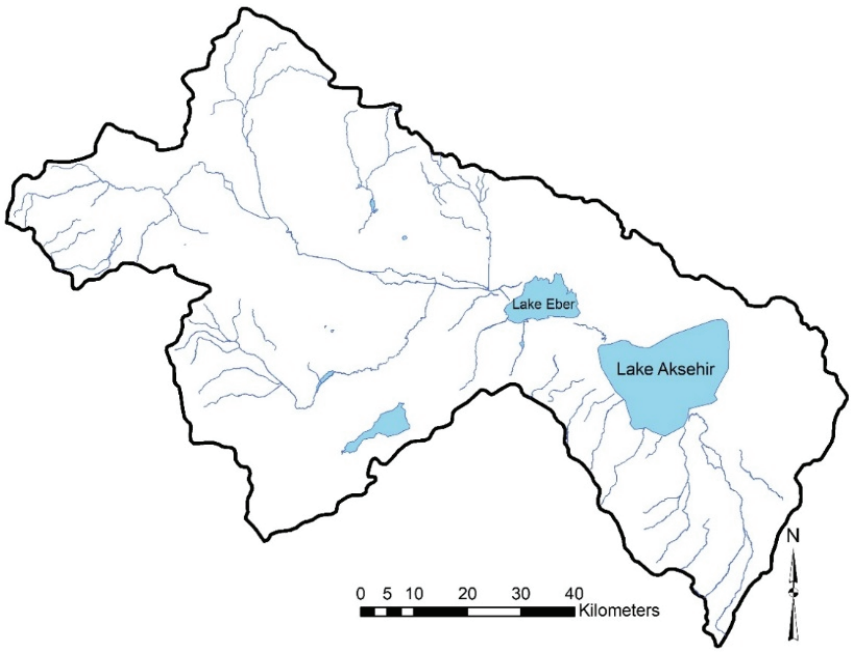

Figure 1 - Location map of Akarcay Basin

4. DATA

Topographical data used in this study were obtained from the General Directorate of Mapping, Turkey in the form of 1/25000 scaled 107 maps. Area properties were derived from maps in raster format. The Manning's roughness coefficients (*n*) of each area are presented in Table 1. Forested areas have higher Manning's roughness coefficients than urban areas. Also, the coefficients of river bed and highway are very close to each other and attain minor values. In these parts, flow velocity is high because of impermeable layer and less roughness. It is known that most of rivers and shallow waters in the watershed have natural cross sections and bed form. But the water level changes in the rivers are affected by anthropogenic impacts such as irrigation for agriculture. Synthetic flood hydrograph methods were used to be able to eliminate these impacts and determine flood discharge. 1/5000 high scaled 6 maps were taken from the General Directorate for Land Registry and Cadastre, Turkey for the University Campus of Afyon Kocatepe which is flash-flood prone due to high groundwater level. In addition, it was observed that the campus has high soil moisture and flow accumulation increases after any heavy rainfall event. At the same time, most of the campus area is known to be marshy area. The highway in front of the campus plays a very important role for transportation and connection between Afyon-Eskisehir cities and Gazligol County, which has a large capacity in terms of thermal water and health tourism. The high detailed maps were in the paper format, so they were digitalized using the GIS modeling technique.

Turkish Ministry of Forestry and Water Management provides geographically some environmental data by online access but not downloadable from geodata application. The data on the basin boundaries, gauging station locations, forests, highways, railways, river lengths, water bodies, water storage structures such as dams, hydraulic structures, bathymetry, administrative boundaries, etc. were accessible.

Table 1 - The selected Manning's roughness coefficients (n) in the study area [44]

Area	*n*
River	0.03
Forest	0.10
Light forest	0.08
Highway and railway	0.02
Other	0.06

Hydrological data was taken from the State Hydraulic Works (DSI) of Turkey. The observed data is obtained by annual instantaneous maximum discharge and monthly mean discharge in m^3/s (Figure 2). The calibration process for flood discharges was provided by annual instantaneous maximum discharge. Some gauging stations of the rivers in Akarcay Basin were compared with their minimum discharges and they are classified by intermittent and non-intermittent rivers. Figure 3 demonstrates the maximum water levels change in 1-1.5 m and confirms that the basin has shallow waters.

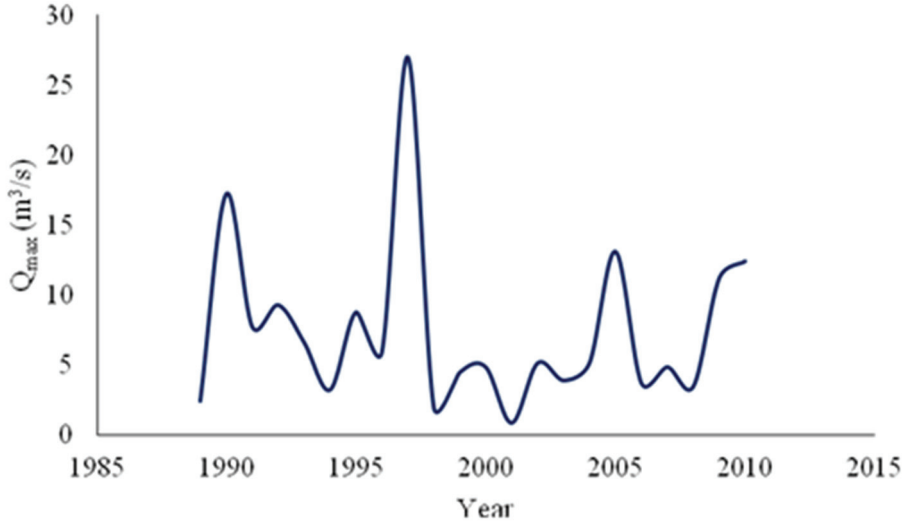

Figure 2 - Annual instantaneous maximum discharge of D11A021 gauging station

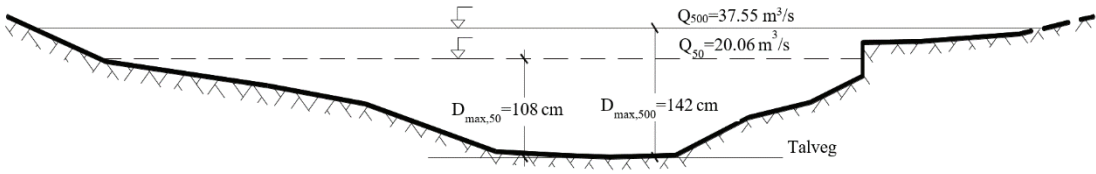

Figure 3 - The cross section at the point of D11A024 gauging station

Meteorological data were taken from the General Directorate of Meteorology (MGM). Monthly total precipitation, evaporation and temperature data were evaluated while investigating rainfall-runoff relationship. Only monthly total precipitation data was considered because the cause of flash floods is based on snow melting and heavy rainfall during spring season in the basin.

5. MODEL APPLICATIONS

Two hydrodynamic models were used to assess flood risk in Akarcay Basin. DEM data was prepared for the purpose of use in software. Then, area properties were extracted as a polygon from 1/25000 scaled digital maps in shapefile format. FESWMS and AdH models solve the flow equations using the finite element method. They are separated by mesh type as 8-node or 9-node quadrilateral (FESWMS) and 6-node triangle (AdH). The boundaries of river and floodplains were constructed in the software (Figure 5). The peak flood discharges are presented as input in the models (Table 2). Calculated peak flood discharges are in the 100-year return period.

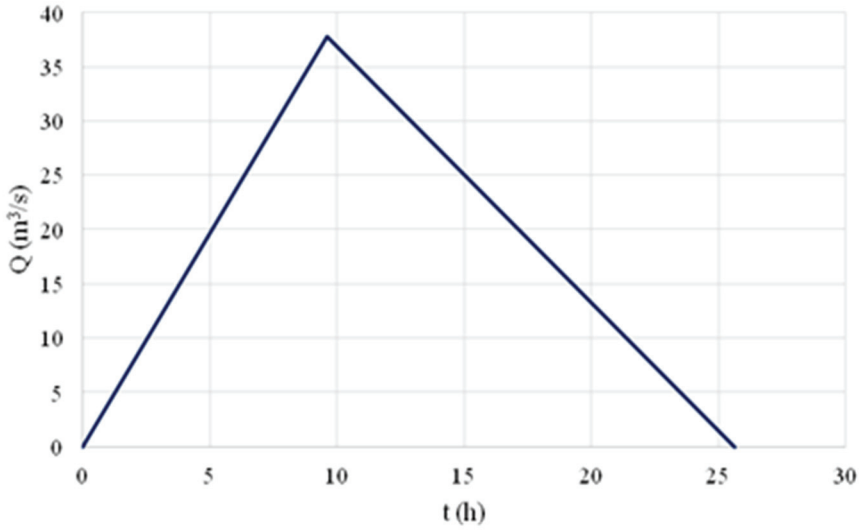

Figure 4 - The triangular Mockus flood hydrograph at the inlet of Akarcay Basin

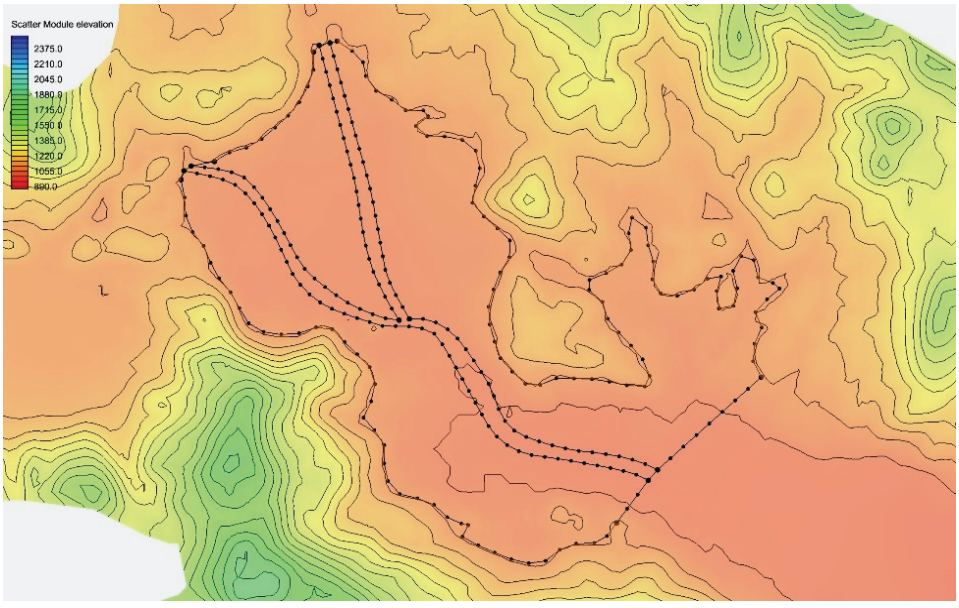

Figure 5 - Boundary conditions for inlets and outlet of the Akarcay Basin

Time of peak, t_p is calculated from Eq. (8) as 9.6 h. Time of peak and recession time of flood hydrograph are summed up for the aim of finding the base time of the flood hydrograph. The triangular Mockus flood hydrograph is demonstrated in Figure 4.

Table 2 - Observed and calculated peak flood discharges

Method	Q (m^3/s)
Observed	32.60
SCS	80.82
Mockus	37.82
Regression	29.65

5.1. FESWMS Model

FESWMS model runs under supercritical and subcritical flow regimes. Also, this model can be used to simulate flow in rivers and floodplains where vertical velocities are small in comparison to horizontal velocities, using wetting-drying conditions. FESWMS solves the following equations simultaneously:

$$\frac{\partial z_w}{\partial t} + \frac{\partial q_1}{\partial x} + \frac{\partial q_2}{\partial y} - q_m = 0 \tag{12}$$

$$\frac{\partial q_1}{\partial t} + \frac{\partial}{\partial x}\left(\frac{q_1^2}{d} + \frac{1}{2}gd^2\right) + \frac{\partial}{\partial y}\left(\frac{q_1 q_2}{d}\right) + gd\frac{dz_b}{\partial x} + gn^2\frac{q_1\sqrt{q_1^2+q_2^2}}{d^{7/3}}\sqrt{1+\left(\frac{dz_b}{dx}\right)^2+\left(\frac{dz_b}{dy}\right)^2} - 2d\varepsilon_{xx}\frac{\partial^2\bar{u}}{\partial x^2} - \varepsilon_{xy}\frac{\partial}{\partial y}\left(\frac{\partial\bar{u}}{\partial x}+\frac{\partial\bar{v}}{\partial y}\right) = 0 \tag{13}$$

$$\frac{\partial q_2}{\partial t} + \frac{\partial}{\partial x}\left(\frac{q_1 q_2}{d}\right) + \frac{\partial}{\partial y}\left(\frac{q_2^2}{d} + \frac{1}{2}gd^2\right) + gd\frac{dz_b}{\partial y} + gn^2\frac{q_2\sqrt{q_1^2+q_2^2}}{d^{7/3}}\sqrt{1+\left(\frac{dz_b}{dx}\right)^2+\left(\frac{dz_b}{dy}\right)^2} - 2d\varepsilon_{yy}\frac{\partial^2\bar{v}}{\partial y^2} - \varepsilon_{yx}\frac{\partial}{\partial x}\left(\frac{\partial\bar{u}}{\partial x}+\frac{\partial\bar{v}}{\partial y}\right) = 0 \tag{14}$$

where Eq. (12) is the continuity equation and Eqs. (13) and (14) are momentum equations in x and y directions, respectively. In the equations, t=time (s); d=water depth (m); g=acceleration due to gravity (m/s^2); z_w and z_b=water surface elevation and bed elevation above certain datum (m); q_1 and q_2= unit discharge fluxes (m^2/s) defined as $\bar{u}d$ and $\bar{v}d$, respectively; $\bar{u}$ and $\bar{v}$ (m/s)=depth-averaged velocities of an element in the streamwise and transverse directions, respectively; q_m=resultant inlow or outflow from that element (m/s); ε_{xx} and ε_{yy}=normal components of the eddy viscosity (m^2/s) in the x and y directions, respectively; and ε_{xy} and ε_{yx}=shear components of the eddy viscosity (m^2/s) applied to the x-y plane.

Initial and boundary conditions were determined in the model. Water surface elevation for the outlet and peak flood discharge for the inlets were determined as shown in Figure 6. The required other parameters as Eddy viscosity coefficients (V_o) 100 and 50 for land and river, respectively. The coefficient is used to define turbulence characteristics. So, Eddy viscosity coefficient is higher in floodplain areas than the river. Wind and wave effects weren't considered because of insufficient data. Under steady flow, the user inputs are boundary conditions a discharge upstream and a stage downstream. The model calculates stages

throughout the interior points, keeping the discharge constant. Under unsteady flow, the user inputs a discharge hydrograph at the upstream boundary and a discharge-stage rating at the downstream boundary. The model calculates discharges and stages throughout the interior points. All scenarios were applied under steady state case assuming constant flood discharge. The boundary conditions were determined according to flood discharges and dry conditions were taken into consideration considering that the rivers in the basin are dry during certain periods of the year for the initial conditions.

For the aim of flood modeling of the basin, FESWMS model was used in the whole of the Akarcay Basin and AdH model was used for the subbasins of Akarcay Basin with 80.82 m^3/s peak discharge, which is found by SCS method against 100-year return period. Flood propagation with FESWMS model is demonstrated by Figures 7-10. Flood propagation is examined in regard of 4 different places (Afyon, Bolvadin, Cay, Suhut) altitudes for the aim of determination as water level thresholds (Figures 7-10). Altitude affects the flooded area's forward propagation. When the altitude increases, the flooded area increases and vice versa. Flooded areas are calculated as 503.96, 422.13, 1126.16 and 1596.61 km^2. Mesh modules are defined as water levels during flood event. Flow velocities and magnitudes are demonstrated by Figure 11. The flow velocities are calculated taking into consideration Suhut (highest altitude) threshold. The maximum velocity is calculated as 1.91 m/s in the Akarcay Basin.

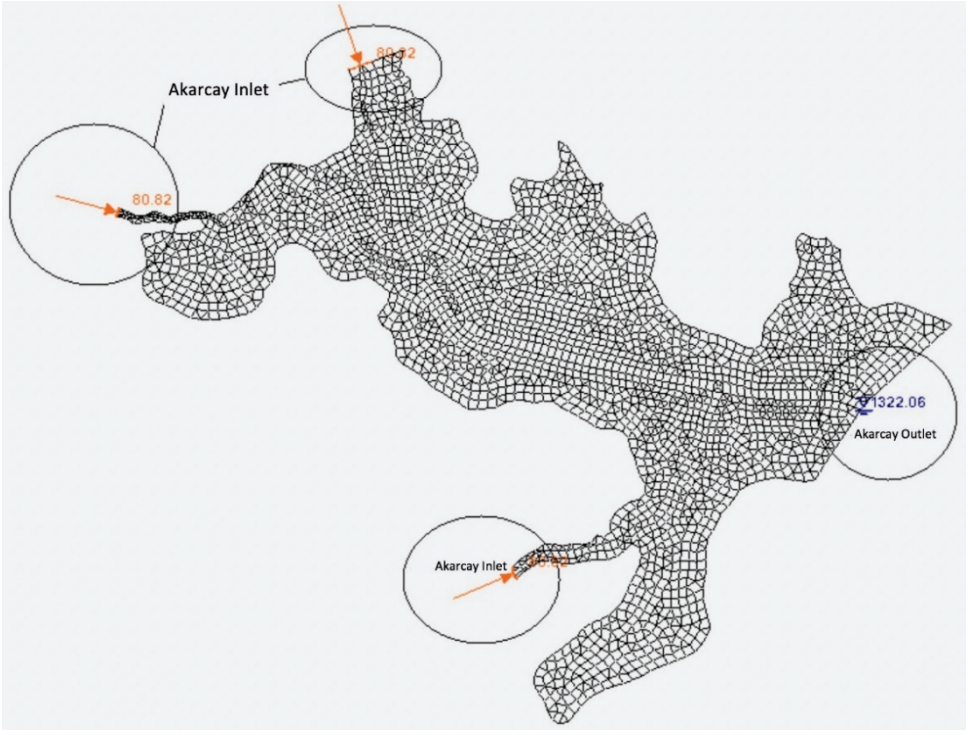

Figure 6 - Boundary conditions for inlets and outlet of the Akarcay Basin

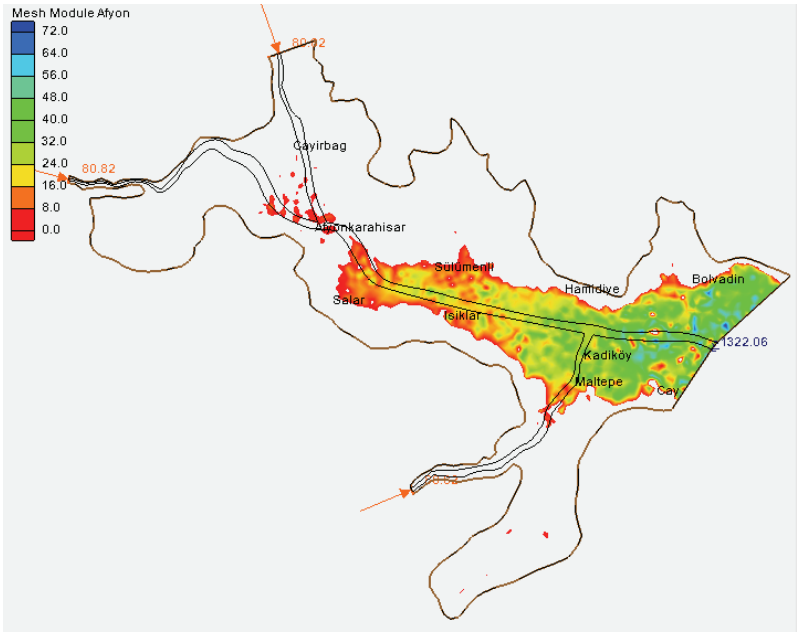

Figure 7 - Flood risk map of the Akarcay Basin in FESWMS model according to altitude of Afyon in threshold

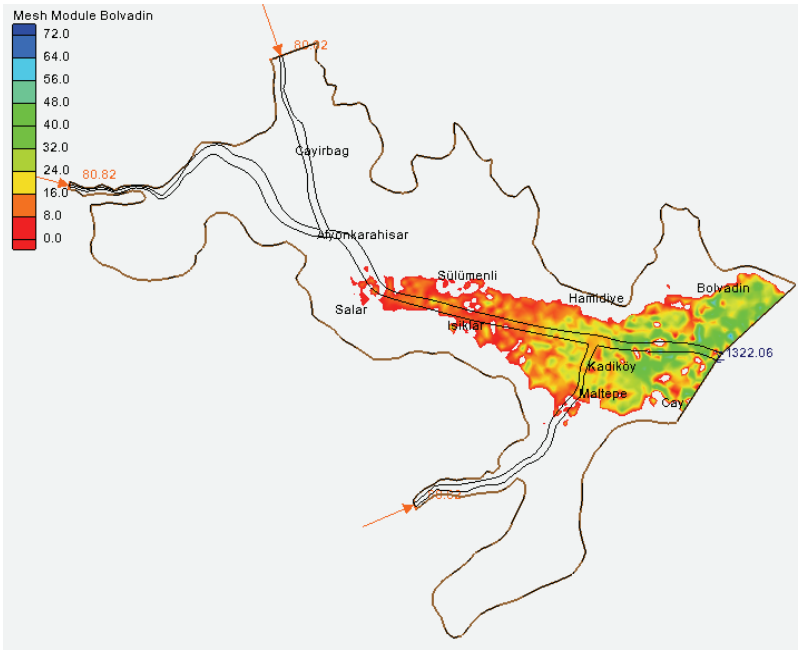

Figure 8 - Flood risk map of the Akarcay Basin in FESWMS model according to altitude of Bolvadin in threshold

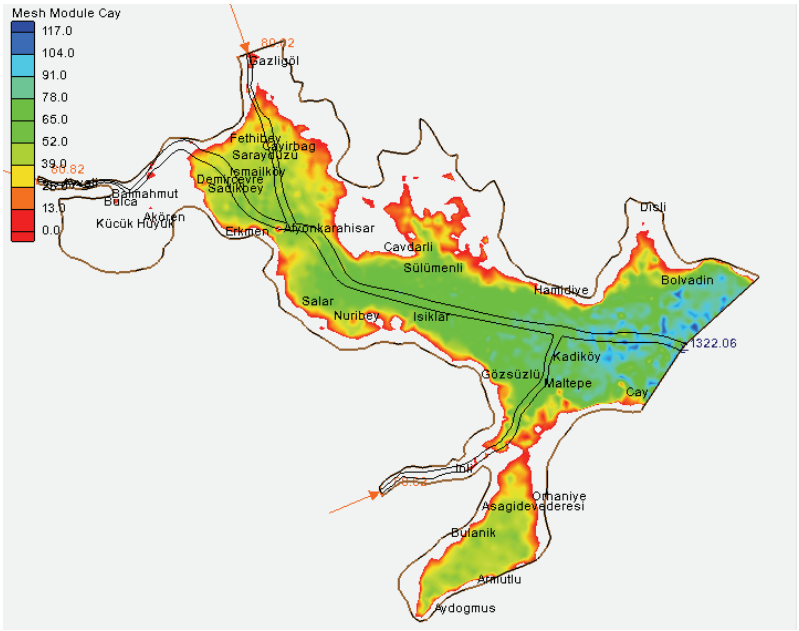

Figure 9 - Flood risk map of the Akarcay Basin in FESWMS model according to altitude of Cay in threshold

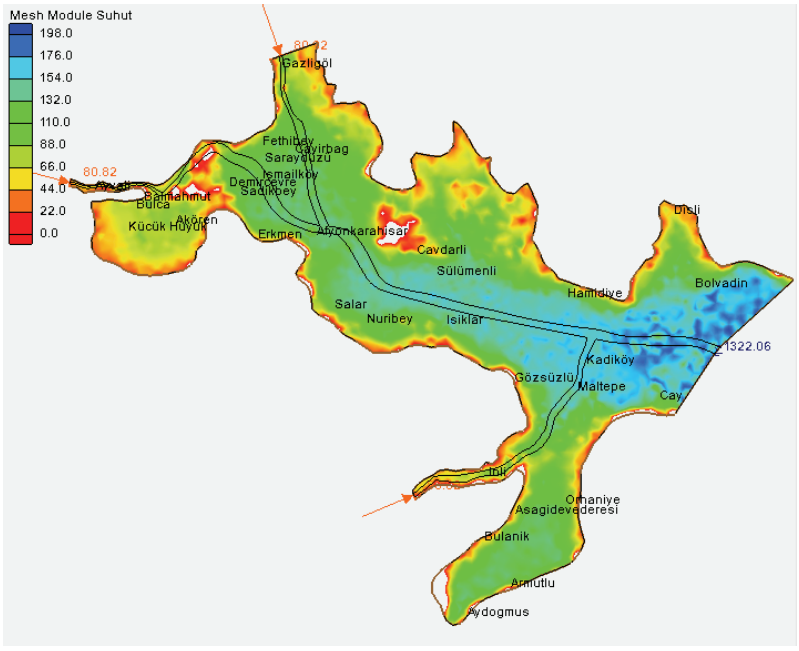

Figure 10 - Flood risk map of the Akarcay Basin in FESWMS model according to altitude of Suhut in threshold

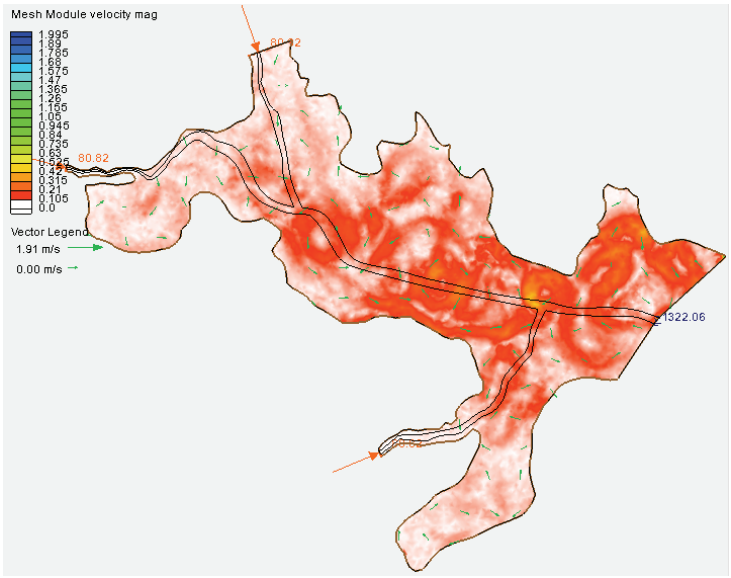

Figure 11 - Flow velocities and magnitudes during the 100-year return period flood event

5.2. AdH Model

AdH model uses 3D Navier-Stokes and 2D (depth averaged) shallow water equations. Although 3D models allow a detailed reproduction of flow processes in compound channels, so far, a number of limiting factors usually prevented their application as flood models. The computational burden is still considerably larger for 2D models, particularly for dynamic shallow flows with significant changes in domain extent. Also, 3D model is preferred for the solution of flow mechanism complexity in urban areas. The ability of AdH to allow the domain to wet and dry as flow conditions or tides change is suitable for shallow marsh environments, floodplains and the like. AdH can simulate subcritical and supercritical flow conditions within the same domain [1]. For overland flow conditions, urban and others were considered. The model was run for 36 and 72 hours at time interval of 1 hour. At the end of computations, flooded area was calculated.

When the parameters which are used in FESWMS model, are also used in the AdH model, flooded areas in the Akarcay Basin are presented in Figure 12. Afyon, Bolvadin and Suhut plains are analyzed separately with AdH model which is used for shallow water modeling. Constant water depth is averagely taken as 0.6 m by handling observed data. Variable water levels change between 1-3 m. After running the AdH model, the results are manifested in the Google Earth software and the motion of flood waters is followed during the flood event. With these results, the recession of flood waters can be observed. Flood propagation with AdH model is demonstrated by Figures 12-13. The darkness of the blue color indicates the increasing water level. The black lines inside the working area represent the boundaries of the river bed. Flood risk map of Afyonkarahisar City Center from localized AdH model results (Figure 14). The calculated flooded areas from AdH model are demonstrated in Table 3.

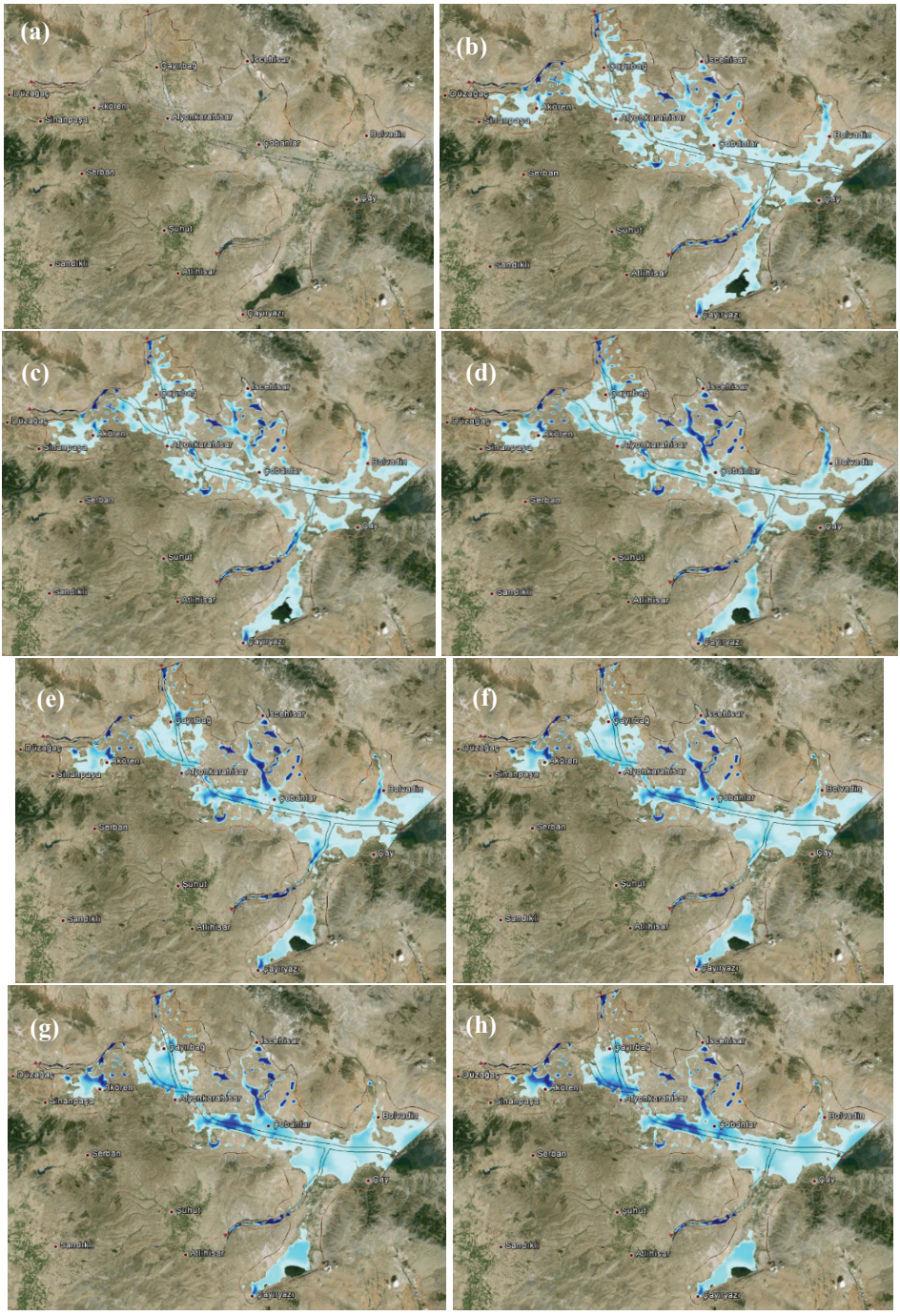

Figure 12 - Flooded areas of Akarcay for different time steps until 72 h during flood event; (a) 0 h, (b) 12 h, (c) 14 h, (d) 24 h, (e) 36 h, (f) 48 h, (g) 60 h, (h) 72 h

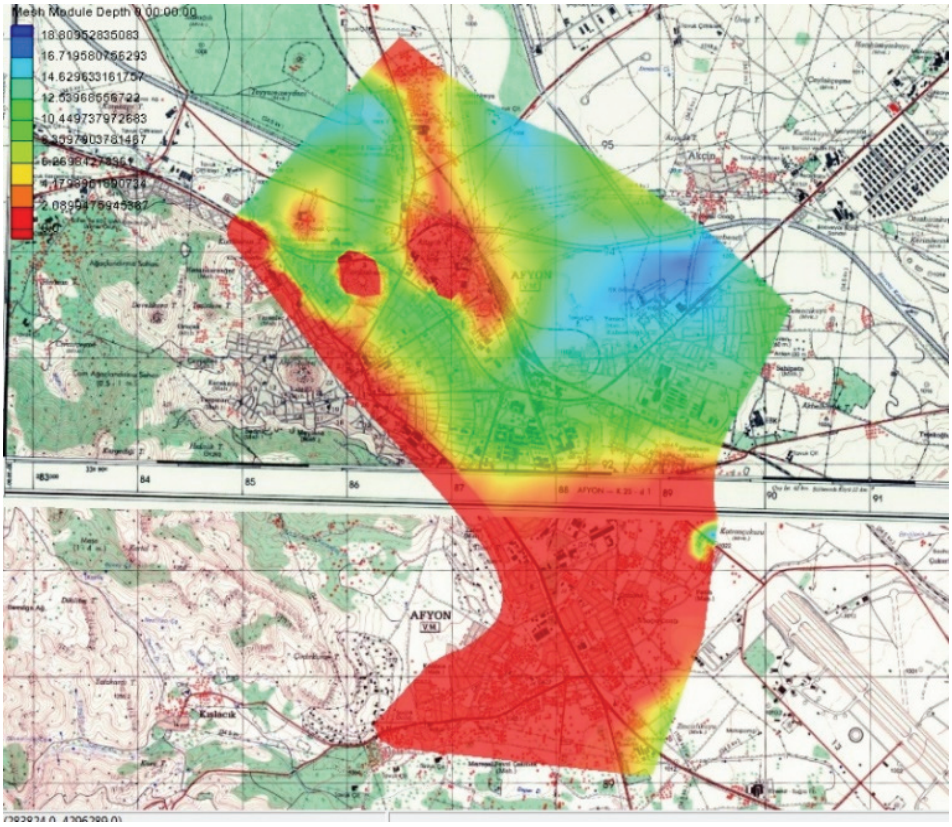

Figure 13 - Flood risk map of Afyonkarahisar City Center from localized AdH model results

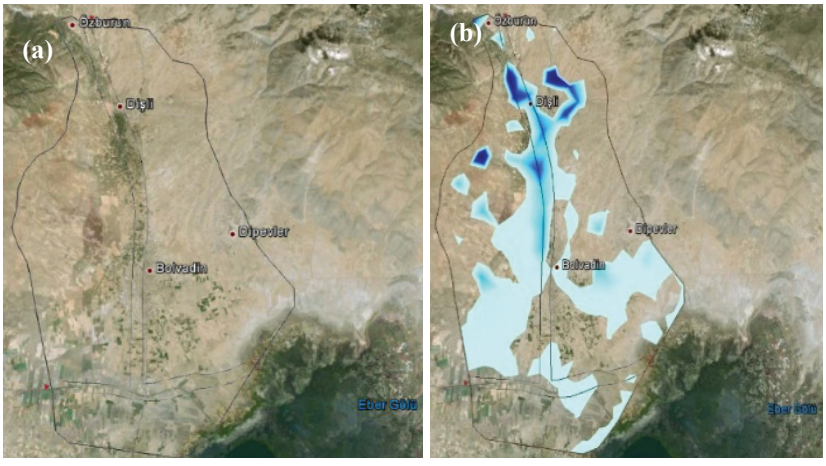

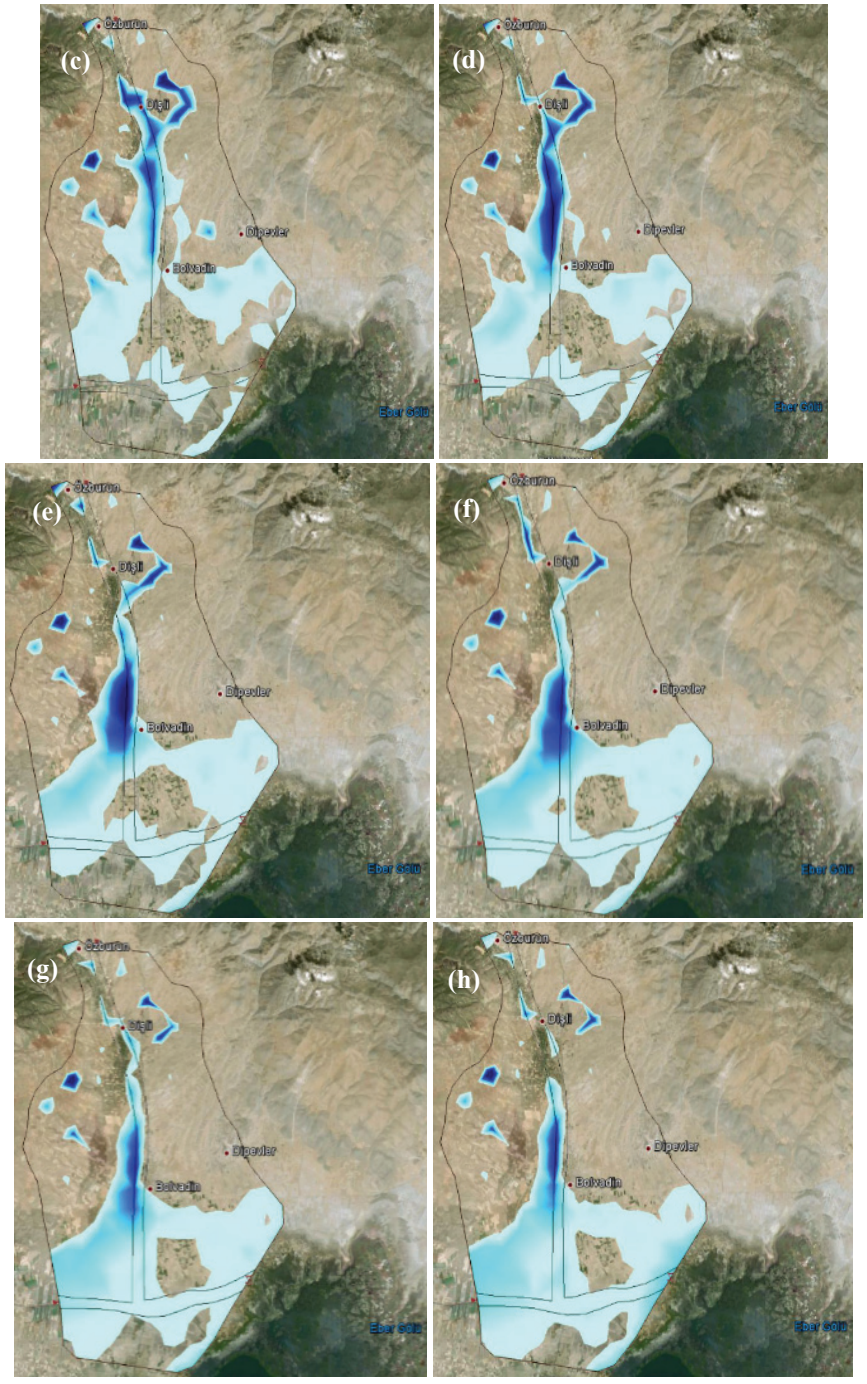

Figure 14 - Flooded areas of Bolvadin near Lake Eber for different time steps until 72 h during flood event; (a) 0 h, (b) 12 h, (c) 15 h, (d) 24 h, (e) 36 h, (f) 48 h, (g) 60 h, (h) 72 h

Table 3 - Flooded areas in the regions of Akarcay Basin for 36 h and 72 h simulation time

	Simulation time (h)	
	36	72
Region	Area (km^2)	
Afyon	218.65	252.60
Bolvadin	150.81	164.21
Suhut	134.06	137.73
Akarcay	804.72	914.83

6. DISCUSSIONS

In the analyzed models, the changes of the water levels were examined and the areas to be inundated at the time of the flood were calculated. When flood effect caused by a flow rate value of 80.82 m^3/s worked out by flood analysis results calculated through FESWMS and AdH according to a 100-year return period in the whole of the Akarcay basin and affected settlement areas as well as total areas are taken into consideration.

FESWMS model results:

In the analysis that Afyonkarahisar center gorge is referenced (Figure 7), a total of 503.96 km^2 of floods will take place in the Uydukent side, Cayirbag, Sulumenli, Isiklar, Salar, Maltepe, Hamidiye, Kadikoy, Cay and Bolvadin. Bolvadin, Sulumenli, Isiklar, Salar, Maltepe, Hamidiye, Kadikoy, Cay have 422.13 km^2 of flood effect in Bolvadin central elevation (Figure 8).

According to Figure 9, the flood effect of reference in the center of the Cay is Afyonkarahisar center, Gazligol, Kucuk Huyuk, Bulca, Balmahmut, Ayvali, Fethibey, Akoren, Cayirbag, Sarayduzu, Ismailkoy, Demircevre, Sadikbey, Erkmen, Nuribey, Cavdarli, Sulumenli, Isiklar, Salar, Maltepe, Hamidiye, Kadikoy, Gozsuzlu, Orhaniye, Asagidevederesi, Disli, Armutlu, Aydogmus, Inli, Bulanik, Cay and Bolvadin. In this analysis, the area under the total flood was found to be 126.16 km^2.

It is seen that the water velocity results reach about 0.30 m/s values in the plains of Afyon and Bolvadin, and about 0.42 m/s in Ihsaniye, Balmahmut and Suhut regions (Figure 11). Moreover, the maximum water velocity at the basin was found to be 1.91 m/s for a flow rate of 80.82 m^3/s.

AdH model results:

At the next stage, the water velocities for Akarcay Basin and localized Bolvadin County were obtained according to time steps (Figure 12 and 13). Degirmen Creek which passes through Bolvadin then connects with Akarcay River and together discharge to Lake Eber. Also, Bolvadin is the 3rd largest county with population 43842 people and commercial mobility. After the maximum flood in the outflows obtained, the water velocities in the flood areas decreased and then the overflowing water became almost stagnant 36 and 72 hours.

Flood hydrographs which time interval 1 hours that were calculated through the SCS method

were applied. The maximum-flooded area was found to be 914.83 km^2 at the 14^{th} hour for Akarcay Basin. Also, Afyonkarahisar City Center and Saraycik, Garipce, Fethibey, Erenler, Akcin Counties were affected by flood waters according to peak flood discharge (Figure 12). Flooded area was found to be 761.5 km^2 at the end of the 72^{nd} hour for Akarcay Basin along with the regression of flood waters. Again, Afyonkarahisar City Center together with the University Campus and Saraycik, Garipce, Fethibey, Erenler, Akcin Counties were affected by floods. Localized AdH model of flood analysis for Afyonkarahisar City Center was evaluated in Figure 13. It is demonstrated that the places near industrial sites have flood risky areas.

The maximum-flooded area was found to be 164.21 km^2 at the 15^{th} hour for Bolvadin Region. The affected areas from flood waters are Bolvadin County Center and Disli Village which is near Bolvadin and in the North of Bolvadin (Figure 14). Flooded area was found to be 114.76 km^2 at the end of the 72^{nd} hour for Bolvadin Region along with the retreat of flood waters. Afyon, Bolvadin and Suhut regions have important plains in terms of agriculture and settlements. Akarcay region demonstrates flooded area in the whole basin.

FESWMS model versus AdH model:

The FESWMS module outputs are the change in water velocity and water level in the stream during flood. Akarcay river bed length is about 87 km and the data entry only at the inlet and exit points in the basin is limitation of the FESWMS model. In addition, the accuracy of the model is variable due to the lack of cross-section identification as in other flood programs.

The ADH module is dynamically operated and the amount of water overflowing the river bed after flood, the areas under water, the changes in water flow rates and water levels can be obtained as output. Due to the dynamic identification of the ADH model, the water heights at the exit point have also changed as compared to the base. But, due to the dynamic setup of the model, the analysis time is longer than the steady-state.

In basin-based analysis, the flood area calculated in the FESWMS module was also obtained by the work done in the ADH module. However, it appears that the fields are not equal, calculated flood areas in the FESWMS module are wider than the field with AdH. This is due to the above limitation of the FESWMS model, so, ADH is expected to provide more accurate results in the Akarcay basin.

7. CONCLUSIONS

In order to avoid flood risks, it is necessary to perform flood analysis before the flood and to take necessary precautions to reduce or prevent flood damage. Various flood analysis software has been developed for this purpose. FESWMS and AdH modules of SMS (Surface water Modeling System) software which is one of these softwares were discussed in this work and flood analysis of the Akarcay basin was performed by using modules. Erratic rainfall and discharges as well as impermeable ground, topographic structures increase flood risk at the Akarcay basin. Thus, the measures at stated locations are important in terms of prevention of flood risk. In this study, quite difficult flood calculations were made through computer, thıs allowing visualization of flooded areas in the 3D form.

For this purpose, FESWMS and AdH models of the SMS software were used. FESMWS

model was built for the steady state condition and used for calculating peak flood discharges by the four methods mentioned above. The model was run to provide users water velocity and water surface elevation as output. The model was run at one hourly time intervals. AdH model was run under dynamic conditions. Flooded areas, water velocity and water surface elevation are the model outputs there.

The main river reaches 87 km throughout Akarcay. Maximum water velocity was calculated as 1.91 m/s. One limitation of FESWMS model is that it only allows data input where there are basin inputs. In addition, the accuracy of the model is variable due to the lack of cross section identification as in other flood modeling programs. According to the ADH model, the FESWMS model predicts that larger areas will be flooded. It is recommended to use the AdH model for precise calculation because of the limited limitations according to FESWMS.

According to results, Erenler, Cayirbag and Fethibey Villages near the University campus are under flood risk. The local population subsist on agriculture and animal husbandry. Also, Sivrikaya Creek passes through University Campus which also has flood risk. Additionally, most of the campus area is marshy land.

With the ease of use of the SMS program interface, it is thought that this work will lead to applications such as flood, sediment transport, multi-directional modeling studies such as water quality and the design of water structures. In addition to hydrological and meteorological data such as rainfall, evaporation, temperature and wind speed results are to be obtained sensitively in the investigated area, the sensitivity of the values can be increased by operating the program on days, hours and minutes basis using digital maps higher than 1/25000 scale. For the first time with the study, hydrodynamic-flood models are developed for Akarcay Basin using FESWMS and AdH models. For future studies, changing earth should be taken into consideration with manmade channels, crowded population and growing settlements, water quality etc. Real time working systems and models are newly developing. After required experimental setups with data observation and data transfer, this type of real time hydrodynamic models can be applied worldwide.

Symbols

A : Drainage area

A' : The smallest circle area which covers drainage boundary

CN : Curve Number

D : Total duration of rainfall

d : Water depth

g : Acceleration due to gravity

h_a : Annual rainfall depth of selected return period

h_e : Maximum flow height

L : Length of drainage channel

P : Monthly total precipitation

Q_p : Peak discharge

q_1 : Unit discharge flux defined as $\bar{u}d$

q_2 : Unit discharge flux defined as $\bar{v}d$

q_m : Resultant inlow or outflow from that element

q_p : Unit peak discharge

R_d : Basin shape factor

S : Average slope of drainage area

S' : Potential maximum retention

t : Time

t_c : Time of concentration

t_p : Time of peak

$\bar{u}$: Depth-averaged velocity of an element in the streamwise direction

$\bar{v}$: Depth-averaged velocity of an element in the transverse direction

z_b : Bed elevation above certain datum

z_w : Water surface elevation above certain datum

ε_{xx} : Normal component of the eddy viscosity in the x direction

ε_{yy} : Normal component of the eddy viscosity in the y direction

$\varepsilon_{xy}, \varepsilon_{yx}$: Shear components of the eddy viscosity

Acknowledgements

This study is a part of MS thesis of the first author and the study is supported with Scientific Research Project "Flood modelling of Akarcay Basin" (No: 11.FEN.BIL.26) funded by Afyon Kocatepe University.

References

[1] CHL, Adaptive Hydraulics 2D Shallow Water (AdH- SW2D) User Manual (version 4.6), July 2017, Coastal and Hydraulics Laboratory (CHL), US Army Corps of Engineers (USACE), 2017.

[2] Topaloglu, F., Regional Flood Frequency Analysis of the Basins of the East Mediterranean Region. Turk. J. Agric. For., 29, 287-295, 2005.

[3] Burn, D.H., Evaluation of Regional Flood Frequency Analysis with A Region of Influence Approach. Water Resour. Res., 26(10), 2257-2265, 1990.

[4] Burn, D.H., An Appraisal of The "Region of Influence" Approach to Flood Frequency Analysis. Hydrolog. Sci. J., 35(2), 149-165, 1990.

[5] Burn, D.H., Catchment Similarity for Regional Flood Frequency Analysis Using Seasonality Measures. J. Hydrol., 202, 212-230, 1997.

[6] Rossi, F., Fiorentino, M., Versace, P., Two-Component Extreme Value Distribution for Flood Frequency Analysis. Water Resour. Res., 20(7), 847-856, 1984.

[7] Stedinger, J.R., Cohn, T.A., Flood Frequency Analysis with Historical and Paleoflood Information. Water Resour. Res., 22(5), 785-793, 1987.

[8] Zhang, L., Singh, V.P., Bivariate Flood Frequency Analysis Using the Copula Method. J. Hydrol. Eng., 11(2), 150-164, 2006.

[9] Grimaldi, S., Serinaldi, F., Asymmetric Copula in Multivariate Flood Frequency Analysis. Adv. Water Resour., 29, 1155-1167, 2006.

[10] Yue, S., Ouarda, T.B.M.J., Bobee, B., Legendre, P., Bruneau, P., The Gumbel Mixed Model for Flood Frequency Analysis. J. Hydrol., 226, 88-100, 1999.

[11] Acreman, M.C., Sinclair, C.D., Classification of Drainage Basins According to Their Physical Characteristics; An Application for Flood Frequency Analysis in Scotland. J. Hydrol., 84, 365-380, 1986.

[12] Bates, P.D., De Roo, A.P.J., A Simple Raster-Based Model for Flood Inundation Simulation. J. Hydrol., 236, 54–77, 2000.

[13] Horritt, M.S., Bates, P.D., Evaluation of 1D and 2D Numerical Models for Predicting River Flood Inundation. J. Hydrol., 268, 87-99, 2002.

[14] Sanders, B.F., Evaluation of On-line DEMs for Flood Inundation Modeling. Adv. Water Resour., 30, 1831-1843, 2007.

[15] Yamazaki, D., Ikeshima, D., Tawatari, R., Yamaguchi, T., O'Loughlin, F., Neal, J.C., Sampson, C.C., Kanae, S., Bates, P.D., A High-Accuracy Map of Global Terrain Elevations. Geophys. Res. Lett., 44, 5844-5853, 2017.

[16] Ciervo, F., Papa, M.N., Medina, V., Bateman, A., Simulation of Flash Floods in Ungauged Basins Using Post-Event Surveys and Numerical Modelling. J. Flood Risk Manag., 8, 343-355, 2015.

[17] Bradford, S.F., Sanders, B.F., Finite-Volume Model for Shallow-Water Flooding of Arbitrary Topography. J. Hydraul. Eng., 128(3), 289-298, 2002.

[18] de Almeida, G.A.M., Bates, P., Ozdemir, H., Modelling Urban floods at Submetre Resolution: Challenges or Opportunities for flood Risk Management? J. Flood Risk Manag., https://doi.org/10.1111/jfr3.12276, 2016.

[19] Falter, D., Dung, N.V., Vorogushyn, S., Schroter, K., Hundecha, Y., Kreibich, H., Apel, H., Theisselmann, F., Merz, B., Continuous, Large-Scale Simulation Model for Flood Risk Assessments: Proof-Of-Concept. J. Flood Risk Manag., 9, 3-21, 2016.

[20] Papanicolaou, A.N., Elhakeem, M., Wardman, B., Calibration and Verification of A

2D Hydrodynamic Model for Simulating Flow Around Emergent Bendway Weir Structures. J. Hydraul. Eng., 137(1), 75-89, 2011.

[21] Rossell, R.P., Ting, F.C.K., Hydraulic and Contraction Scour Analysis of A Meandering Channel: James River Bridges Near Mitchell, South Dakota. J. Hydraul. Eng., 139(12), 1286-1296, 2013.

[22] Larsen, R.J., Ting, F.C.K., Jones, A.L., Flow Velocity and Pier Scour Prediction in a Compound Channel: Big Sioux River Bridge at Flandreau, South Dakota. J. Hydraul. Eng., 137(5), 595-605, 2011.

[23] Cook, A. Merwade, V., Effect of Topographic Data, Geometric Configuration and Modeling Approach on Flood Inundation Mapping. J. Hydrol., 377, 131-142, 2009.

[24] Pasternack, G.B., Bounrisavong, M.K., Parikh, K.K., Backwater Control on Riffle–Pool Hydraulics, Fish Habitat Quality, And Sediment Transport Regime in Gravel-Bed Rivers. J. Hydrol., 357, 125-139, 2008.

[25] Brown, R.A., Pasternack, G.B., Engineered Channel Controls Limiting Spawning Habitat Rehabilitation Success on Regulated Gravel-Bed Rivers. Geomorphology, 97, 631-654, 2008.

[26] Brown, R.A., Pasternack, G.B., Comparison of Methods for Analysing Salmon Habitat Rehabilitation Designs for Regulated Rivers. River Res. Appl., 25, 745-772, 2009.

[27] Cavagnaro, P., Revelli, R., Numerical Model Application for the Restoration of the Racconigi Royal Park (CN, Italy). J Cult. Herit., 10, 514-519, 2009.

[28] Jennings, A.A., Modeling Sedimentation and Scour in Small Urban Lakes. Environ. Modell. Softw., 18, 281-291, 2003.

[29] Mouton, A.M., Schneider, M., Peter, A., Holzer, G., Muller, R., Goethals, P.L.M., Pauw, N.D., Optimisation of A Fuzzy Physical Habitat Model for Spawning European Grayling (Thymallus Thymallus L.) in the Aare River (Thun, Switzerland). Ecol. Model., 215, 122-132, 2008.

[30] Zanichelli, G., Caroni, E., Fiorotto, V., River Bifurcation Analysis by Physical and Numerical Modeling. J. Hydraul. Eng., 130(3), 237-242, 2004.

[31] Stockstill, R.L., Daly, S.F., Hopkins, M.A., Modeling Floating Objects at River Structures. J. Hydraul. Eng., 135(5), 403-414., 2009.

[32] Sharp, J.A., McAnally, W.H., Numerical Modeling of Surge Overtopping of A Levee. Appl. Math. Model., 36, 1359-1370, 2012.

[33] Jones, L., Adaptive Control of Ground-Water Hydraulics. J. Water Res. Plan. Man., 118(1), 1-17, 1992.

[34] Danchuk, S., Willson, C.S., Effects of Shoreline Sensitivity on Oil Spill Trajectory Modeling of the Lower Mississippi River. Environ. Sci. Pollut. R., 17, 331-340, 2010.

[35] Lai, X., Jiang, J., Liang, Q., Huang, Q., Large-Scale Hydrodynamic Modeling of the Middle Yangtze River Basin with Complex River–Lake Interactions. J. Hydrol., 492, 228-243, 2013.

[36] Martin, S.K., Savant, G., McVan, D.C., Two-Dimensional Numerical Model of the Gulf Intracoastal Waterway near New Orleans. J. Waterw. Port Coast., 138(3), 236-245, 2012.

[37] McAlpin, T.O., Sharp, J.A., Scott, S.H., Savant, G., Habitat Restoration and Flood Control Protection in the Kissimmee River. Wetlands, 33, 551-560, 2013.

[38] Nguyen, H.V., Cheng, J.C., Hammack, E.A., Maier, R.S., Parallel Newton-Krylov Solvers for Modeling of A Navigation Lock Filling System. Procedia Computer Science, 1, 699-707, 2012.

[39] Nguyen, H.V., Cheng, J.C., Berger, C.R., Savant, G., A Mass Conservation Algorithm for Adaptive Unrefinement Meshes Used by Finite Element Methods. Procedia Computer Science, 9, 727-736, 2012.

[40] Eller, P.R., Cheng, J.C., Maier, R.S., Dynamic Linear Solver Selection for Transient Simulations Using Multi-Label Classifiers. Procedia Computer Science, 9, 1523-1532, 2012.

[41] Pettway, J.S., Schmidt, J.H., Stagg, A.K., Adaptive Meshing in A Mixed Regime Hydrologic Simulation Model. Computat. Geosci., 14, 665-674, 2010.

[42] Savant, G., Berger, C., McAlpin, T.O., Tate, J.N., Efficient Implicit Finite-Element Hydrodynamic Model for Dam and Levee Breach. J. Hydraul. Eng., 137(9), 1005-1018, 2011.

[43] Burgan, H.I., Flood Modelling of Akarcay Basin. MS Thesis, Afyon Kocatepe University, 2013.

[44] Chow, V.T., Open-channel Hydraulics. New York: McGraw-Hill, 1959.

TEKNİK DERGİ MANUSCRIPT DRAFTING RULES

1. The whole manuscript (text, charts, equations, drawings etc.) should be arranged in Word and submitted in ready to print format. The article should be typed on A4 (210 x 297 mm) size paper using 10 pt (main title 15 pt) Times New Roman font, single spacing. Margins should be 40 mm on the left and right sides and 52.5 mm at the top and bottom of the page.
2. Including drawings and tables, articles should not exceed 25 pages, technical notes 6 pages.
3. Your contributed manuscript must be sent over the DergiPark system. (http://dergipark.gov.tr/tekderg)
4. The text must be written in a clear and understandable language, conform to the grammar rules. Third singular person and passive tense must be used, and no inverted sentences should be contained.
5. Title must be short (10 words maximum) and clear, and reflect the content of the paper.
6. Sections should be arranged as: (i) abstract and keywords, (ii) title, abstract and keywords in the other language, (iii) main text, (iv) symbols, (v) acknowledgements (if required) and (vi) references.
7. Both abstracts should briefly describe the object, scope, method and conclusions of the work and should not exceed 100 words. If necessary, abstracts may be re-written without consulting the author. At least three keywords must be given. Titles, abstracts and keywords must be fitted in the first page leaving ten line space at the bottom of the first page and the main text must start in the second page.
8. Section and sub-section titles must be numbered complying with the standard TS1212.
9. Symbols must conform to the international rules; each symbol must be defined where it appears first, additionally, a list of symbols must be given in alphabetic order (first Latin, then Greek alphabets) at the end of the text (before References).
10. Equations must be numbered and these numbers must be shown in brackets at the end of the line.
11. Tables, drawings and photographs must be placed inside the text, each one should have a number and title and titles should be written above the tables and below the drawings and photographs.
12. Only SI units must be used in the manuscripts.
13. Quotes must be given in inverted commas and the source must be indicated with a reference number.
14. Acknowledgement must be short and mention the people/ institutions contributed or assisted the study.
15. References must be numbered (in brackets) in the text referring to the reference list arranged in the order of appearance in the text. References must include the following information:

    If the reference is an article: Author's surname, his/her initials, other authors, full title of the article, name of the journal, volume, issue, starting and ending pages, year of publication.

    Example : Naghdi, P. M., Kalnins, A., On Vibrations of Elastic Spherical Shells. J. Appl. Mech., 29, 65-72, 1962.

    If the reference is a book: Author's surname, his/her initials, other authors, title of the book, volume number, editor if available, place of publication, year of publication.

    Example : Kraus. H., Thin Elastic Shells, New York. Wiley, 1967.

    If the reference is a conference paper: Author's surname, his/her initials, other authors, title of the paper, title of the conference, location and year.

    If the source is a thesis: Author's surname, his/her initials, thesis title, level, university, year.

    If the source is a report: Author's surname, his/her initials, other authors, title of the report, type, number, institution it is submitted to, publication place, year.
16. Discussions to an article published in Teknik Dergi should not exceed two pages, must briefly express the addressed points, must criticize the content, not the author and must be written in a polite language. Authors' closing remarks must also follow the above rules.
17. A separate note should accompany the manuscript. The note should include, (i) authors' names, business and home addresses and phone numbers, (ii) brief resumes of the authors and (iii) a statement "I declare in honesty that this article is the product of a genuinely original study and that a similar version of the article has not been previously published anywhere else" signed by all authors.
18. Copyright has to be transferred to UCTEA Turkish Chamber of Civil Engineers. The standard copyright form signed by the authorised author should therefore be submitted together with the manuscript.

CONTENTS

ISSN: 1300-3453